CAPTURA DE CO_2 EM MATERIAIS CIMENTICIOS ATRAVÉS DE CARBONATAÇÃO ACELERADA

Alex Neves Junior

Tese de Doutorado apresentada ao Programa de Pós-Graduação em Engenharia Civil, COPPE, da Universidade Federal do Rio de Janeiro, como parte dos requisitos necessários à obtenção do título de Doutor em Engenharia Civil.

Orientadores: Romildo Dias Toledo Filho
Jo Dweck
Eduardo de Moraes Rego Fairbairn

Rio de Janeiro
Fevereiro de 2014

CAPTURA DE CO_2 EM MATERIAIS CIMENTICIOS ATRAVÉS DE CARBONATAÇÃO ACELERADA

Alex Neves Junior

TESE SUBMETIDA AO CORPO DOCENTE DO INSTITUTO ALBERTO LUIZ COIMBRA DE PÓS-GRADUAÇÃO E PESQUISA DE ENGENHARIA (COPPE) DA UNIVERSIDADE FEDERAL DO RIO DE JANEIRO COMO PARTE DOS REQUISITOS NECESÁRIOS PARA A OBTENÇÃO DO GRAU DE DOUTOR EM CIÊNCIAS EM ENGENHARIA CIVIL.

Examinada por:

_____
Prof. Romildo Dias Toledo Filho, D.Sc

_____
Prof. Jo Dweck, D.Eng

_____
Prof. Eduardo de Moraes Rego Fairbairn, D.Ing

_____
Prof. Guilherme Chagas Cordeiro, D.Sc

_____
Prof[a]. Elisabeth Ermel da Costa Monteiro, D.Sc

_____
Prof[a]. Maria Luisa Aleixo Gonçalves, D.Sc

_____
Prof. Valter José Fernandes Junior, D.Sc

RIO DE JANEIRO, RJ – BRASIL
FEVEREIRO DE 2014

Neves Junior, Alex

Captura de CO_2 em Materiais Cimentícios através da Carbonatação Acelerada / Alex Neves Junior – Rio de Janeiro: UFRJ/COPPE, 2014.

XI, 179 p.: il.; 29,7cm.

Orientadores: Romildo Dias Toledo Filho

Jo Dweck

Eduardo de Moraes Rego Fairbairn

Tese (doutorado) – UFRJ/COPPE/Programa de Engenharia Civil, 2014

Referências Bibliográficas: p.31-36.

1. Captura de CO_2 em pastas cimentícias. 2. Carbonatação acelerada. 3. Cimento de Alta Resistência Inicial Resistente à Sulfatos. 4. Análise térmica. 5. Propriedades mecânicas 6. Porosidade 7. Propriedades microestruturais. 8. Compósitos cimentícios. I. Toledo Filho, Romildo Dias et al. II Universidade Federal do Rio de Janeiro, COPPE, Programa de Engenharia Civil. III. Título.

Agradecimentos

A minha gratidão é toda primeiramente à Deus, pois como aconteceu até essa etapa e com certeza em todas as próximas que virão, Ele estará ao meu lado nos desafios que se apresentarão na minha vida. Sem Ele não terminaria esse doutorado.

Agradeço à minha família, na figura dos meus pais Alex Neves, Maria de Lourdes Turbino Neves, meus irmãos Ricardo Turbino Neves, Karol Turbino, Aline Turbino Neves e Mario Junior que me apoiaram em todos os momentos e foram o combustível extra nesta jornada, o amor dispensado por vocês foi fundamental.

De forma especial a Luciana, minha noiva, que viveu comigo cada momento deste desafio, me ajudou com as correções gramaticais e soube entender e me fortalecer para conclusão desta tese. Obrigado amor.

Agradeço ao professor Romildo Dias Toledo Filho por ter me aceitado no programa de doutorado, ter acreditado em mim e depositado confiança na minha capacidade de realizar um trabalho com um tema tão atual e relevante, mesmo sabendo de todas as atividades paralelas que desenvolvia e as viagens que realizava durante este doutorado ao conduzi-lo com a docência.

Ao professor Eduardo, pelo ajuda na correção dos artigos.

Agradeço aos amigos Leandro Neves Duarte, Danilo Hiroshi Konda e Paulo Borges, por entenderem o desafio do doutorado desde o início e me ajudarem a cumprí-lo mesmo com as atividades de docência na UFMT.

Agradeço a todos os colegas que fiz ao longo destes quatro anos de doutorado, mas principalmente, ao Ederli pela amizade e adaptação na mudança para o Rio de Janeiro, Marco Antônio pela amizade e conselhos no ambiente de trabalho, Camila pela força e ajuda no entendimento de vários ensaios, Saulo pela ajuda na confecção dos compósitos, Carlos Rosigali pela amizade e pelos cafezinhos na copa, Maria Rita pela amizade no ambiente de trabalho, Mariana pelo auxílio nos ensaios de NCDTA, Marcelo Viana pelas análises térmicas realizadas na USP.

A todos os técnicos laboratoriais e administrativos, cito, a Luzidelle, Sandra e Paulinho pelo apoio na parte administrativa, Rosângela pela paciência no auxílio das análises

térmicas, Adailton e Clodoaldo pela amizade no ambiente de trabalho, Ivan por auxiliar na confecção dos blocos, Flávio Sarquis e Santiago pela instrumentação das amostras, Arnaldo e Manuel pelo apoio na oficina e pelas conversas de futebol, Rogério, Flávio Silva e Eduardo, pelo apoio nos ensaios, Renan e Rodrigo na obtenção dos ensaios mecânicos, Philipe pela ajuda na caraterização dos materiais, Alessandro e Júlio pelo preparo dos corpos de prova, Emanuel pelos ensaios de nanoindentação, Profª Rosane pelos ensaios de RMN, Antonieta pelos ensaios de MEV, Guilherme Cordeiro pelos ensaios de DRX e ao Prof Frank Cartledge, que mesmo sem conhecer pessoalmente, deixou a sua contribuição auxiliando na interpretação dos resultados de RMN.

Em especial, separo um parágrafo para demostrar a minha gratidão ao professor Jo Dweck, que não foi apenas um orientador, mas um pai, um inspirador e um amigo que fiz neste doutorado. Ajudou-me a crescer não só como acadêmico, mas principalmente como homem. Com seu estímulo e desafios quebrei barreiras pessoais, as quais não imaginava poder transpor, e por acreditar em minha capacidade, não só cresci culturalmente, mas profissionalmente apresentando trabalhos em congressos de relevância internacionais em Portugal, Japão e Grécia. Obrigado professor Jo por tudo, pois este doutorado não teria sido concluído sem a sua intensa participação em todos os seus detalhes e etapas.

Essa pesquisa foi financiada pelo CNPq durante o período de 07/2009 a 07/2013.

“Alguém que nunca cometeu erros nunca tratou de fazer algo novo.”

Albert Einstein

Resumo da Tese apresentada à COPPE/UFRJ com parte dos requisitos necessários para a obtenção do grau de Doutor em Ciências (D.Sc)

CAPTURA DE CO_2 EM MATERIAIS CIMENTICIOS ATRAVÉS DE CARBONATAÇÃO ACELERADA

Alex Neves Junior

Fevereiro/2014

Orientadores: Romildo Dias Toledo Filho

Jo Dweck

Eduardo de Moraes Rego Fairbairn

Programa: Engenharia Civil

A presente Tese teve por objetivo estudar a captura de gás carbônico (CO_2) em materiais à base de cimento Portland de Alta Resistência Inicial e Resistente a Sulfatos (ARI-RS), principalmente por reação daquele gás com hidróxido de cálcio ($Ca(OH)_2$), formando carbonato de cálcio ($CaCO_3$). Após analisar a formação do $Ca(OH)_2$ nas primeiras idades por termogravimetria (TG), as melhores condições de captura de CO_2 foram definidas em corpos de prova retangulares, em uma câmara climática de carbonatação acelerada com controles de temperatura e umidade relativa, sendo quantificada em base à massa inicial de cimento por TG. O desenvolvimento de dois protótipos, um de análise térmica diferencial e outro de termogravimetria, ambos não convencionais, permitiu acompanhar e analisar o processo de carbonatação em tempo real e em larga escala. Diversos ensaios e análises instrumentais mostraram que 1h de carbonatação é o tempo mais indicado para aumentar a resistência mecânica em relação à medida sem carbonatação.

Abstract of Thesis presented to COPPE/UFRJ as a partial fulfillment of the requirements for the degree of Doctor of Science (D.Sc)

CO_2 CAPTURE IN CEMENTITIOUS MATERIALS THROUGH ACCELERATED CARBONATION

Alex Neves Junior

Fevereiro/2014

Advisors: Romildo Dias Toledo Filho

Jo Dweck

Eduardo de Moraes Rego Fairbairn

Department: Civil Engineering

This thesis aimed to study the capture of carbon dioxide (CO_2) by cementitious in materials based on High Initial Strength Sulfate Resistant Portland cement (HS SR PC), mainly by reaction of that gas with calcium hydroxide ($Ca(OH)_2$), forming calcium carbonate ($CaCO_3$). After analyzing the formation of $Ca(OH)_2$ at the early stages by thermogravimetry (TG), the best conditions of CO_2 capture were defined in rectangular specimens, in a climatic chamber of accelerated carbonation, with temperature and relative humidity controls, being quantified on initial cement mass basis by TG. The development of two prototypes, one of differential thermal analysis and other of thermogravimetry, both non-conventionals, allowed monitoring and analyzing the carbonation process in real time and in large scale. Several experiments and instrumental analysis showed that 1h of carbonation is the most appropriate time to increase the mechanical strength as compared with no carbonation.

Sumário

Lista de Figuras

.

Lista de Tabelas

Capítulo 1.

Introdução

É de conhecimento geral que as mudanças climáticas globais têm alterado conceitos referentes à exploração dos recursos naturais e do desenvolvimento humano. A busca pela sustentabilidade tem-se incorporado de uma maneira mais substancial como alvo estratégico da cadeia produtiva humana em todos os seus aspectos, e a engenharia civil, no âmbito dessas mudanças, tem acompanhado de forma intensa essa filosofia. Há uma preocupação de instituições governamentais, centros de pesquisa e organizações não governamentais com a adoção de tecnologias que minimizem os efeitos causados por essas mudanças e contribuam no melhoramento da qualidade de vida da humanidade.

Estudos científicos [1] recentes estimam um aumento entre 0,3 – 6°C na temperatura média da Terra até o final de 2100. Segundo vários cientistas do *IPCC* (Painel Intergovernamental sobre Mudanças Climáticas), o aquecimento global seria causado pelo excesso dos chamados *gases do efeito estufa*, lançados pelas atividades humanas na atmosfera desde 1750 e que agora, ultrapassam consideravelmente os valores pré-industriais.

Entre os principais gases responsáveis pelo aquecimento global, se encontra o dióxido de carbono (CO_2), cujas emissões globais provenientes das atividades humanas ultrapassaram os 32 bilhões de toneladas em 2011 [2]. Cerca de metade das emissões é absorvida pelas florestas e/ou armazenadas em reservatórios submersos nos oceanos, porém a outra metade se acumula na própria atmosfera. Estima-se que as emissões de CO_2 totalizem 1750 giga toneladas até 2050, superando o limite estabelecido de 1000 giga toneladas estipulado pela comunidade científica, para que temperatura do planeta até o final do século não ultrapasse os 2°C [1].

A indústria cimenteira colabora com uma parcela de 5 a 8% das emissões globais de CO_2, entre o consumo de energia gerado durante o seu transporte e as etapas envolvidas durante o processo produtivo até a obtenção do *clinquer* [3]. De acordo com HABERT et al. [4], analisando todo o ciclo de produção do cimento, cerca de 95% do CO_2 é liberado durante a produção e apenas 5% no transporte do material e nos produtos derivados. Considerando que a produção global de cimento é de 3,5 bilhões de toneladas anuais e estimando que o mesmo alcance 5,5 bilhões anuais até 2050, só a indústria cimenteira poderá ser responsável por 30% do total das emissões mundiais de CO_2 [3].

A produção do *clinquer* envolve a calcinação (queima) do calcário ($CaCO_3$) para a obtenção do óxido de cálcio, representada pela reação abaixo:

$$CaCO_3 \longrightarrow CaO + CO_2$$

Considerando que o calcário, o óxido de cálcio e o CO_2 têm pesos molares respectivamente iguais a 100, 56 e 44, significa que quando 100 kg de calcário se transformam em óxido de cálcio, 56% se transformará realmente em óxido de cálcio, enquanto que 44% serão emitidas na forma de CO_2. Considerando que o *clinquer* é composto por aproximadamente 65% de óxido de cálcio [5] e o restante por óxido de silício e outros óxidos metálicos, a produção de 100 kg de *clinquer* corresponde à emissão de aproximadamente 51kg de CO_2.

Com esses dados, a partir das metas de emissão de poluentes estabelecidas pelo *IPCC*, um dos maiores desafios principalmente para a indústria cimenteira, é o de incorporar planos de ação que minimizem os impactos gerados por sua cadeia produtiva. Entre as soluções reconhecidas podemos citar a substituição parcial do *clínquer* por produtos e subprodutos industriais pozolânicos contendo sílica e/ou alumina ou pozolanas naturais [6], uso de outras matérias-primas como fontes de óxido de cálcio, entre elas a escória com a vantagem da não emissão de CO_2, redução do volume de concreto empregado a partir do aumento do seu desempenho mecânico, principalmente com os avanços da nanotecnologia [7] e mudanças na cadeia produtiva com o uso de fontes alternativas de combustíveis que minimizem a quantidade de CO_2 gerado e aumentem a eficiência energética do processo, gerando, por exemplo, créditos de carbono [8-11].

Com o crescimento dos mercados de créditos de carbono, tem crescido também o emprego do termo "Sequestro de Carbono", nome que é dado às técnicas adotadas na captura do CO_2 da atmosfera. A forma mais comum de se "sequestrar" o carbono é a que naturalmente é realizada pelas florestas através da fotossíntese, porém podemos ainda citar como alternativas aplicáveis, a injeção do CO_2 em reservatórios geológicos e poços de petróleo depletados [12], os processos químicos de carbonatação mineral em meio aquoso a altas temperaturas e pressões [13] e a reincorporação do CO_2 emitido pelas cimenteiras no próprio cimento produzido [14] [15].

Em relação à opção supracitada de reincorporação do CO_2 emitido pela indústria cimenteira, uma solução viável que envolve diretamente o próprio cimento Portland e que é proposta neste trabalho, é a captura através da carbonatação de materiais cimentícios durante o seu processo produtivo, onde o CO_2 é fixado na matriz cimentícia na forma de $CaCO_3$ [16] [17] [18] [19] [20] [21].

Por outro lado, apesar do potencial ecológico, a reação de carbonatação em materiais cimentícios como argamassas e concretos é reconhecidamente um fenômeno deletério, que pode comprometer a durabilidade do material, podendo ocasionar o fissuração por retração química da matriz [22] [23] e/ou depassivação das armaduras no caso de estruturas de concreto armado [24].

Os objetivos da presente pesquisa são:

- Analisar o processo de formação dos principais produtos hidratados em pastas de cimento Portland ARI-RS nos estágios iniciais de sua hidratação, em função do relação água-cimento utilizado, visando principalmente o hidróxido de cálcio para posterior uso na captura de CO_2.
- Determinar as condições operacionais ótimas para se maximizar a captura de CO_2 em pastas de cimento Portland ARI-RS nas poucas idades, através das reações de carbonatação, bem como estimar a quantidade de CO_2 capturado nessas matrizes.
- Caracterizar mecânica e micro estruturalmente pastas carbonatadas nas condições ótimas de captura anteriormente estabelecidas.
- Estudar o comportamento mecânico à flexão e a durabilidade à ciclos de molhagem e secagem de duas matrizes: 1) de cimento Portland e 2) cal hidratada

com pozolanas, ambas reforçadas com fibras longas de sisal e tratadas com CO_2 à poucas idades.

Os resultados dos experimentos desenvolvidos na presente Tese foram escritos na forma de artigos, que constam como anexos, dos quais alguns já foram publicados em jornais internacionais indexados e outros estão em revisão para posterior submissão a outros jornais científicos do setor. Cada artigo trata de uma etapa da pesquisa, como apresentado a seguir:

Artigo A: Estudo por termogravimetria da influência da relação água/cimento (a/c) de pastas de cimento Portland ARI-RS, na formação dos produtos de hidratação (carbonatáveis) nas primeiras 24h de cura.

Artigo B: Estudo da hidratação de pastas de cimento Portland ARI-RS com elevada relação água x cimento nas primeiras 24h com o uso da termogravimetria (TG) e de análise térmica diferencial não convencional (sigla NCDTA em inglês) e a sua relação com ensaio de penetração por Vicat.

Artigo C: Determinação por termogravimetria das condições ótimas de captura de CO_2 em pastas de cimento Portland ARI-RS em câmara controlada através da carbonatação acelerada.

Artigo D: Estudo por termogravimetria da influência do tempo de exposição ao CO_2 e o comportamento mecânico das pastas de cimento Portland ARI-RS, nas condições ótimas de captura estabelecidas.

Artigo E: Estudo da carbonatação de pastas de cimento Portland ARI-RS nas primeiras idades de cura por novos sistemas DTA e termogravimetria não convencionais, desenvolvidos para uso em maior escala de processamento.

Artigo F: Caracterização mecânica e morfológica de pastas de cimento Portland ARI-RS obtidas em condições de captura de CO_2 estabelecidas.

Artigo G: Caracterização microestrutural de pastas de cimento Portland ARI-RS obtidas em condições de captura de CO_2 estabelecidas.

Artigo H: Estudo do comportamento mecânico e da durabilidade de compósitos cimentícios reforçados com fibras longas de sisal submetidas à carbonatação acelerada.

A estrutura da Tese é composta, além do presente capítulo introdutório, de uma revisão bibliográfica, metodologia/resultados e conclusões.

O capítulo sobre revisão bibliográfica inicia-se apresentando as características principais da reação de carbonatação e os fatores que influenciam a cinética da reação. O texto continua relatando o reconhecido efeito deletério da carbonatação nas estruturas de concreto armado e o efeito da fissuração causada pela retração por carbonatação e segue, por outro lado, expondo uma visão geral das pesquisas encontradas na literatura que tratam do benefício ambiental do uso da reação de carbonatação como mecanismo de fixação do CO_2 em materiais cimentícios como pastas, argamassas e concretos, bem como do uso da carbonatação em compósitos cimentícios reforçados com fibras vegetais para aumento da durabilidade. A lacuna do conhecimento é apresentada mostrando a importância da pesquisa. O capítulo sobre metodologia e resultados resume as metodologias utilizadas para se atingir os objetivos da presente Tese.

Uma conclusão geral apresentando os resultados mais relevantes do trabalho é feita no último capítulo.

Em cada um dos artigos que compõem os anexos da Tese, em que são apresentados e discutidos resultados dos experimentos realizados, encontram-se revisões bibliográficas assim como conclusões específicas dos respectivos assuntos.

Capítulo 2

Revisão Bibliográfica

A carbonatação é uma reação química em que os produtos de hidratação alcalinos do cimento, sendo o hidróxido de cálcio ($Ca(OH)_2$) o principal deles, reagem com CO_2 em um processo de dissolução/precipitação, gerando produtos a base de carbonato e gel de sílica.

A reação principal de carbonatação entre o $Ca(OH)_2$ e o CO_2 é apresentada na forma simplificada abaixo:

$$Ca(OH)_2 + CO_2 \xrightarrow{H_2O} CaCO_3 + H_2O$$

Como nas reações de hidratação, a carbonatação é de natureza exotérmica, o calor gerado acelera o processo de cura do meio reacional em relação ao procedimento convencional de cura úmida [21][25]. Durante a carbonatação, a água não é consumida durante a reação, mas necessária para desencadeá-la, sendo a quantidade presente nos poros preponderante na velocidade da reação [26]. A ausência de umidade inibe a reação, porém a saturação dos poros reduz a velocidade de difusão do gás [27].

A taxa de reação de carbonatação é também regulada pelas condições durante o tratamento. Ambientes com elevada pressão e concentração de CO_2 (tratamento supercrítico) aumentam a velocidade de difusão e por consequência a taxa de carbonatação [25][28][29]. A temperatura ambiente influencia a velocidade da reação, sendo proporcional ao aumento da temperatura [30]. Aumentos de 10°C podem dobrar a taxa de reação [31]. Os níveis de carbonatação são também regulados pela umidade relativa do ambiente de exposição. Mudanças na umidade relativa do ambiente alteram o teor de umidade dos poros e do material como um todo e, por consequência, a

velocidade de difusão do CO_2 para o interior da matriz. Estudos apontam como condições ótimas para carbonatação umidades relativas entre 50 e 70% [31-33].

A composição química do cimento Portland utilizado é outro fator que influencia a reação de carbonatação, pois cimentos com adições minerais, apesar de propiciarem o refinamento dos poros da matriz diminuindo a sua porosidade e dificultando a difusão do CO_2, na realidade podem acelerar a frente de carbonatação, ao preponderar o efeito da reserva alcalina segundo STUMPP et al. [28]. De acordo com NUNES et al.[34] o teor remanescente de $Ca(OH)_2$ (reserva alcalina) é um dos fatores que pode restringir a difusão do CO_2 para o interior da matriz, pois o progresso da carbonatação apenas será possível após o consumo total do $Ca(OH)_2$ na zona de interface para formação de $CaCO_3$.

Além da contribuição do CH [$Ca(OH)_2$], , as fases de silicatos de cálcio hidratados (C-S-H) sofrem modificações estruturais devido à reação de carbonatação, porém de forma mais lenta da que ocorre com o primeiro [35]. A reação de carbonatação ao consumir os íons Ca^+, oriundos do $Ca(OH)_2$ e presentes na solução dos poros, induz por equilíbrio químico a uma compensação através da liberação de Ca^+ do C-S-H através da queda do pH. Este processo altera a relação Ca/Si do C-S-H modificando a sua composição e transformando o C-S-H em um gel de sílica [27].

A reação de carbonatação que envolve o C-S-H, pode ser vista pela equação abaixo [36]:

$$3CaO.2SiO_2.3H_2O + 3CO_2 \rightarrow 3CaCO_3.2SiO_2.3H_2O$$

Desta forma, misturas de materiais cimentícios com pozolanas, devido a maior formação de C-S-H e consequente aumento da disponibilidade de Ca^+ na composição da matriz, contribuem para o aumento das fases carbonatadas e da frente de carbonatação [28][37].

Por outro lado, a reação de carbonatação tem sido um assunto exaustivamente explorado na engenharia civil do ponto de vista da durabilidade, principalmente em função do conhecido efeito deletério gerado nas estruturas de concreto armado. Neste caso o CO_2, ao longo do tempo, age na interface concreto/armadura em um processo químico que ao reduzir o *pH* da matriz cimentícia, elimina a película protetora de óxido de ferro que

reveste a armadura, ocasionando a despassivação da mesma, o que acelera a sua corrosão comprometendo o seu funcionamento estrutural [38-39].

Outro efeito nocivo causado pela reação de carbonatação que compromete a durabilidade e precisa ser explorado, é a fissuração que ocorre por uma retração diferencial entre a superfície e o interior do material cimentício carbonatado, chamada de retração por carbonatação, que tem origem durante o processo de secagem [40][30]. Nestes casos a fissuração é explicada pela sobreposição de vários fenômenos: formação de cristais de $CaCO_3$ com estruturas e dimensões moleculares distintas (aragonita, calcita e vaterita), reorganização da microestrutura, forças de capilaridade entre outras, que somadas, contribuem para o aumento das fissuras superficiais e aceleram a taxa de carbonatação [23][41][42].

Por outro lado, embora se deva evitar a carbonatação excessiva, a literatura tem mostrado que respeitando determinadas condições impostas e considerando algumas aplicações, o tratamento de materiais cimentícios com CO_2 pode trazer benefícios ao material do ponto de vista mecânico e de durabilidade, a partir da redução da porosidade da matriz pela precipitação dos cristais de $CaCO_3$ nos poros [43-46].

Estudos de BUKOWSKI et al. [47], usando argamassas na proporção aglomerante/areia 1:1 e proporção água/aglomerante 0,191, com as amostras submetidas a dois tipos de fluxos de CO_2 (estático e dinâmico), após a compactação do material em pequenos cilindros, apresentaram resultados de resistência à compressão satisfatória.

Em outro estudo, WAGH et al.[48] analisaram argamassas de cimento com areia de sílica, com a proporção de cimento variando de 100 a 30%, comprimidas em moldes cilíndricos, onde se verificou que as amostras carbonatadas alcançaram a resistência equivalente aos 28 dias com apenas algumas horas.

TERAMURA et al. [49] ao ensaiarem corpos de prova de argamassas com 100 x 100 x 12mm, utilizando CO_2 na concentração de 100% e pressão atmosférica de 0,4 MPa, verificaram que, além da resistência à flexão aumentar linearmente com o grau de carbonatação, a maior resistência à flexão atingida foi de 4,8MPa e que a relação água/cimento ótima para eficiência da reação foi de 0,5.

ROSTAMI et al. [18] estudando pastas submetidas à carbonatação acelerada durante 2h após 18h de hidratação, constataram um aumento da resistência mecânica em 61% em

relação às referências, explicadas pela formação de cristais de $CaCO_3$ junto ao C-S-H (silicato de cálcio hidrocarbonatado).

Estudos de ZORNOZA et al.[50], revelaram que a aplicação da carbonatação acelerada em pastas com catalisadores de craqueamento catalítico (FC3R), além de reduzir a alcalinidade das matrizes, permitiram aumentar a quantidade de produtos como silicoaluminatos de cálcio hidratados, melhorando a resistência.

Ao mesmo tempo em que é possível melhorar as propriedades do material, a reação de carbonatação pode ser aproveitada como alternativa ambiental para o sequestro do CO_2 liberado pela indústria cimenteira durante sua produção, a partir do seu reaproveitamento, por exemplo, em cadeias produtivas de blocos ou peças pré-moldadas de concreto instaladas próximas das próprias unidades fabris, gerando créditos de carbono, em um processo químico inverso onde o CO_2 é fixado (capturado) no material produzido na forma de $CaCO_3$ ou outra [17][19][21][25][51] como mostram as etapas do processo de forma esquemática abaixo:

$$Calcário + argila \rightarrow \quad clinquer + \overset{\nearrow}{CO_2} + \overset{\nearrow}{H_2O}$$

$$Clinquer + aditivos \rightarrow Cimento$$

$$Cimento + CO_2\ Recuperado + Agregados + H_2O \rightarrow Concreto + CaCO_3$$

Segundo SHAO et al.[17], considerando a produção mundial, a captura de CO_2 através da carbonatação de materiais cimentícios durante a sua produção, apresenta um potencial líquido de sequestro entre 0,98 à 1,8 milhão de toneladas de CO_2 anuais com uma eficiência entre 84% e 87,1% no processo.

Na Tabela 1, SHAO et al.[17] comparam os níveis de captura de diversos materiais de construção cimentícios com o potencial global, considerando a produção anual dos respectivos materiais.

Tabela 1: Potencial Anual de Sequestro de CO_2 em Produtos de Concreto feitos nos E.U.A e Canadá (SHAO et al. [17])

	Blocos de concreto	*Paver*	Placas	Placa fibrosa
Produção anual	4.300.000.000 unidades	74.000.000 m²	75.000.000 m²	910.000.000 m²
Cimento usado no produto (Mt)	5,9	2,6	0,595	4,8
Captura de CO2, %	9,80%	9,80%	12,20%	19%
Potencial de sequestro do CO2 recuperado (Mt)	0,578	0,255	0,073	0,907
Resistência com duas horas de carbonatação (MPa)	10,3±0,6	10,3±0,6	7,8±0,2	10,5±1,2
Resistência aos 28 dias (MPa)	20,5±0,9	20,5±0,9	7,8±0,5	11,7±0,5

Os resultados apresentados comprovam que produtos a base de cimento Portland, como blocos e placas que não utilizam reforço de aço, são candidatos ideais para se fixar o CO_2 durante a sua fabricação, alcançando níveis de resistência satisfatórios com poucas horas de tratamento em relação à cura convencional aos 28 dias e reaproveitando ao mesmo tempo o CO_2 emitido durante o processo produtivo. SHAO et al. [17] destacam que neste processo, o suprimento contínuo de CO_2 é tecnicamente viável e eficaz para implementação em escala industrial, por garantir a manutenção das condições de pressão e concentração de gás, ideais para o ambiente de cura proposto.

Em um processo que induz a captura através da formação do $CaCO_3$ no cimento, PATHI et al.[52], mostram também a viabilidade de se capturar CO_2 incorporando o $CaCO_3$ na "farinha" obtida pelo processo de produção do cimento como adsorvente, através de ciclos de carbonatação.

A substituição parcial de cimento por pozolanas artificiais ou naturais tem permitido reforçar com fibras vegetais materiais cimentícios, ao reduzir a elevada alcalinidade das matrizes responsáveis pela mineralização das fibras [53][54]. Além da oportunidade de captura de CO_2, a redução do $Ca(OH)_2$ pela carbonatação constitui outra aplicação

interessante para o aumento da durabilidade e resistência mecânica destes materiais [21][55][56].

TOLEDO FILHO et al.[57], trataram com CO_2 em câmara controlada com temperatura de 26,5°C, umidade relativa de 60% e concentração de CO2 em 9,8%, compósitos reforçados com fibras de coco e sisal, após 24h de cura, verificando uma melhora na durabilidade do compósito após 109 dias de exposição.

JONH et al.[58], estudando envelhecimento de painéis fabricados com argamassa contendo escória de alto forno, cal e gesso reforçadas com fibras de coco, verificaram que a ação do CO_2 após 12 anos de exposição natural preservou as fibras.

Recentemente, ALMEIDA et al.[59] testaram com 28 dias e após 200 e 400 ciclos de envelhecimento acelerado, compósitos reforçados com polpas de eucalipto submetidos à carbonatação acelerada após 2 dias de cura convencional e verificaram melhora nas propriedades mecânicas do material, através da redução da porosidade, aumento da densidade e adesão da interface fibra-matriz.

TONOLI et al.[60] carbonatando telhas reforçadas com fibras de sisal durante 7 dias, alcançaram um aumento da carga máxima de flexão em 25% e melhoraram a tenacidade em 80% em relação às referências não carbonatadas.

QI et al.[61], carbonatando compósitos reforçados com fibras de madeira de média densidade (sigla MDF em inglês), durante 3-5min, melhoraram o desempenho mecânico em 50-70% em relação aos curados convencionalmente, alcançando 22-27% do grau de carbonatação total.

Ainda mais atraente do ponto de vista ambiental é a carbonatação de compósitos à base de cal e livres de cimento, reforçados com fibras vegetais. Nestes casos, a atividade pozolânica compete com a reação de carbonatação no consumo de $Ca(OH)_2$ [62-66]. Apesar do potencial de serem totalmente carbonatadas, FAHARI et al.[64], recomenda que os compósitos de cal apresentem cimento Portland em sua composição para melhorar a sua resistência mecânica.

Outra alternativa de captura de CO_2 é a que ocorre através do uso do resíduo de concreto demolido (RCD), tendo em vista as grandes áreas superficiais não carbonatadas envolvidas nesses materiais, como aponta estudos de LAGERBLAD et al

[27], porém, neste caso, a captura ocorre pelo fenômeno da "adsorção" superficial do CO_2 [67][35] .

Estudando a eficiência de captura de CO_2 em materiais absorventes à base de cal com resíduos de concreto demolido, MOGHTADERI et al.[68] verificou uma eficiência no processo de captura maior que 56,4%, obtendo materiais com elevada resistência mecânica e durabilidade com baixo custo.

A imobilização de resíduos tóxicos através da reação de carbonatação usando cimento Portland como aglomerante é outra estratégia que apresenta grandes vantagens ambientais [69]. Estudos conduzidos por LANGE et al.[70], mostraram que a carbonatação, além de acelerar as reações de hidratação, gerou materiais com elevada resistência mecânica e reduzida lixiviação, tornando-o interessante para descarte no solo e outras aplicações menos nobres.

Em outro estudo, BORGES et al.[71], comparando a carbonatação natural e acelerada de pastas contendo escória de alto forno para o encapsulamento de resíduos nucleares, mostraram uma correlação satisfatória entre ambos os tratamentos, com a reação de carbonatação sendo governada pela quantidade de $Ca(OH)_2$ disponível antes do processo.

Além da viabilidade demostrada de se capturar o CO_2 durante o processo produtivo de materiais cimentícios, existe ainda o aspecto econômico a se considerar ao se medir a quantidade do CO_2 efetivamente absorvido, em vista dos créditos de carbono que podem ser obtidos com a implementação deste processo. Entre as estratégias de medição da quantidade de CO_2 capturado por materiais cimentícios, temos a que é realizada através do monitoramento de massa, pois a reação de carbonatação, ao envolver a formação de novos produtos na matriz, além de influenciar os existentes, modifica a porosidade e altera também a densidade do material obtido.

Neste sentido, com a ajuda de uma câmara de carbonatação acelerada conforme Figura 1, vários autores estudaram os efeitos do CO_2 em pastas, argamassas e concretos [16-19].

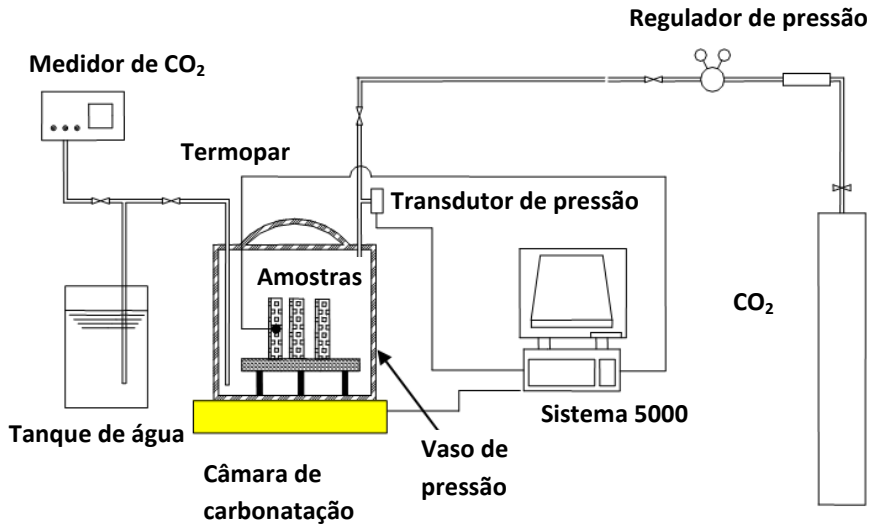

Figura 1: Configuração experimental de uma câmara de carbonatação (SHAO et al. [21])

Nestes experimentos, a quantidade de CO_2 absorvida pôde ser estimada através do ganho de massa dado pela equação 1 que considera a massa da amostra antes e após a carbonatação, incluindo a massa de água perdida durante a reação e a massa inicial de cimento Portland da mistura.

Deste modo:

$$G.deMassa(\%) = \frac{(Massa)_{antes,CO2} - (Massa)_{depois,CO2} + (Massa)_{P.de.Água}}{(Massa)_{S.do.Aglomerante}} \quad (1)$$

Onde:

$(Massa)_{antes,CO2}$ – Massa da amostra antes da carbonatação.

$(Massa)_{depois,CO2}$ – Massa da amostra depois da carbonatação.

$(Massa)_{P.de.Água}$ – Massa de perda de água.

$(Massa)_{S.do.Aglomerante}$ – Massa inicial do aglomerante.

A partir da equação 1, SHAO et al. [21], avaliando o comportamento do CO_2 em pastas confeccionadas com cimento, cinza volante e cal nas primeiras idades, alcançaram níveis de captura da ordem de 12,6% usando cimento; 11,3% usando cinzas e 23,8%

usando a cal. Verificaram ainda que a captura de 12,6% de CO_2 em relação à massa de cimento representa apenas 25% da eficiência da carbonatação, podendo ser potencialmente ampliada.

Além disso, SHAO et al.[21], estudando a captura de CO_2 em concretos nas primeiras idades, constataram a capacidade de captura superior a 16% de CO_2 em um período de exposição de 2h, sob pressão de 0,5MPa, adquirindo uma resistência maior do que as amostras curadas convencionalmente em menor tempo.

Resultados obtidos por YE [25] carbonatando materiais cimentícios em câmara controlada durante 2 horas, usando pressão de injeção de CO_2 de 5 bar e concentração de CO_2 em torno de 100%, alcançaram resistências à compressão superiores a 40 MPa e módulos de ruptura superiores a 6 MPa, com níveis de absorção em torno de 7 a 8%.

Outro método adotado para avaliação da quantidade de CO_2 capturado é através do método da curva de massa e variação de pressão de CO_2. Estas curvas são obtidas com a câmara de carbonatação posicionada sobre uma balança eletrônica, registrando o ganho de massa *in situ* das amostras com a ajuda de sensores de pressão de injeção de gás no sistema, em função do tempo durante todo o processo de tratamento. O ganho de massa e a variação de pressão começam a ser monitorados a partir do momento em que o CO_2 é injetado na câmara, constituindo-se parâmetros indicadores de captura.

Usando esta metodologia, SHAO et al.[17] verificaram a capacidade de captura de CO_2 de quatro materiais típicos da construção de acordo com a Figura 2, constatando que embora a pressão de carbonatação se mantivesse próxima, as temperaturas máximas entre os produtos foram bastante diferentes entre si.

Os mesmos autores, avaliando a curva de massa referente à captura de CO_2 de cada um dos produtos analisados mostrados na Figura 3, verificaram que, embora os elevados picos de temperatura indiquem uma elevada taxa de carbonatação, não indicaram necessariamente uma maior taxa de absorção.

Pelos resultados, SHAO et al.[17] perceberam que a pasta, embora apresentasse maior liberação de calor, a sua capacidade de absorção de CO_2 era inferior ao do compósito. As curvas de massa também mostraram claramente que a maior parte da reação, na maioria dos produtos, ocorria nos primeiros 30 minutos, no caso dos compósitos durando um pouco mais, o que poderia justificar a maior captura de CO_2 nos mesmos.

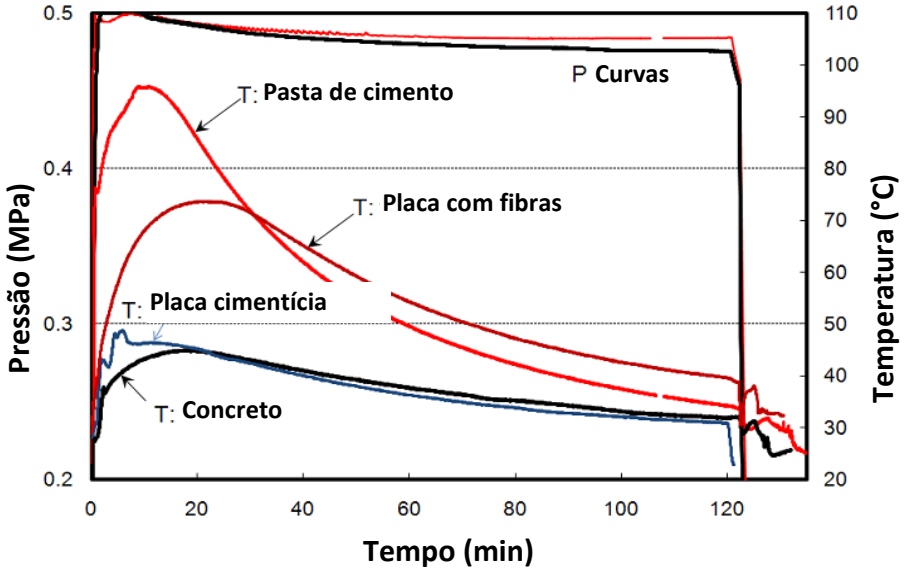

Figura 2: Curvas de Temperatura e Pressão para Diferentes Produtos Pré-Fabricados (SHAO *et al.*[17])

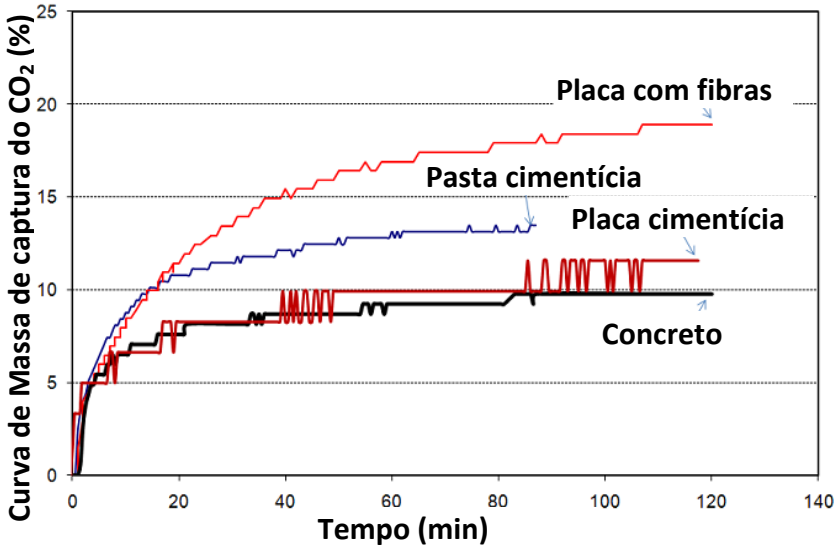

Figura 3: Curvas de Massa para Diferentes Produtos Pré-Fabricados Submetidos à Cura com Carbonatação (SHAO *et al.*[17])

Segundo SHAO et al.[16], a estimativa do CO_2 capturado pode ser efetuada também através da composição química do cimento Portland usado, conforme equação 2 abaixo:

$$CO_2(\%) = 0{,}785(CaO - 0{,}7SO_3) + 1{,}09MgO + 1{,}42Na_2O + 0{,}935K_2O \quad (2)$$

SHAO et al.[16], em um estudo com blocos de concreto tratados com CO_2, usando a equação 2, constataram uma capacidade de absorção de CO_2 de 10% em relação à

quantidade inicial de cimento, mostrando que em escala industrial o processo pode representar mais de 6000 ton de CO_2 capturado.

Apesar de maiores tempos de tratamento promoverem uma maior absorção de CO_2, SHAO et al.[21], alertam para um limite de duração da reação de carbonatação, a partir do qual o ganho de massa começa a decrescer devido à densificação das camadas e a própria perda de umidade durante a reação.

Além do monitoramento de massa, a técnicas analíticas como a termogravimetria e termogravimetria derivativa (TG/DTG), podem ser ferramentas interessantes para auxiliar na determinação da quantidade de CO_2 capturado através da carbonatação, pois as faixas de decomposição correspondentes à desidroxilação do $Ca(OH)_2$ (380-450°C) e a descarbonatação do $CaCO_3$ (500-750°C), estão bem definidas pela literatura [40][73]. Alterações que ocorrem nos silicatos hidratados devido à carbonatação podem ser também constatadas através de modificações nos picos referentes à água total combinada até 380°C [18].

A literatura apresenta estudos de matrizes cimentícias carbonatadas usando-se as técnicas de TG e DTG. KNOPF et al.[74], estudaram matrizes cimentícias carbonatadas em condições de elevada pressão e concentração, analisando a evolução da frente de carbonatação através da diminuição do pico de $Ca(OH)_2$ simultaneamente ao crescimento do pico de $CaCO_3$.

DWECK et al.[75], propuseram um estudo comparativo por termogravimetria, considerando diferentes idades de hidratação de pastas de cimento Portland e $CaCO_3$, mostrando que além da maior eficácia da TG/DTG em relação ao DTA na caracterização dos produtos de hidratação, foi possível identificar fases de $CaCO_3$ menos cristalinas e não aparentes por Difração de Raios X.

Em outro trabalho, VILLAIN et al.[76], mediram por TG/DTG, o grau de carbonatação em concretos contendo agregados calcários, diferenciando os carbonatos oriundos dos agregados e os formados pela reação de carbonatação. Os resultados mostraram que a calcita (forma bem cristalizada do $CaCO_3$) que se decompõe apenas sob elevadas temperaturas, apresenta faixas inferior (650-950°C) e superior (760-950°C) de decomposição, com a decomposição da vaterita resultante da carbonatação do C-S-H

ocorrendo a temperaturas menores do que a calcita e os picos de $CaCO_3$ referentes aos agregados calcários, de difícil diferenciação devido à sobreposição dos mesmos.

Também através da termogravimetria, ROSTAMI et al.[21] estudando pastas cimentícias carbonatadas a poucas idades durante 2h, observaram um potencial de captura de CO_2 de 8% em relação à massa de cimento, correspondendo a um grau de carbonatação de 16%.

Outra tecnologia promissora proposta por CHEN et al.[72], é através do uso de adsorventes a base de cálcio em cimentos ricos em aluminatos com a adição de agentes formadores de poros, que ao proporcionar um aumento da porosidade da matriz, permitem aumentar o potencial de captura nestes materiais.

Além dessas, outras técnicas para avaliação da quantidade de CO_2 são reportados pela literatura como o uso da análise por infravermelho de CO_2, difração de Raios X quantitativa, gamadensimetria e medições da profundidade de carbonatação por fenolftaleína [16] [17][19][21][25].

Embora em níveis menores de absorção devido à baixa concentração de CO_2 no ar atmosférico (~0,03%), é possível também medir a quantidade de CO_2 capturado em concretos de baixa porosidade durante sua vida útil. KJELLSEN et al.[77], utilizando tabelas que correlacionam parâmetros como região de aplicação do concreto, condição de exposição, classe de resistência, cobrimento e adições presentes na mistura como cinza volante, sílica ativa ou calcário, estimaram durante um período de 100 anos de carbonatação, a quantidade de CO_2 capturado por concretos, assumindo uma vida útil de 70 anos para o material em uso na estrutura e um período posterior à demolição de 30 anos. Segundo esses autores, considerando que cerca de 75% do CaO original do cimento é carbonatado, então a quantidade de CO_2 (kg) capturado por m³ de concreto poderia ser estimada multiplicando o resultado da equação 3 pelo volume de concreto considerado.

$$CO_2(Captura) = a = 0{,}75 \times C \times CaO \times \frac{M_{CO2}}{M_{CaO}} (kg/m^3) \qquad (3)$$

Onde:

C - Quantidade de cimento Portland por m^3 de concreto.

CaO - fração de massa de CaO no *clinquer* de cimento, geralmente 65%.

M_{CO2} e M_{CaO} - massas molares do CO_2 e CaO, respectivamente.

Resultados obtidos por de KJELLSEN et al.[77], mostraram que aproximadamente 50% de todo o volume de concreto utilizado na fabricação de blocos estruturais de concreto na Dinamarca podem ser carbonatados no período de vida útil de 70 anos. Usando a mesma metodologia, POMMER et al.[5] mostraram um potencial de captura de CO_2 de até 81% em relação ao volume total de concreto para vigas e de até 72% para telhas de concreto em um período de 100 anos de uso.

Deste modo, a literatura aponta que o sequestro do CO_2 em materiais cimentícios, a partir da reação de carbonatação, pode se dar de duas formas: durante a vida útil do material em um processo mais lento, ou ocorrendo simultaneamente à hidratação de matrizes jovens em ambiente com elevada concentração de CO_2, onde a capacidade de captura tende a ser maior. Porém, apesar da habilidade dos materiais cimentícios em absorver CO_2 através da carbonatação, principalmente nas primeiras idades, não há um consenso na literatura sobre o momento adequado (idade de hidratação) para o início da exposição de matrizes jovens ao CO_2 e as condições ideais para se maximizar a captura.

Esta pesquisa propõe, a partir de um programa experimental com pastas, elucidar estas questões estabelecendo o momento propício para o início da carbonatação acelerada, a partir de um tempo inicial de hidratação em ambiente com temperatura de 25°C e concentração de CO_2 em 20%, assim como as condições referentes à umidade relativa, relação água/cimento e tempo de exposições necessárias para aumentar o potencial de sequestro sem comprometer o desempenho mecânico e a durabilidade do material.

Apesar do uso do evidenciador (fenolftaleína) ser uma das técnicas consagradas utilizadas para se estimar a quantidade de CO_2 capturado em um volume de material cimentício, não há na literatura uma proposta de estudo da frente de carbonatação por termogravimetria que ao mesmo tempo integre os resultados das curvas obtidas nas diferentes profundidades em uma mesma base de comparação, que permita calcular a quantidade de CO_2 fixado para um volume de material cimentício conhecido.

Embora existam diversas aplicações de calorímetros adiabáticos e semi adiabáticos para estudo das reações de hidratação, não existem modelos de sistemas abertos e em

ambientes controlados de temperatura e umidade, que permitam estudar em tempo real a hidratação e outros fenômenos como a carbonatação simultaneamente.

Apesar de a literatura apresentar sistemas de monitoramento de massa em tempo real para cálculo de captura de CO_2, com a câmara de carbonatação sobre a balança, não há estudos de captura apresentados a partir de sistemas com o medidor de massa dentro de um ambiente controlado monitorando o fenômeno em tempo real.

Resumidamente, a presente pesquisa traz uma contribuição para o avanço do conhecimento no assunto em pauta, com investigações relacionadas a:

- Condições ambientais de tratamento e as características das pastas de cimento Portland ARI-RS, para maximização da captura de CO_2 a poucas idades.
- Estimativa da quantidade de CO_2 capturado em pastas, através da integração dos resultados obtidos do perfil de carbonatação por termogravimetria em base à massa inicial de cimento, conhecidos o volume e quantidade inicial de cimento na mistura.
- Monitoramento em tempo real da variação de temperatura e massa de pastas em ambiente controlado de carbonatação acelerada.
- Caracterização mecânica e microestrutural das pastas nas condições ótimas de captura encontradas.
- Estudo da tenacidade, desempenho mecânico à flexão e de durabilidade a ciclos de molhagem e secagem, de duas famílias de compósitos (uma de cimento Portland e outra de cal) reforçadas com fibras longas de sisal e carbonatadas nas condições ótimas de captura encontradas.

Capítulo 3

Metodologia e Resultados

3.1 Estudos Preliminares da Hidratação de Pastas de Cimento Portland de Alta Resistência Inicial Resistente à Sulfatos. (Artigos A e B)

Estudos sobre pastas apresentam uma vantagem pelo número reduzido de variáveis envolvidas em relação aos outros tipos de matrizes. Compreender a influência da relação água/cimento na quantidade de produtos de hidratação formados, na cinética da reação de hidratação e a sua relação com o processo de endurecimento de pastas nas primeiras 24h, é de suma importância no estabelecimento das condições ideais para captura de CO_2 em matrizes cimentícias.

A termogravimetria e a termogravimetria derivativa (TG/DTG) foram técnicas analíticas amplamente exploradas nesta tese para os estudos propostos e portanto as alíquotas extraídas tiveram um cuidado especial desde a sua coleta, preparo e condicionamento.

Nas idades designadas, as alíquotas extraídas dos corpos de prova eram imediatamente colocadas em frascos de vidro contendo acetona, para interrupção da hidratação, onde após secagem eram transferidos para pequenos sacos plásticos e condicionados em dessecador até o momento do ensaio.

Com o intuito de se garantir a precisão dos resultados obtidos e excluir a interferência da água livre presente nas pastas na determinação de água combinada, antes de cada procedimento de análise no aparelho, as amostras eram secas no interior do equipamento a partir de 25 até 35°C à uma taxa de aquecimento de $1°C.min^{-1}$ seguido por uma isoterma de 35°C durante 1h. Posteriormente aplicava-se uma taxa de

aquecimento de 10°C.min^{-1} de 35 a 1000°C, para análise de perdas de massa de água combinada e CO_2 das principais fases presentes.

Os estudos preliminares foram divididos em duas partes.

Na primeira parte da pesquisa, análises térmicas (TG/DTG) de pastas nas relações água/cimento (a/c) 0,35, 0,45 e 0,55 em diferentes idades iniciais de hidratação (1, 8, 14 e 24h), foram realizadas com o intuito de se verificar a influência da relação água/cimento na formação dos produtos de hidratação usando cimento Portland ARI-RS, calculando principalmente a quantidade de $Ca(OH)_2$ produzida nestas idades e estimando também a água total combinada, a água das fases tobermorita + etringuita, da gipsita e dos outros produtos de hidratação formados.

A metodologia de cálculo apresentada nesta pesquisa, de conversão dos resultados em base a massa inicial da amostra (obtidos por "*default"* nos equipamentos de análise térmica) para resultados em base a massa inicial de cimento, possibilitou calcular e comparar os resultados corretamente ao estabelecer para as curvas obtidas, uma base de comparação de mesma composição, além de possibilitar entender melhor que transformações ocorriam com a massa de cimento presente em cada amostra.

Verificou-se que a pasta com relação a/c 0,55 formava mais $Ca(OH)_2$, permitindo concluir que o aumento no teor de água das pastas (maiores relações água/cimento) aumentava a quantidade de produtos de hidratação formados, principalmente do $Ca(OH)_2$ importante para fixação do CO_2.

Na segunda parte, em função dos resultados obtidos na primeira, foi complementado o estudo, onde além das três relações a/c inicialmente propostas, foram escolhidas mais três pastas com elevada relação a/c (0,65, 0,75 e 0,85) com o intuito de se confirmar a tendência de formação de produtos de hidratação com o aumento da relação a/c obtida na primeira parte.

Os equipamentos de análise térmica diferencial (DTA) conhecidos no mercado medem as diferenças de temperatura entre uma referência (inerte) e a amostra, com ambos submetidos a um dispositivo externo de aquecimento ou resfriamento. Neste trabalho, foi desenvolvido um sistema de monitoramento de efeitos térmicos em tempo real, denominado pelos autores de análise térmica diferencial não convencional (NCDTA). Desta forma, ensaios de NCDTA e de penetração por Vicat, foram realizados nas 6

relações a/c (0,35, 0,45, 0,55, 0,65, 0,75 e 0,85) propostas, para se estudar as curvas de hidratação das pastas em tempo real e a sua relação com o processo de endurecimento nas primeiras 24h de reação. Para as relações a/c 0,65, 0,75 e 0,85, foram calculadas, em base à massa inicial de cimento, a quantidade de $Ca(OH)_2$, água total combinada e água da tobermorita + etringita para 4 e 24h de hidratação.

Através dos resultados comparativos entre as curvas de NCDTA e os resultados dos ensaios de penetração por Vicat, foi possível constatar que apesar do aumento no teor de água aumentar o período de indução e retardar a hidratação a partir da relação a/c=0,45, o tempo de início de pega e o grau de hidratação das pastas continuavam a aumentar, mostrando que ocorria um limite na formação dos produtos de hidratação para a relação a/c=0,66, correspondente ao limite de miscibilidade do cimento com água na pasta. Os dados obtidos das curvas TG/DTG em base a massa inicial de cimento, para as relações a/c 0,65, 0,75 e 0,85, confirmaram que para 4 ou 24h de hidratação, a quantidade de $Ca(OH)_2$, água total combinada e água da tobermorita + etringita, além de serem as maiores, eram praticamente iguais, indicando que a água acima do grau de miscibilidade com cimento, que inclusive forma uma fase em separado, não participa do processo de hidratação.

3.2 Definição dos Parâmetros Experimentais de Captura de CO_2 em Pastas de Cimento Portland de Alta Resistência Inicial Resistente à Sulfatos. (Artigos C e D).

Para início dos estudos de carbonatação, foram moldadas pastas nas relações a/c 0,5, 0,6 e 0,7, em formas metálicas retangulares (115 x 115 x 25 mm). As pastas foram tratadas inicialmente em condições de fluxo unidirecional CO_2 durante 8h, em uma câmara climática, desde o início da hidratação, mantendo-se constantes a temperatura em 25°C, a concentração de CO_2 no volume da câmara em 20% e a umidade relativa (UR) em três diferentes condições: 60, 80 e 100%. De cada corpo de prova foram coletadas amostras para análise térmica de 2 regiões distintas (topo e meio) e calculados os respectivos teores de $CaCO_3$ em base à massa inicial de cimento em cada amostra.

O procedimento de coleta das amostras para análise térmica, de cada região estudada, ocorreu com o auxílio de uma furadeira vertical com broca de 3mm, com a limpeza da broca e o resfriamento da mesma entre cada etapa de coleta. As amostras em pó

extraídas do corpo de prova tiveram a hidratação interrompida com acetona como descrito anteriormente nas idades desejadas até as análises. A massa média das alíquotas retiradas, para análise térmica, das diferentes regiões consideradas do corpo de prova, foi de 10mg.

Os resultados preliminares com 8h de hidratação e carbonatação, comparando-se a quantidade de $CaCO_3$ formado no topo e no meio, mostraram que as pastas preparadas com a/c=0,5 carbonatadas a 80% de UR, e com a/c=0,7 carbonatadas a 60% de UR, capturaram a maior quantidade de CO_2 em base à massa inicial de cimento do que os demais casos.

Considerando os resultados obtidos com 8h, as pastas com relação a/c 0,5 e 0,7 nas condições mais indicadas de umidade relativa, respectivamente 80 e 60%, foram carbonatadas durante 24h, simultaneamente à sua hidratação, considerando duas formas de tratamento: fluxo unidirecional e multidirecional de CO_2. Para o tratamento em fluxo multidirecional, os corpos de prova foram desmoldados após as pastas estudadas atingirem os respectivos tempos do patamar de percolação, estimados entre os resultados de penetração por Vicat e confirmados por ensaio de pulso ultrassônico.

Para os corpos de prova carbonatados em fluxo multidirecional, após o tratamento com CO_2 durante 24h, foram coletadas amostras apenas de 3 regiões (topo, topo-meio e meio) para realização de análises por TG/DTG, devido à simetria na carbonatação dos referidos corpos de prova.

Com os resultados do teor de $CaCO_3$ formado em cada região, em base à massa inicial de cimento, foram estabelecidas curvas da frente de carbonatação em função da profundidade de cada caso. Conhecendo o volume do corpo de prova, o teor inicial de $CaCO_3$ presente na composição química do cimento e a quantidade de cimento utilizada para preparar cada mistura, foi possível integrar os resultados obtidos de cada região estudada e calcular a quantidade de CO_2 capturado no volume por diferença de $CaCO_3$ formado.

A partir das quantidades de CO_2 capturados em cada caso, verificou-se que no fluxo unidirecional a quantidade de $CaCO_3$ formado é bem maior no topo do que nas demais regiões, em função da saturação de água nos poros do topo, o que diminuiu a velocidade de difusão do CO_2 para o interior do corpo de prova. Com o transcorrer da hidratação, o

excesso de $CaCO_3$ precipitado no topo formou uma película que impediu que a frente de carbonatação prosseguisse, diminuindo assim o potencial de captura.

A vantagem do fluxo multidirecional em relação ao anterior acontece, pois, transcorrido um tempo inicial de hidratação, quando parte da água já foi consumida para hidratação e os poros encontram-se menos obstruídos, o que favorece a difusão do gás. Há também uma maior disponibilidade inicial de $Ca(OH)_2$ para reagir com o CO_2, pois a pasta neste instante atravessa a fase de aceleração.

As pastas com relação a/c=0,7, carbonatadas durante 24h, nas condições de UR=60%, após 6h iniciais de hidratação, consumiram todo o $Ca(OH)_2$ e promoveram a maior captura de CO_2, correspondendo a aproximadamente 7% da massa inicial de cimento.

Alcançadas as condições favoráveis de captura, foram moldados 10 corpos de prova cilíndricos (25 x 50mm), sendo 5 como referência (sem carbonatação) e outros 5 carbonatados nas condições ótimas de captura, para serem testados à compressão aos 28 dias. Os resultados mostraram que a carga de ruptura dos cilindros carbonatados foram 51% menores que os da referência, constatando-se que o tempo de 24h de exposição ao CO_2, apesar de maximizar a captura, comprometia a matriz, especificamente o do C-S-H, revelada posteriormente pelos resultados da TG/DTG.

A fim de compatibilizar os parâmetros de captura de CO_2 encontrados, com a resistência à compressão das pastas, foram moldados corpos de prova cilíndricos (25 x 50mm), escolhendo 5 diferentes tempos de exposição ao CO_2 (1, 2, 4, 8 e 12h), mantendo-se os parâmetros de carbonatação previamente estabelecidos. Para cada tempo de exposição foram coletadas amostras de 4 regiões distintas do cilindro (r=0, 0,42, 0,84 e 1,25), na direção radial, para análise térmica (TG/DTG), imediatamente após a carbonatação.

Após o tratamento com CO_2, os cilindros foram cortados pela metade na direção longitudinal com o auxílio de uma pequena serra circular e usando uma pequena espátula, retiradas as alíquotas para análise térmica das regiões designadas. Foi seguido o mesmo procedimento supracitado para interrupção da hidratação das amostras através da acetona.

Também, para cada tempo de exposição ao CO_2 foram moldados 5 cilindros para serem testados à compressão aos 14 dias. Os resultados da análise térmica mostraram que até as duas primeiras horas, a carbonatação não atingiu as regiões mais internas do cilindro,

limitando-se à superfície, e que apenas após 2h de exposição ao CO_2 é que a resistência à compressão dos cilindros carbonatados decresceu em relação às referências não carbonatadas.

3.3 Estudo da Hidratação e Carbonatação em Tempo Real de Pastas de Cimento Portland de Alta Resistência Inicial e Resistente à Sulfatos em Câmara Controlada (Artigo E).

Os estudos preliminares realizados por NCDTA (seção 3.1) permitiram acompanhar as diversas etapas da reação de hidratação de pastas de cimento Portland ARI-RS e estudar a influência da relação a/c na cinética de hidratação. Esta parte da pesquisa se propôs a complementar tal conhecimento, desenvolvendo um novo modelo de NCDTA, em ambiente controlado de temperatura e umidade e em maior escala de processamento, comumente utilizada em pesquisas na área de engenharia civil, para auxiliar no estudo, em tempo real, da hidratação e carbonatação de pastas cimentícias, aplicando as condições experimentais de captura definidas. Neste modelo, termistores foram colocados na posição horizontal dentro de fôrmas metálicas retangulares (115 x 115 x 25mm) isoladas do ambiente da câmara com poliestireno expandido (isopor). Com esse novo modelo de NCDTA desenvolvido foram acompanhadas as primeiras 24h de hidratação das pastas nas relações a/c iguais a 0,5, 0,6 e 0,7, variando-se a umidade relativa em 60, 80 e 100%, na ausência do CO_2. Posteriormente, apenas para a relação a/c=0,7, os ensaios foram repetidos, aplicando as condições ótimas de captura de CO_2 encontradas.

Diferentemente da termogravimetria convencional, que registra a perda de massa em tempo real, a partir do aquecimento controlado da amostra por uma fonte externa de calor, além do acompanhamento da variação de temperatura dos meios reacionais em tempo real, um sistema de termogravimetria não convencional (sigla NCTG em inglês), foi montado dentro da câmara climática para o monitoramento, também em tempo real, da variação de massa efetiva promovida pela reação de carbonatação. Dessa forma, cilindros (25 x 50mm) de pastas na relação a/c=0,7 foram submetidos à carbonatação durante 24h nas condições ótimas de captura de CO_2 anteriormente apresentadas.

Através das curvas NCDTA e NCTG assim obtidas, foi possível estudar os efeitos endotérmicos da perda de água e exotérmicos da hidratação e carbonatação,

estabelecendo uma correlação entre esses efeitos térmicos e as variações de massa respectivas e simultaneamente ocorridas. Comparações de curvas NCTG em diversas situações experimentais permitiram calcular a quantidade de CO_2 capturado nos cilindros, que corresponderam a um aumento de massa de 15,95%.

3.4 Estudo das propriedades mecânicas, microestruturais e de porosidade de pastas de Cimento Portland de Alta Resistência Inicial e Resistente à Sulfatos tratadas com CO_2 (Artigos F e G).

Alcançadas as condições para maximizar a captura de CO_2, os corpos de prova carbonatados foram caracterizados quanto a suas propriedades mecânicas e microestruturais, assim como foram realizados ensaios para determinar sua porosidade. Além das pastas de referência (sem carbonatação) processadas, foram preparadas pastas de cimento Portland ARI-RS para serem tratadas com CO_2 nos dois tempos de carbonatação estudados (1 e 24h), obedecendo às condições ótimas de captura estipuladas.

Os ensaios mecânicos realizados aos 28 dias confirmaram os resultados previamente obtidos aos 14 dias (seção 3.2), onde as pastas carbonatadas durante 1h apresentaram resistência mecânica superior à referência e às carbonatadas durante 24h.

Os resultados mostraram que as pastas com 1h de carbonatação formam após 28 dias, produtos finais, que apesar de mais resistentes, apresentam porosidade ligeiramente maior do que as pastas de referência e muito menor do que as pastas submetidas a carbonatação por 24h. As imagens obtidas por MEV permitiram explicar os elevados índices de absorção de água dos produtos finais obtidos nas pastas carbonatadas por 24h e a degradação superficial causada pelo CO_2 nas pastas carbonatadas por 1h, que aumentaram ligeiramente a porosidade global e os índices de absorção de água dos produtos finais, em relação aos de referência.

Os espectros de DRX e RMN corroboraram resultados apresentados na literatura, principalmente para as pastas carbonatadas por 24h. Nestes casos, os resultados de RMN permitiram confirmar as grandes modificações estruturais das fases de silicato de cálcio hidratadas promovidas pela carbonatação. Como nos resultados obtidos por TG/DTG, os resultados de DRX confirmaram o consumo da portlandita ($Ca(OH)_2$) e a intensa formação de $CaCO_3$, pelos picos correspondentes à calcita.

3.5 Avaliação do Comportamento Mecânico de Compósitos Reforçados com Fibras de Sisal Tratadas com CO_2 (Artigo H)

No artigo H, foi estudada a aplicação das condições de captura de CO_2 encontradas para as pastas, em duas famílias de compósitos: uma de cimento Portland (CSAND) e outra de cal, metacaulinita e cinza volante (LMKFA), ambas reforçadas com fibras longas de sisal de 50mm. Para comparar a eficiência da carbonatação das matrizes de cimento Portland no consumo do $Ca(OH)_2$, foram confeccionadas matrizes de cimento Portland com metacaulinita e cinza volante (CMKFA) sem carbonatação.

Os compósitos CSAND foram tratados com CO_2, considerando os dois tempos de carbonatação estudados para as pastas: 1 e 24h, comparando-as com os compósitos CSAND de referência (sem carbonatação) e CMKFA. Para os compósitos LMKFA foi feita apenas a carbonatação por 1h, sendo comparados os resultados com os respectivos compósitos de referência não carbonatados.

Uma parte dos compósitos finais obtidos foram ensaiados à flexão em 4 pontos aos 28 dias, outra parte após 10 e 20 ciclos de molhagem e secagem em uma câmara de ventilação forçada. Para cada compósito ensaiado foram extraídas alíquotas para análise térmica (TG/DTG) das matrizes e das fibras por MEV. Os índices de tenacidade foram calculados para cada compósito conforme a norma Belga NBN B15-238.

Os resultados mostraram que os compósitos CMKFA apresentaram desempenho mecânico e durabilidade melhores do que os compósitos CSAND em todos os casos. Os tratamentos com CO_2 durante 24h dos compósitos CSAND não foram suficientes para consumir todo o $Ca(OH)_2$ das respectivas matrizes. Com 20 ciclos de molhagem e secagem a tenacidade dos compósitos CSAND ficou comprometida em relação aos compósitos CMKFA.

Os compósitos LMKFA tratados com CO_2 por 1h apresentaram desempenho mecânico melhor do que as respectivas referências em todos os casos. As curvas TG/DTG dos compósitos LMKFA com 20 ciclos de molhagem e secagem carbonatados por 1h, mostraram uma tendência de lixiviação dos produtos formados, porém os resultados mecânicos de flexão para os compósitos LMKFA de referência apresentaram fissuração prematura da matriz.

Apesar da carbonatação não ter consumido todo o $Ca(OH)_2$ dos compósitos CSAND, as respectivas imagens de MEV mostraram que as fibras de sisal apresentaram certa integridade estrutural.

Capítulo 4

Conclusões

- As análises térmicas aplicadas a diversas condições experimentais ensaiadas permitiram melhor estudar e entender os mecanismos de carbonatação.

- As referidas análises permitiram estabelecer as condições ideais para captura de CO_2 em pastas de cimento Portland de Alta Resistência Inicial Resistente a Sulfatos, sem prejuízo de suas propriedades mecânicas.

- Pastas de cimento Portland ARI-RS, preparadas com relação a/c=0,7, tratadas com CO_2 durante 24h, com uma concentração de 20%, em ambiente com temperatura de 25°C e umidade relativa de 60%, após 6 horas iniciais de hidratação sem carbonatação, definem as condições que maximizam a captura de CO_2.

- Por termogravimetria pode se quantificar a massa de CO_2 fixada nas condições ideais de captura, que foi de aproximadamente 7% da massa inicial de cimento utilizada na preparação das respectivas pastas.

- As pastas carbonatadas por 24h, apesar do aumento na capacidade de absorção de CO_2 nas condições ideais de captura, apresentaram uma sensível piora na resistência mecânica em relação às não carbonatadas e elevados índices de absorção de água devido à elevada porosidade da matriz assim formada.

- A carbonatação por 1h, apesar de diminuir o nível de captura de CO_2, permitiu que as amostras carbonatadas apresentassem resistência mecânica superior às não carbonatadas, apesar de exibirem um pequeno aumento nos índices de absorção de água, devido à intensa carbonatação superficial das amostras.

- Maiores tempos de exposição ao CO_2 nas condições ótimas de captura, embora formem fases sólidas carbonatadas mais densas conforme verificado por RMN, comprometem a estrutura final dos corpos de prova hidratados, aumentando significativamente sua porosidade global, fato confirmado por MEV, e em consequência, diminuindo sensivelmente sua resistência mecânica final.

- Os novos sistemas de análise térmica diferencial não convencional (sigla NCDTA em inglês) e termogravimetria não convencional (sigla NCTG em inglês) desenvolvidos em ambiente controlado de temperatura e umidade, demonstraram serem ferramentas eficazes para o estudo simultâneo da hidratação e da carbonatação em tempo real de pastas em maior escala de processamento.

- Esses novos sistemas desenvolvidos permitem estabelecer uma correspondência entre os efeitos térmicos e as variações de massa ocorridos durante os processos de hidratação e carbonatação, e estimar a quantidade de CO_2 capturado em pastas com moldes comumente utilizados em ensaios de materiais cimentícios na engenharia civil.

- Conforme resultados obtidos por TG/DTG, em condições ótimas de captura estabelecidas, a carbonatação durante 24h dos compósitos de cimento Portland reforçados com fibras longas de sisal (CSAND) não consome totalmente o $Ca(OH)_2$ formado, como ocorreu nas pastas, tendo estes compósitos apresentado desempenho mecânico pior que os carbonatados por 1h.

- Em condições ótimas de captura estabelecidas, compósitos de cimento, metacaulinita e cinza volante (CMKFA) apresentaram comportamento mecânico final melhor que os compósitos CSAND, em todas as condições estabelecidas, com nítido comportamento de "*strain hardening"*.

- Os compósitos preparados com cal, metacaulinita e cinza volante (LMKFA) tratados com CO_2 durante 1h apresentaram desempenho mecânico melhor que os não carbonatados, ocorrendo porém, degradação da matriz dos compósitos de referência com 20 ciclos de molhagem e secagem.

REFERÊNCIAS

[1] Disponível em <http://www.ipcc.ch/> Acesso em 21 out. 2013.

[2] Disponível em <http://edgar.jrc.ec.europa.eu/index.php> Acesso em 21 out. 2013.

[3] Disponível em <http://agencia.fapesp.br/17215> Acesso em 21 out. 2013.

[4] HABERT, G., BILLARD, C., ROSSI, P., *et al*. "Cement Production Technology Improvement Compared to Factor 4 Objectives", **Cement and Concrete Research**, v.40, n.5, pp. 820-826, 2010.

[5] POMMER, K., PADE, C., 2005 (Oct), **Guidelines - Uptake of Carbon Dioxide in the Life Cycle Inventory of Concrete**, ISBN: 87-7756-757-9, Danish Technological Institute.

[6] FAIRBAIRN, E.M.R., AMERICANO, B.B., CORDEIRO, G.C., PAULA, T.P., TOLEDO FILHO, R.D., SILVOSO, M.M. "Cement replacement by sugar cane bagasse ash: CO_2 emissions reduction and potential for carbon credits." **Journal of Environmental. Management.** V.91, n.9, pp 1864-1871, 2010.

[7] RAKI, L., BEAUDOIN, JJ., ALIZADEH R. "Nanotechnology Applications for Sustainable Cement-Based Products", **Nanotechnology in Construction,** n.3 , pp. 119-124, 2009.

[8] LI, J., THARAKAN, P., MACDONALD, D., LIANG, X., et al. "Technological, economic and financial prospects of carbon dioxide capture in the cement industry", **Energy Policy**, v.61, pp 1377-1387, 2013.

[9] DUBOIS, L., THOMAS, D. "Experimental study of post-combustion CO_2 capture by Chemical Absorption: Screening of Aqueous Amine(s)-based solvents", **Energy Procedia,** v.37, pp. 1648-1657, 2013.

[10] HANDAGAMA, NB., KOTDAWALA, RR., VAJPEYI, A., 2013, "Heat integration of a cement manufacturing plant with an absorption based carbon dioxide capture process" **United States Patents Application Publication**.

[11] COSTA, B. L.C, 2012, *Quantificação das Emissões de CO_2 Geradas na Produção de Materiais Utilizados na Construção Civil no Brasil*. Dissertação* de M.Sc., COPPE/UFRJ, Rio de Janeiro, RJ, Brasil.

[12] PLASYNSKI, S., DAMIANI, D. "Carbon Sequestration through Enhanced Oil Recovery", U. S. Department of Energy, Office of Fossil Energy, National Energy Technology Laboratory**.** Disponível em: <http://www.netl.doe.gov/publications/factsheets/program/Prog053.pdf>, Acesso em 25 out. 2013.

[13] CHANG, EE., WANG, YC., PAN, SY., et al. "CO_2 capture by using blended hydraulic slag cement via a slurry reactor", **Aerosol and Air Quality Research**, v.12, n.6, pp 1433-1443, 2012.

[14] RUIFENG, D., ZAOXIAO Z., HONGFANG L.,et al. "Recovery of waste heat in cement plants for the capture of CO_2", **Frontiers of Chemical Science and Engineering**, v.6, pp 104-111, 2012.

[15] Disponível em < http://www.uspto.gov/about/ipm/calera.jsp> Acesso em 21 out. 2013.

[16] SHAO Y., MIRZA MS., WU X. "CO_2 sequestration using calcium–silicate concrete", **Canadian Journal of Civil Engineering**, n.33, v.6, pp 776-784, 2006.

[17] SHAO Y., MONKMAN S., WANG S., "Market analysis of CO_2 sequestration in concrete building products". *2nd International Conference on Sustainable Construction Materials and Technologies*. Italy, Ancona, 28–30 June 2010.

[18] ROSTAMI V., SHAO Y., BOYD AJ. "Microstructure of cement paste subject to early carbonation curing". **Cement Concrete Research**, n.42, v.1, pp 186–93, 2012.

[19] SHAO Y., MONKMAN S., BOYD AJ., "Recycling carbon dioxide into concrete: a feasibility study." *Concrete Sustainability Conference*. Canada: McGill University, Department of Civil Engineering, 2010. Disponível em <http://www.concretetechnologyforum.com/2010CSCProceedings/documents/Shao%20Paper%204-15-10.pdf>, acesso em 25 out 2013.

[20] HABERT G., ROUSSEL N. "Study of two concrete mix-design strategies to reach carbon mitigation objectives". **Cement and Concrete Composites**, n.31, pp 397–402, 2009.

[21] SHAO Y., ZHOU X., MONKMAN S., "A new CO_2 sequestration process via concrete products production. *EIC Climate Change Technology*, Canada, Ottawa, 10-12 May 2006.

[22] JEONGA J., SARDINIB P., RAMÉZANIC H., et al. "Modeling of the induced chemo-mechanical stress through porous cement mortar subjected to CO_2: Enhanced micro-dilatation theory and 14C-PMMA method", **Computational Materials Science** v. 69, pp 466–480, 2013.

[23] JEFFREY J C., JEFFREY J., THOMAS B., et al. "Decalcification shrinkage of cement paste", **Cement and Concrete Research,** v.36, pp 801 – 809, 2006.

[24] CUNHA, ACQ., HELENE, PRL,. 2001, "Despassivação das armaduras de concreto por ação da carbonatação", **Boletim Técnico da Escola Politécnica da USP, Departamento de Engenharia de Construção Civil**, São Paulo.

[25] YE, G., 2003, "*Carbon Dioxide Uptake By Concrete Through Early-Age Curing*". M.Sc Dissertation**,** Department of Civil Engineering and Applied Mechanics, McGill University, Montreal, Canadá.

[26] SIMATUPANG, MH., HABIGHORST, C. "Investigations on the Influence of the Addition of Carbon Dioxide on the Production and Properties of Rapidly Set Wood-Cement Composites", **Cement and Concrete Composites**, v.17, pp 187-197, 1995.

[27] LAGERBLAD, B., 2005 (Febr), "**Carbon Dioxide Uptake During Concrete Life Cycle – State of Art**" – In: CBI Report 2**,** Swedish Cement and Concrete Research Institute.

[28] STUMPP, M. J., 2003, "*Carbonatação de Concretos com Altos Teores de Adições Minerais e de Cal Hidratada*". Dissertação* de M.Sc., UFSM/ PPGEC, Santa Maria, RS, Brasil.

[29] FUKUSHIMA, T., 1988 "Theoretical investigation on the influence of various factors on carbonation of concrete", Building research Institute (Japan), **BRI Research Paper No 127 (ISSN 0453-4972),**Japan. Disponível em: <http://www.kenken.go.jp/english/contents/publications/paper/127.html>, acesso em 25 out 2013.

[30] NEVILLE, AM., **Propriedades do concreto**., 2.ed.2, São Paulo: Pini, Rev. Atual, 1997

[31] KULAKOWSKI, MP., 2002, "*Contribuição ao estudo da Carbonatação em Concretos e Argamassas Compostos com Adição de Sílica Ativa*." Tese* de D.Sc., PPGEM, Porto Alegre, RS, Brasil.

[32] ISABEL, G., ANDRADE, C., MORA, P., et al. "Sequestration of CO_2 by Concrete Carbonation", **Environmental Science & Technology**, v.44, n.8, pp. 3181-6, 2010.

[33] PAULETTI, C., 2004. "*Análise Comparativa de Procedimentos para Ensaios Acelerados de Carbonatação*." Dissertação* M.Sc., PPGEC/UFRGS, Porto Alegre, RS, Brasil.

[34] NUNES, FL., HELENE, PLR., 1998, "Influência da Dosagem na Carbonatação dos Concretos" **Boletim Técnico da Escola Politécnica da USP, Departamento de Engenharia de Construção Civil**, São Paulo.

[35] HASELBACH, L. "Potential for Carbon Dioxide Absorption in Concrete", **Journal of Environmental Engineering**, v.135, n.6, pp. 465-472, 2009.

[36] SULAPHA, P., WONG, SF., WEE, TH., et al. "Carbonation of Concrete Containing Mineral Admixtures", **Journal of Materials in Civil Engineering**, v.15, n.2, pp. 134-143, 2003.

[37] OSBORNE, G.J. "Carbonation of blast furnace slag cement concretes." **Durability of Building Materials,** v.4 p 81-96, 1989.

[38] TALUKDAR, S., BANTHIA, N., GRACE, JR. "The effects of structural cracking on carbonation progress in reinforced concrete: is climate change a concern?", *3rd International Conference on the Durability of Concrete Structures*, Queen's University Belfast, September,2012.

[39] CHI, JM., HUANG, R., YANG, CC. "Effects of carbonation on mechanical properties and durability of concrete using accelerated testing method", **Journal of Marine Science and Technology**, vol.10, n. 1, pp. 14-20, 2002.

[40] HEWLETT PC. **Lea's Chemistry of cement and concrete.** 4 ed. London, Arnold,1998.

[41] MATSUSHITA, F., YOSHIMICHI, A., SHIBATAB., S. "Calcium silicate structure and carbonation shrinkage of a tobermorite-based material.", **Cement and Concrete Research**, v.34, I.7, pp.1251–1257, 2004.

[42] HOUST, YF., "Carbonation shrinkage of hydrated cement paste", Disponível em <http://infoscience.epfl.ch/record/29449/files/Houst_CS_1997> Acesso em 25 out 2013.

[43] MO, L., PANESAR, DAMAN, K. "Accelerated carbonation - A potential approach to sequester CO_2 in cement paste containing slag and reactive MgO." **Cement and Concrete Composites**, v.43, pp.69-77, 2013.

[44] YUAN, C., NIU, D., CHEN, N., et al. "Influence of carbonation on microstructure of concrete.", **Guisuanyan Tongbao**, v.32, n.4, pp.687-691, 2013.

[45] WANG, W., LI, S., XING, F., et al. "Behaviors of carbonation resistance of phosphoaluminate cement pastes." **Jianzhu Cailiao Xuebao**, v.15, n.3, pp.334-339, 2012.

[46] MO, L., PANESAR, DAMAN, K. "Effects of accelerated carbonation on the microstructure of Portland cement pastes containing reactive MgO.", **Cement and Concrete Research**, v.42, n.6, pp.769-777, 2012.

[47] BUKOWSKI, JM., BERGER RL. "Reactivity and Strength Development of Activated Non-Hydraulic Calcium Silicates", **Cement and Concrete Research**, v.9, pp.57-68, 1979.

[48] WAGH, AS., SINGH, D., AND KNOX, LJR. "Lab studying Greenhouse Effect on Concrete Setting", **Concrete International**, v.17, pp.41-42, 1995

[49] TERAMURA, S., ISU, N. "New Building Material from Waste Concrete by Carbonation", **Journal of Materials in Civil Engineering**, pp.288-293, 2000.

[50] ZORNOZA, E., GARCES, P., MONZO, J., et al. "Accelerated carbonation of cement pastes partially substituted with fluid catalytic cracking catalyst residue (FC3R)." **Cement and Concrete Composites**, v.31. n.2, pp.134-138, 2009.

[51] QIN, C., YIN, J., AN, H., et al. "Performance of Extruded Particles from Calcium Hydroxide and Cement for CO_2 Capture.", **Energy and Fuels**, v.26, n.1, pp.154-161, 2012.

[52] KLAUS P., DAM-JOHANSEN, K., HJULER SK., et al. "CO_2 Capture by Cement Raw Meal." **Energy and Fuels**, v.27, n.9, pp.5397-5406, 2013.

[53] PEREIRA, CL., SAVASTANO, H.J.R., PAYA, J., et al. "Use of highly reactive rice husk ash in the production of cement matrix reinforced with green coconut fiber." **Industrial Crops and Products**, v.49, pp.88-96, 2013.

[54] SILVA F. A., TOLÊDO FILHO R.D., FAIRBAIRN E.M.R. "Accelerated aging characteristics of sisal fiber-cement based composites made with a CH free cementitious matrix". *In: Brazilian Conference Non-Conventional Materials and Technologies in Ecological and Sustainable Construction* – Brasil Nocmat 2006.

[55] BENTUR, A., MINDESS, S., Fibre Reinforced Cementitious Composites. 2ed. Technology and Engineering, 1990

[56] TOLÊDO FILHO RD., SCRIVENER, K., ENGLAND, GL., et al. "Durability of alkali-sensitive sisal and coconut fibres in cement mortar composites." **Cement and Concrete Composites**, v.22, pp.127-143, 2000.

[57] TOLÊDO FILHO RD., SCRIVENER, K., ENGLAND, GL., et al. "Development of vegetable fibre–mortar composites of improved durability." **Cement and Concrete Composites,** v.25, pp.185–196, 2003.

[58] JOHN, VM., CINCOTTO, MA., SJOSTROM, C., et al. "Durability of slag mortar reinforced with coconut fibre", **Cement and Concrete Composites**, v. 27, pp. 565-574, 2005.

[59] ALMEIDA AEFS., TONOLI GHD., SANTOS SF, et al. "Improved durability of vegetable fiber reinforced cement composite subject to accelerated carbonation at early age." **Cement and Concrete Composites**, v.42, pp.49-58, 2013.

[60] TONOLI GHD., SANTOS SF, JOAQUIM AP., SAVASTANO JRH. "Accelerated carbonation on vegetable fibre reinforced cementitious roofing tiles." *10th IIBCC* São Paulo, November 15-18, 2006.

[61] QI, H., COOPER, PA., WAN, H., 2004, "The recycling of MDF fiber into wood-cement composites with carbon dioxide injection.", **Inorganic-Bonded Composite Materials** ,v.9.

[62] SAVASTANO HJR., JOHN, VM., AGOPYAN, V., et al. "Weathering of vegetable fibre-clinker free cement composites.", **Materials and Structures,** v.35, I. 1, pp. 64-68, 2002.

[63] CARVALHO, MA., JÚNIOR, CC., SAVASTANO H.JR., et al. "Microstructure and mechanical properties of gypsum composites reinforced with recycled cellulose pulp." **Materials and Research**, vol.11, n.4, 2008.

[64] FARAHI, E., PURNELL, P., SHORT, NR. "Supercritical carbonation of calcareous composites: Influence of mix design", **Cement and Concrete Composites**, v.43, pp.12–19, 2013.

[65] CULTRONE, GT., SEBASTIAN, E., HUERTAS, MO. "Forced and natural carbonation of lime-based mortars with and without additives: Mineralogical and textural changes." **Cement and Concrete Research,** v.35, pp. 2278– 2289, 2005.

[66] GEORGESCU M., MOHANU, I., VOICU, G., COȚOFANĂ, V., 2012, "Physical-chemical processes at hardening of some lime-limestone-volcanic tuff composites", **U.P.B. Scientific Bulletin**., Series B, v.74, I.1.

[67] HASELBACH, L., SHUGUO, M. “Potential for Carbon Adsorption on Concrete: Surface XPS Analyses”, **Environmental Science and Technology**, v.42, n.14, pp 5329-5334, 2008.

[68] MOGHTADERI, B., ZANGANEH, J., SHAH, K., et al. “Application of Concrete and Demolition Waste as CO_2 Sorbent in Chemical Looping Gasification of Biomass.” **Energy and Fuels**, v.26, n.4, pp.2046-2057, 2012.

[69] PAN, SY., CHIANG, PC., CHEN, YH., et al. “Ex Situ CO_2 capture by carbonation of steelmaking wastewater in a rotating packed bed.” **Environmental Science Technology**, v.47, n.7, pp. 3308-3315, 2013.

[70] LANGE, LC., HILLS, CD., POOLE. AB. “A Preliminary Investigation into the Effects of Carbonation on Cement-Solidified Hazardous Wastes”, **Environmental Science and Technology**, v.30, n.1, pp. 25-30, 1996.

[71] BORGES, PHR., MILESTONE, NB., COSTA, JO., et al. “Carbonation durability of blended cement pastes used for waste encapsulation.” **Materials and Structures** (Dordrecht, Netherlands), v.45 n.5, pp. 663-678, 2012.

[72] CHEN, H., ZHAO, C., YANG, Y. “Enhancement of attrition resistance and cyclic CO_2 capture of calcium-based sorbent pellets.”, **Fuel Processing Technology**, v.116, pp. 116-122, 2013.

[73] TAYLOR HFW. “**Cement Chemistry**,” 2ed. London, 1997.

[74] KNOPF, FC., ROY, A., SAMROW, HA., et al. “High-Pressure Molding and Carbonation of Cementitious Materials”, **Industrial and Engineering Chemistry Research**, v.38, n.7, pp. 2641-2649, 1996.

[75] DWECK, J., BUCHLER, PM., COELHO, ACV., et al. “Hydration of a Portland cement blended with calcium carbonate”, **Thermochimica Acta**, v.346, n. 1-2, pp. 105-113, 2000.

[76] VILLAIN, G., THIERY, M., PLATRET, G., et al. “Measurement Methods of Carbonation Profiles in Concrete: Thermogravimetry, Chemical Analysis and Gammadensimetry”, **Cement and Concrete Research**, v.37, n.8, pp. 1182-1192, 2007.

[77] KJELLSEN, KO., GUIMARAES, M., NILSSON, A., 2005 (Dec), **The CO_2 Balance of Concrete in a Life Cycle Perspective**, ISBN: 87-7756-758-7, Danish Technological Institute.

ANEXOS

ARTIGO A – Neves Junior A, Toledo Filho R.D, Dweck J, Fairbairn E.M.R. Early Stages Hydration of High Initial Strength Portland Cement – Part I – Thermogravimetric Analysis on Calcined Mass Basis. Journal of Thermal Analysis and Calorimetry, v. 108, p. 725-731, 2012.

Early Stages Hydration of High Initial Strength Portland Cement – Part I – Thermogravimetric Analysis on Calcined Mass Basis.

Alex Neves Junior[a], Romildo Dias Toledo Filho[a], Jo Dweck[b] and Eduardo de Moraes Rego Fairbairn[a]

[a] Civil Engineering Program – COPPE – Rio de Janeiro Federal University, Brazil

[b] School of Chemistry - Rio de Janeiro Federal University, Brazil.

Journal of Thermal Analysis and Calorimetry

2012

Abstract

Thermogravimetry (TG) and Derivative Thermogravimetry (DTG) were used to analyze the early stages of hydration of a high initial strength and sulphate resistant Portland cement (HS SR PC) within the first 24 hours of setting. The water/cement (W/C) mass ratios used to prepare the pastes were 0.35, 0.45 and 0.55. The hydration behavior of the pastes was analyzed through TG and DTG curves obtained after different hydration times on calcined cement mass basis to have a same composition basis to compare the data. The influence of the W/C ratio on the kinetics of the hydration process was done through the quantitative analysis of the combined water of the main hydration products formed in each case. TG and DTG curve data calculated on calcined mass basis of all the results were converted to initial cement mass basis to have an easier way to analyze the influence of the water/cement ratio on the free and combined water of the different main hydrated phases. The gypsum content of the pastes was totally consumed in 8 hours for all cases. A significant part of the hydration process occurs within the first 14 hours of setting and at 24h the highest hydration degree, indicated by the respective content of formed calcium hydroxide, occurs in the case of the highest initial water content of the paste.

Keywords: HS SR cement, early stage hydration, TG, DTG, calcined mass basis

1.Introduction

Thermogravimetric (TG) and Derivative Thermogravimetric (DTG) analysis have helped to understand and to study the behavior of cementitious materials during their hydration stages. Among these applications, there are: identification of the main different present phases [1, 2, 3] studies of the hydration degree [4, 5, 6, 7], studies of the effects of different additives [8, 9, 10, 11, 12] and the analysis of pozzolanic activities of mineral additives [2, 8, 9, 10, 13, 14].

When thermal analysis is performed without a previous drying step, distinct type of reactions may occur during the thermal decomposition of a cementitious paste: drying and dehydration steps, a dehydroxilation and a decarbonation. The first two steps include the loss of free water from the pores and from the water released from any C-S-

H structured phase including tobermorite. (Capillary, interstitial and physically combined water) [14, 15].

When thermal analysis is performed after an initial drying step at temperatures between 28 and 35°C, the main decomposition steps of the hydrated phases are: dehydration of tobermorite (non necessarily in crystalline form) and ettringite (50-200°C); dehydration of the dihydrated calcium sulphate (110-145°C); dehydration of calcium hydroxide (380-460°C); decomposition of calcium carbonate (520-730°C) [16, 17].

In this study, the evaluation of the influence of water/cement ratio in the kinetics of the hydration reactions was done by using TG and DTG analysis at different times during the first 24 hours of setting, estimating the contents of Free Water, Combined Water released from Tobermorite and Ettringite phases, Total Combined Water and Portlandite, in the different water/cement ratio studied pastes.

2.Materials

For this study, a High Initial Strength and Sulphate Resistant Portland Cement (HS SR PC) [18] was used, which allows reaching high strengths still at the early hydration stages. The development of high initial strength is due to the use of a different proportion of limestone and clay in the production of the clinker than that used in usual Portland cement manufacture, as well as through a higher milling degree of the cement, in order to accelerate the reaction with the water, by the higher specific external area of the particles and consequently reaching a higher strength in a shorter time. This kind of cement may have a maximum of 5% of carbonates additions with aggregation of blast furnace slag or pozzolanic materials [19]. Its chemical composition and the granulometric distribution curve of the HS SR PC is presented respectively on the Table 1 and in Figure 1

Table 1 – Composition of the cement

Compound	Content / %
CaO	66.92
SiO_2	16.45
Al_2O_3	5.00
SO_3	4.44
Fe_2O_3	3.30
TiO_2	0.40
K_2O	0.35
MnO	0.28
SrO	0.25
ZnO	0.03
ZrO_2	0.02
LOI	2.55

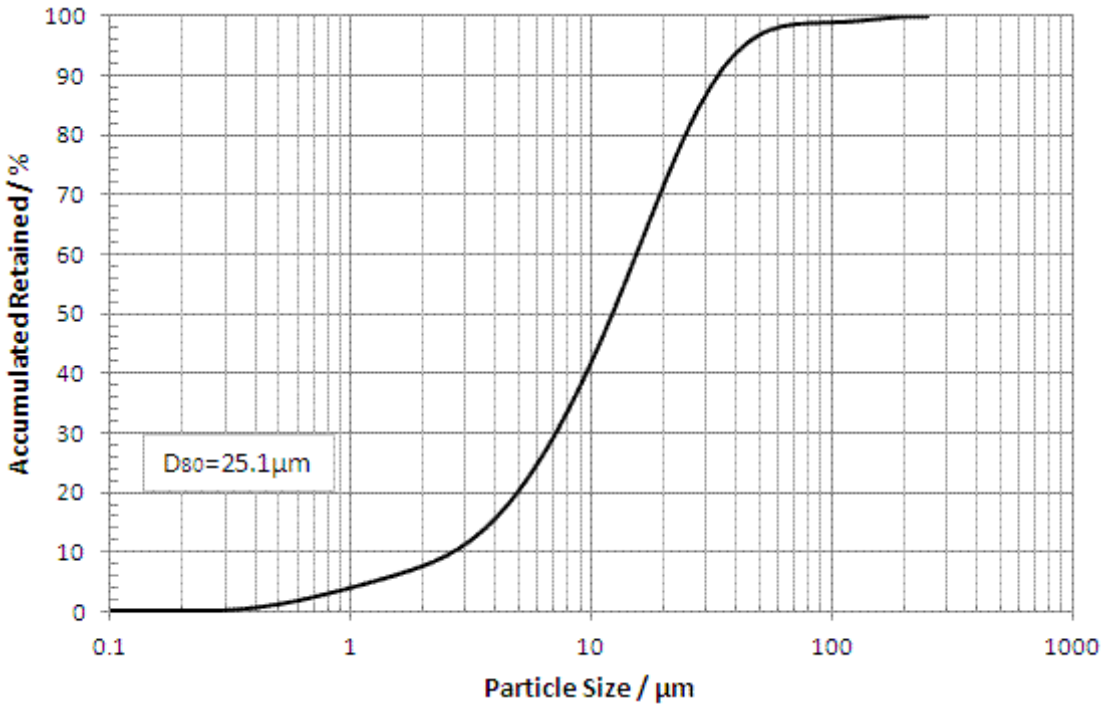

Fig.1- Cement particle size distribution

3. Methods

Pastes with water/cement mass ratios (W/C) of 0.35; 0.45 and 0.55 were prepared. The cement was inserted in plastic bags previously containing the proper amount of deionized water with which homogenization was manually done for one minute after the bag was tightly closed and maintained in a controlled temperature chamber at 30°C. After that, a sample of about 10mg, was collected for each analysis from respective

stored bag at the established times of the experiments, which were of 1h, 8h, 14h and 24h. To minimize the external environment influence, the time between collection and insertion of the sample in the thermal analysis pan was minimized. When the sample was gelly it was directly put into the pan. When it was solidified, a little amount was first collected and transferred into plastic bag, which was sealed, and then was manually milled. After that it was fastly transferred into the pan.

The thermal analyses were performed in a TA Instruments, SDT Q600 model TGA/DTA/DSC simultaneous apparatus at a heating rate of 10°C.min^{-1}, from 35 to 1000° C, by using 100 mL. min^{-1} of nitrogen flow. Before this, the samples were dried inside the equipment initially at 1°C.min^{-1} from 30 to 35^{o}C, followed by an isothermal step at 35^{o}C for 1 hour, to complete the drying in order to eliminate the residual non combined free water [16]. As during these drying steps the water/cement ratio is decreased significantly, which decreases the cement hydration rate, any possible little acceleration during drying was considered insignificant. The material of reference and sample pans was platinum.

4.Results and Discussion

Figure 2 shows the TG and DTG curves of the HS SR PC.

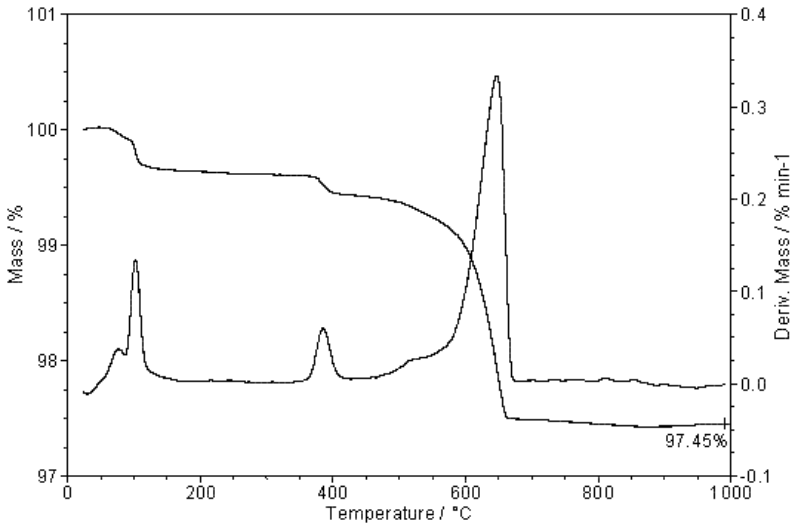

Fig. 2–TG and DTG Curves of the HS SR PC

In Figure 2, the first mass loss step up to 150^{o}C refers to the gypsum dehydration. The second mass loss step from 350 to 450^{o}C is due to calcium hydroxide decomposition. From 450 to 700^{o}C occurs calcium carbonate decomposition.

Typical (TG) and (DTG) curve examples of the pastes prepared with W/C=0.55, on respective sample initial mass basis, are presented respectively in Figures 3 and 4.

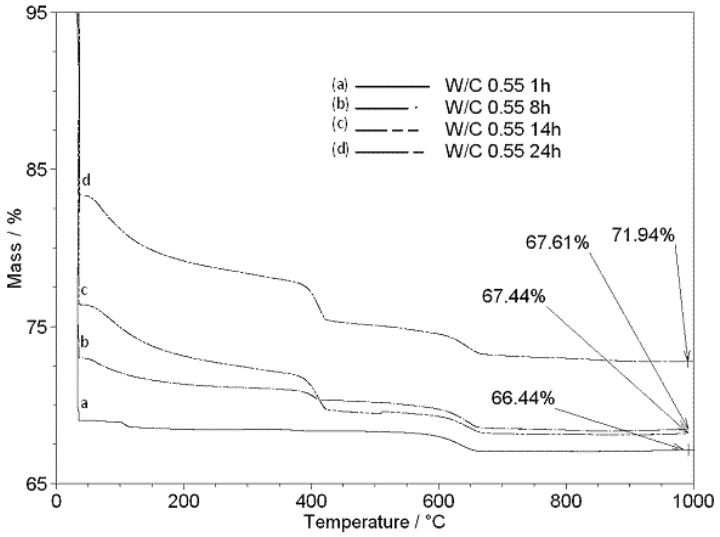

Fig. 3–TG Curves of the pastes prepared with W/C 0.55 at 1h, 8h, 14h and 24h of hydration on initial sample mass basis

We can see from Figure 3 that after the drying step, performed at 35^{o}C, the free water content decreases with time, due to the progress of the hydration and paste setting process, being lower in the 24h paste sample.

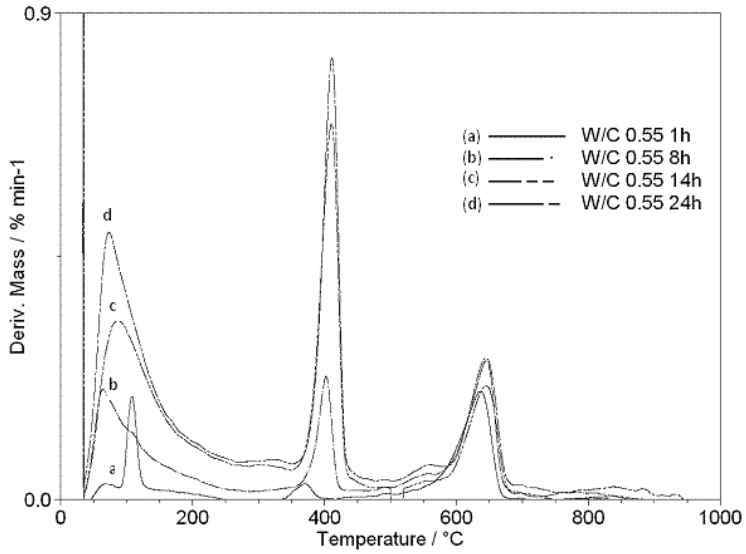

Fig. 4–DTG Curves of the paste with W/C 0.55 at 1h, 8h, 14h and 24h on the sample initial mass basis.

Considering the temperature ranges of the main decomposition steps [16], from Figure 4, which shows the respective DTG curves and peaks, one can evaluate, with major resolution than from respective TG curves shown in Figure 3, the behavior of the decomposition of the main hydrated phases of each paste. It can be seen that the gypsum present in the anhydrous cement is totally consumed at 8 hours of hydration.

It is also noticed from Figure 2 that the anhydrous cement presents a little early hydration, maybe due to storage problems and great reactivity. From 8 to 24h of hydration, the DTG peaks of combined water released from tobermorite and ettringite phases, which occur between 50 and 200°C, increase with hydration time. The same occurs with the combined water loss from the other hydrated phases until 370^{o}C. At this temperature the dehydroxylation of $Ca(OH)_2$ begins, which also increases with the hydration degree until 430°C or 450°C, respectively for the 8 and 24h cases.

It is seen a decrease of the $Ca(OH)_2$ content at 1h, with respect to that of anhydrous cement, possibly due to some carbonation, which may have occurred during sampling at this reaction time, when it has a great reactivity.

From Figure 2 mass loss that occurs and respective DTG peak at the decomposition temperature range of the calcium carbonate, which occurs after the dehydroxilation of calcium hydroxide extending up to 670 a 680°C, we see that carbonate is initially present in the original cement, which was added during its manufacturing.

Comparing the DTG peaks of calcium carbonate decomposition of the pastes with that of original anhydrous cement, we can see a little decrease of peak height. Between 500 and 600°C, a second little and broad peak appears before the higher original calcium carbonate decomposition DTG peak. This can be possibly due to a less crystallized carbonate phase formed during hydration [16].

The TG curves are, by default, shown on respective initial sample mass basis. As the initial masses of the pastes prepared with different W/C ratio have different chemical compositions, the direct comparison among respective TG or DTG curves on respective initial sample basis leads to an erroneous analysis, because the different percentual mass losses do not refer to a same composition.

However, the composition of the residual calcined products of all present cases is composed by the same oxides than the calcined mass of the anhydrous cement. Thus, to

compare the analysis results on a same composition basis, to have correct comparisons, we have converted the TG and DTG data, which are given by the equipment software by default, on respective sample initial mass basis, first on calcined mass basis [12] by dividing all data by respective calcined mass:

$$M_{cb} = \frac{M_i}{M_c}.100$$

Where:

M_{cb} =Mass % at a temperature T on Calcined Mass basis

M_i =Mass % at a temperature T on Initial Sample Mass basis

M_c =Mass % of Calcined Sample on Initial Sample Mass basis

To have an easier and also same basis of comparison, the results obtained on calcined mass basis were transformed on initial cement mass basis, multiplying them by the original cement calcined mass percent:

$$M_{icb} = M_{cb} \frac{M_{cc}}{100}$$

Where:

M_{icb} = Mass % at a Temperature T on Initial Cement Mass Basis

M_{cc} = Mass % of Calcined cement on Initial Cement Mass basis

Thus, on initial cement mass basis, the TG and DTG curves for the paste with 0.55 W/C ratio are shown in Figures 5 and 6 to exemplify these type of data basis change.

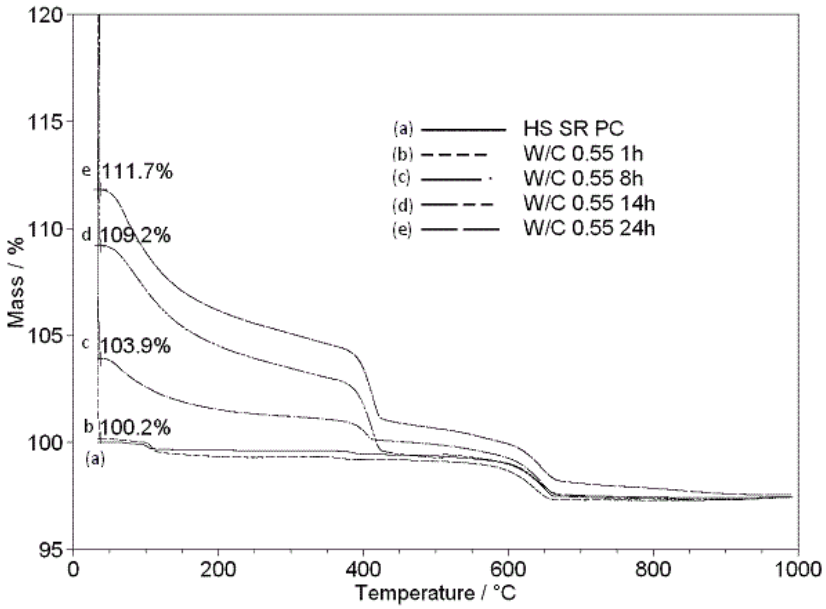

Fig. 5 TG Curves of the cement and the paste with W/C 0.55 at 1h, 8h, 14h and 24h of hydration on cement initial mass basis

From Figures 5 and 6, it can be seen that when the data are transformed on initial cement mass basis, it is possible to have a more correct comparison of the data. The curves tend to disperse when approaching to the lower temperatures, showing the higher free water contents at the begging of respective cases, which are characterized by the initial mass loss during isothermal step of drying 35°C. These curves confirm with more evidence, the increase of the $Ca(OH)_2$ content with the increase of hydration time, because all have as reference, the same respective initial cement mass.

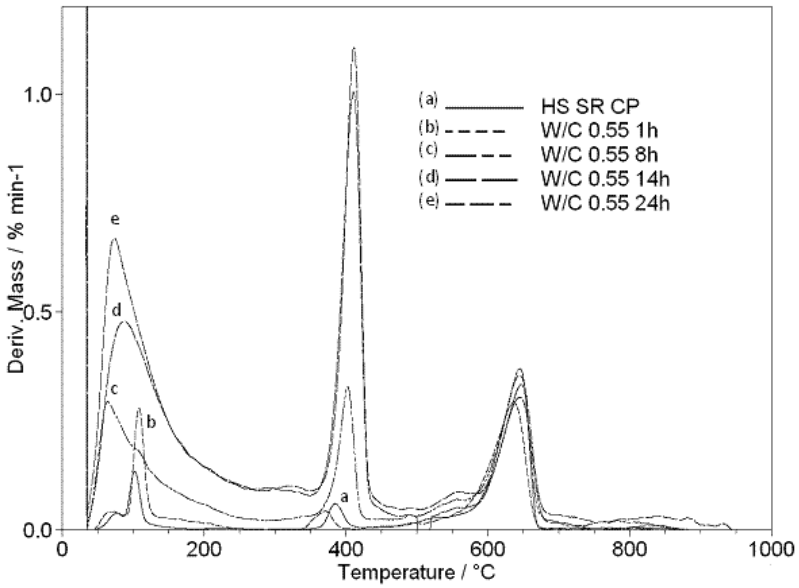

Fig. 6 DTG Curves of the cement and the paste with W/C 0.55 at 1h, 8h, 14h and 24h of hydration on the cement initial mass basis

From the data on initial cement mass basis of each sample, the percentage of the following products can be calculated for each considered hydration time:

- The water released from gypsum decomposition between 90-140°C (when respective DTG peak is apparent);

$$CaSO_4.2H_2O \Leftrightarrow CaSO_4 + 2H_2O$$

- The total combined water released during the products decomposition, including the water loss of dehydroxilation of the $Ca(OH)_2$ between 50-450°C;
- The water released from the Tobermorite and Ettringite decomposition between 50-200°C;
- The water loss during the dehydroxylation of $Ca(OH)_2$, between 380-450°C according to the stoichiometry of the reaction:

$$Ca(OH)_2 \Leftrightarrow CaO + H_2O$$

(Theoretical mass loss = 24.32%);

The comparative histograms of the percentual contents of hydrations products, of the three samples referring to the three used W/C ratios (0.35; 0.45; 0.55) until 24h, are shown from Figures 7, 8, 9 and 10:

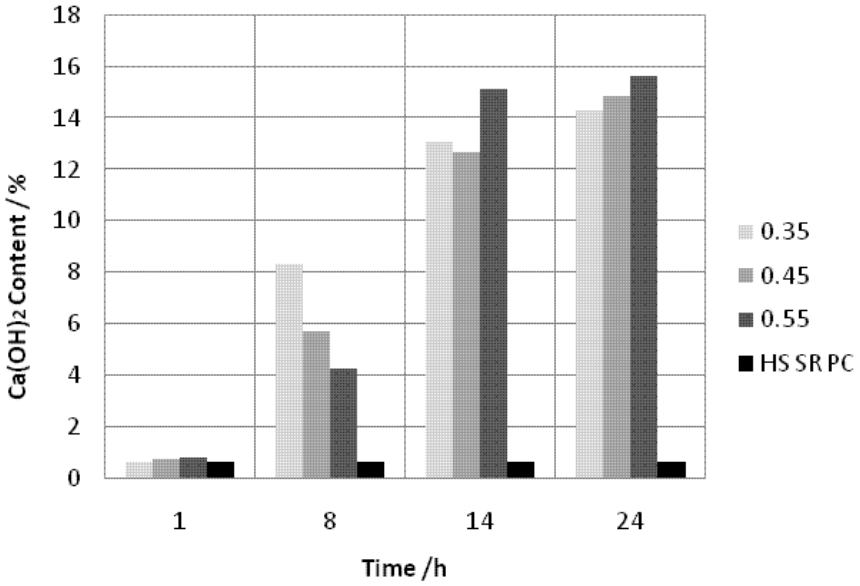

Fig. 7 – $Ca(OH)_2$ content on cement initial mass basis

Figure 7, shows the behavior of the calcium hydroxide content evolution for the three W/C ratios. Until 1h of hydration, the amount of $Ca(OH)_2$ formed is small for the three

pastes. At 8h, the lower is the W/C ratio, the higher is the formation of $Ca(OH)_2$, but at 14h, the sample with the highest W/C value (0.55) forms more $Ca(OH)_2$ than the other ones. Due to its highest free water content present at the first hours, the 0.55 W/C paste promotes the lowest increase of paste temperature, which decelerates the thermal-activation of the hydration reaction. This effect disappears for hydration times higher than 14h, due to the continuous consumption of more available free water for the hydration reactions in the operating conditions, forming more hydrated products than those formed in 0.35 and 0.45 W/C pastes.

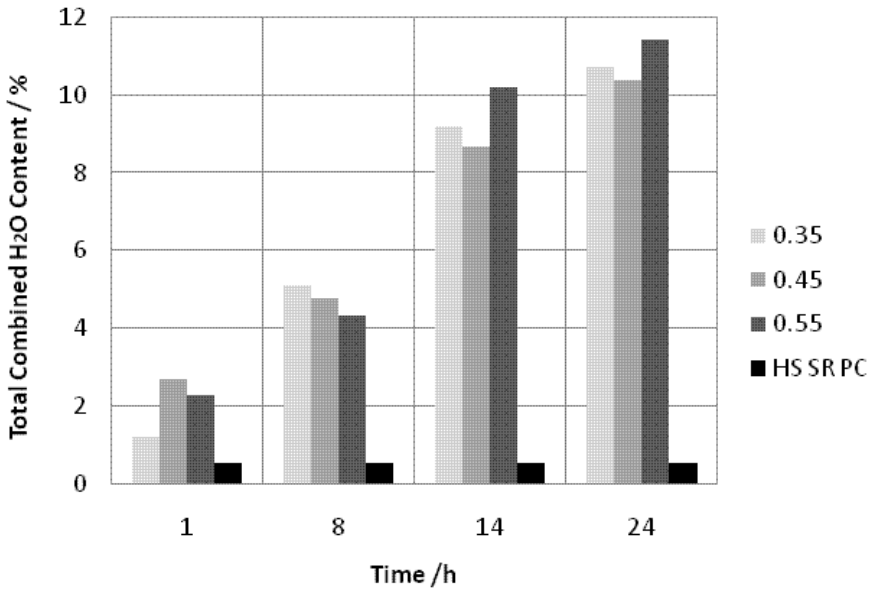

Fig. 8 – Total combined water content on cement initial mass basis

This assumption is confirmed from Figure 8, which shows that after 14h of hydration, the sample with 0.55 W/C ratio presents more total combined water than the other cases, although at 8h, the pastes with less humidity (0.35 and 0.45) present a higher cement hydration degree.

In the first hour, with more water available per cement mass, the pastes with 0.45 and 0.55 W/C ratios quickly form more initial hydration products than the 0.35 W/C paste. In the other hand, in the pastes with the highest W/C ratios, a decrease in the formation of hydration products occurs in the next hydration step until 8 hours of hydration, caused also by the retarding effect caused by ettringite formation during the first hour.

With a lower relative content of initial water the paste with 0.35 W/C ratio presents a lower content of formed hydration products at the end of 24 hour period, with respect to respective initial cement mass. However, the amount of combined water in case of

tobermorite + ettringite phases and in case of total amount of combined water is lower for w/c = 0.45, because the influence of total water content of the different studied pastes, on the kinetics behavior of the hydration reactions, depends on the hydration time.

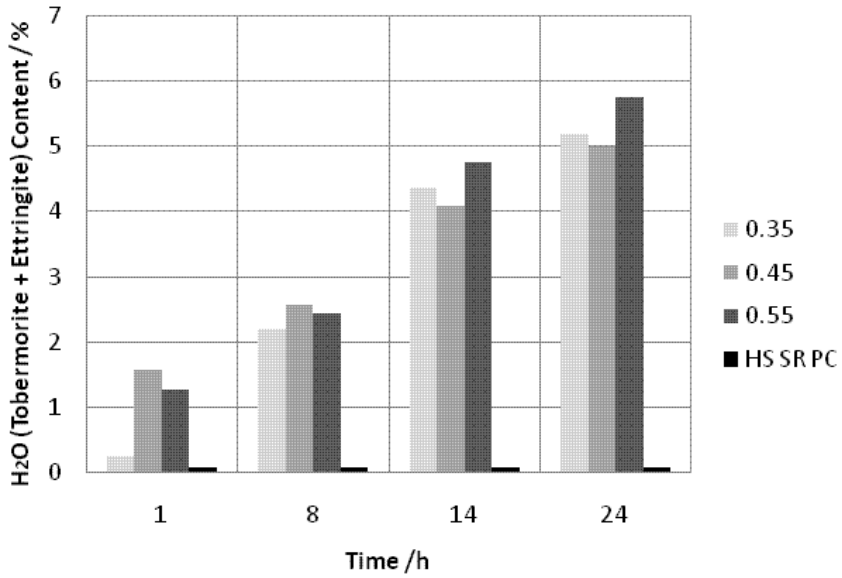

Fig. 9 – Content of water released from tobermorite and Ettringite phases on cement initial mass basis

From Figure 9 it can be seen that after 14h of hydration, the sample with 0.55 W/C ratio, forms more tobermorite and ettringite phases than the other cases. In the first hour, similarly to the total combined water content evolution, in the pastes with 0.45 and 0.55 W/C ratios, there is much more water released mainly from ettringite phase than from 0.35 W/C paste. At 8 hours of hydration a relative decrease occurs with respect to the water lost from tobermorite and ettringite in the pastes with higher W/C ratio.

It must be noticed that in the first hour, the water released from ettringite and tobermorite is mainly due to the dehydration of the former of this compounds, because during this period mostly ettringite is formed. Between 1 and 8 hours, induction period continues, when other hydration reactions slow down and then occurs the beginning of the acceleration period, where mainly are simultaneously formed tobermorite and calcium hydroxide and practically there is no ettringite formation [20]. Thus, the difference between the sum of the water released from tobermorite and ettringite phases at 8 and 1 hours (Dif_{8-1}) is due practically to tobermorite dehydration. As the paste with W/C =0,35 presents the lowest formation of ettringite at 1 hour and the highest value for

Dif_{8-1}, this difference is due mainly to a higher tobermorite formation, which explains the higher simultaneous formation of calcium hydroxide at 8 hours.

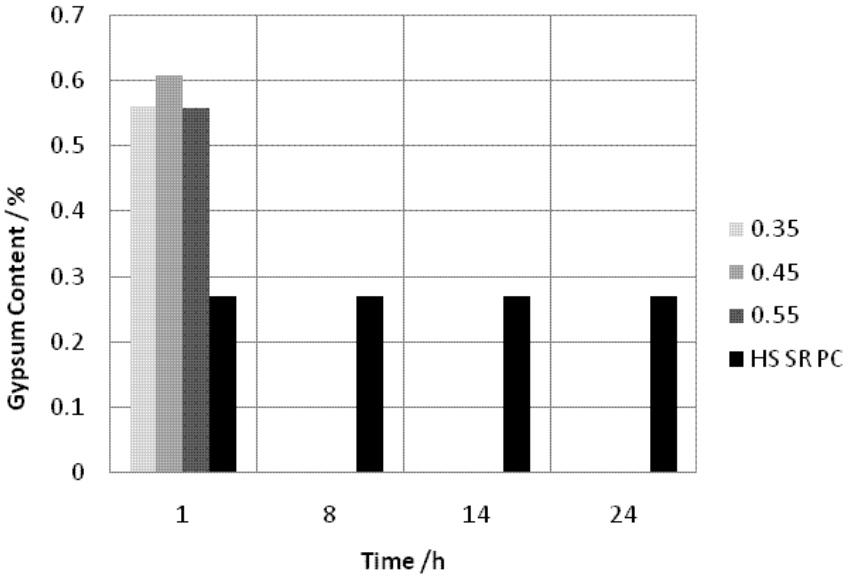

Fig. 10 – Gypsum content on cement initial mass basis

From Figure 10 it is seen that at 1h there is much more gypsum present than in the unhydrated cement which enhances ettringite formation. This fact is due to the rehydration of the of anhydrous calcium sulfate, which is formed during milling step to simultaneously mix and mill the clinker with the gypsum and calcium carbonate added as aggregates [16] of the manufactured cement. After 8h of hydration, the samples lose all the gypsum present in the beginning stages, which is consumed in the formation of ettringite.

5.Conclusions

- The water/cement ratio plays a definite role in the kinetics of the cement hydration reaction kinetics and consequently in the formation of the hydration products.
- Thermogravimetric and Derivative Thermogravimetric Analysis allow one to quantify the hydrated products and to evaluate the influence of the W/C ratio in the reactions that occur in the first 24h of Portland cement hydration.
- Changing TG and DTG data to initial cement mass basis, based on the fact that the calcined compositions of all pastes and that of the calcined anhydrous cement are equal, more accurate values of the different phase contents can be estimated to study

the effect of the W/C ratio on the cement hydration kinetics.

- From the analysis of the contents of the main formed products on cement initial mass basis of each paste as a function of the hydration time, the pastes with 0.55 W/C ratio, form in the first 24h more hydrated products than the other 0.35 and 0.45 W/C cases.
- The influence of total water content of the different studied pastes, on the kinetics behavior of the hydration reaction, depends on the hydration time.
- Between 1 and 8 hours, where there is more available water and the pastes are more diluted, the amount of cement controls the kinetics of hydration reactions and, in this case, the higher available free water promotes a higher cooling effect on the temperature of the paste, decreasing the thermal activation of the hydration reactions. Thus, during this period, the paste with 0.55 W/C ratio, forms less total combined water than in the other lower W/C cases.
- As free water is more consumed, for hydration times equal or higher than 14 hours of hydration, which correspond to the accelerating and post-accelerating cement hydration stages, the available free water controls the hydration process and there is a higher formation of hydrated products. Thus, the paste prepared with W/C=0.55 presents more hydrated products and total combined water than the pastes with W/C = to 0.35 and 0.45.

Acknowledgments The authors acknowledge the experimental assistance of the Chemical School Thermal Analysis and Civil Engineering Structure Laboratories and the financial support of the National Research Council (CNPq).

References

1. Melchert, Maura B. M.; Viana, Marcelo M.; Lemos, Mariana S.; Dweck, Jo; Buechler, Pedro M. Simultaneous solidification of two catalyst wastes and their effect on the early stages of cement hydration. J Therm Anal Calorim, 2011; 105(2), 625-33.

2. Chaipanich, A; Nochaiya, T. Thermal analysis and microstructure of Portland cement-fly ash-silica fume pastes. J Therm Anal and Calorim, 2010; 99(2), 487-93.

3. Stepkowska, E. T.; Perez-Rodriguez, J. L.; Justo, A.; Sanchez-Soto, P. J.; Aviles,

M A.; Bijen, J. M. J. M. Variations in water sorption and in thermogravimetry of a Portland cement . Thermo Acta 1993; 214(1), 97-102.

4. Gruyaert, E.; Robeyst, N.; De Belie, N. Study of the hydration of Portland cement blended with blast-furnace slag by calorimetry and thermogravimetry. J Therm Anal Calorim 2010; 102(3), 941-51.

5. Dweck, J.; Ferreira da Silva, P. F.; Buechler, P. M.; Cartledge, F. K. Study by thermogravimetry of the evolution of ettringite phase during type II portland cement. J Therm Anal Calorim 2002; 69(1), 179-86.

6. Guirado, F.; Gali, S.; Chinchon, J. S. Thermal decomposition of hydrated alumina cement (CAH10). Cem Concr Res, 1998; 28(3), 381-90.

7. Parrott, Leslie J.; Geiker, Mette; Gutteridge, Walter A.; Killoh, David. Monitoring portland cement hydration: comparison of methods. Cem Concr Res, 1990; 20(6), 919-26.

8. De Weerdt, K.; Ben Haha, M.; Le Saout, G.; Kjellsen, K. O.; Justnes, H.; Lothenbach, B. Hydration mechanisms of ternary Portland cements containing limestone powder and fly ash. Cem Concr Res, 2011; 41(3), 279-91.

9. Vessalas, K.; Thomas, P. S.; Ray, A. S.; Guerbois, J.-P.; Joyce, P.; Haggman, J. Pozzolanic reactivity of the supplementary cementitious material pitchstone fines by thermogravimetric analysis. J Therm Anal Calorim, 2009; 97(1), 71-6

10. Trezza, M. A.; Scian, A. N. Waste fuels: their effect on Portland cement clinker. Cem Concr Res, 2005; 35(3), 438-44.

11. Pacewska, B.; Wilinska, I.; Bukowska, M. Hydration of cement slurry in the presence of spent cracking catalyst. J Therm Anal Calorim, 2000; 60(1), 71-8.

12. Dweck, J.;Cunha, A.L.C., Pinto, C.A., Gonçalves, J.P., Büchler, P.M. - Thermogravimetry on calcined mass basis – hydrated cement phases and pozzolanic activity quantitative analysis - J Therm Anal Calorim, 2009; 97, 85–9.

13. Escalante, J. I.; Mendoza, G.; Mancha, H.; Lopez, J.; Vargas, G. Pozzolanic properties of a geothermal silica waste material. Cem Concr Res, 1999; 29(4), 623-25.

14. Mehta, P. K, Monteiro, P. J. M. Concrete, Microstructure, Properties and Materials. 3 ed. IBRACON, 2008. (In Portuguese)

15. Alarcon Ruiz. L, Platret. G, Massieub. E, Ehrlacher. A. The use of thermal analysis in assessing the effect of temperature on a cement paste. Cem. Concr. Res. 2005; 35,609-13.

16. Dweck. J, Buchler. P. M, Coelho. A. C. V, Cartledge. F. K. Hydration of a Portland cement blended with calcium carbonate. Thermoch Acta, 2000; 346: 105-13.

17. Knopf . F .C, Roy. A, Samrow. H. A, Dooley. K. M. High-Pressure Molding and Carbonation of Cementitious Materials Materials and Interfaces. Ind. Eng.Chem.Res, 1999;38, 2641-649.

18. BRAZILIAN ASSOCIATION OF TECHNICAL STANDARDS. High Initial Strenght Portland Cement. NBR 5733; Rio de Janeiro, 1991. (In Portuguese)

19. BRAZILIAN ASSOCIATION OF TECHNICAL STANDARDS. Moderate Sulphate Resistance Portland Cement and Moderate Hydration Heat (MRS) and High Sulphate Resistance. NBR 5737; Rio de Janeiro, 1986. (In Portuguese)

20. Lea´s, Chemistry of Cement and Concrete, 4th Ed., Arnold, London, 1998;270.

ARTIGO B - Neves Junior A, Lemos M.S, Toledo Filho R.D, Dweck J, Fairbairn E.M.R. Early Stages Hydration of High Initial Strenght Portland Cement – Part II – NCDTA and Vicat analysis. Journal of Thermal Analysis and Calorimetry, v. 113, p.659-665, 2013.

Early Stages Hydration of High Initial Strenght Portland Cement – Part II – NCDTA and Vicat analysis.

Alex Neves Junior[a], Mariana Santos Lemos[b], Romildo Dias Toledo Filho[a], Jo Dweck[b] and Eduardo de Moraes Rego Fairbairn[a]

[a] Civil Engineering Program – COPPE – Rio de Janeiro Federal University, Brazil

[b] School of Chemistry - Rio de Janeiro Federal University, Brazil.

Journal of Thermal Analysis and Calorimetry

2013

Abstract

This work complements a quantitative thermogravimetric study of the first 24 hours of hydration of a High Initial Strength and Sulphate Resistant Portland Cement (HS SR PC) by using Non-Conventional Differential Thermal Analysis (NCDTA) and Vicat Needle method. Different water/cement (W/C) ratios from 0.35 to 0.85 were used to evaluate the most indicated operating conditions to maximize calcium hydroxide production for further use in CO_2 capture. Thermogravimetric analysis data performed at 4 and 24h of hydration were also compared to the NCDTA and Vicat data for each kind of paste, to analyze the influence of the W/C ratio on the simultaneous hydration and setting process. The increase of the W/C ratio increases the induction time retards the solidification and setting processes but increases the hydration degree as the W/C ratio is increased from 0.45. At 24 hours, products prepared with 0.35 W/C ratio present a little higher hydration degree than those prepared with W/C = 0.45, because of the highest level of temperature in the reacting mixture in the former case, during the first 8 hours. There is a practical limit of W/C=0.66 to prepare the pastes, due to a limit of the miscibility between HS SR PC and water, above which, the excess of water forms a separated phase that does not interfere in the hydration process.

Keywords: HS SR Portland Cement, Early Stage Hydration, NCDTA, Vicat Analysis.

1.Introduction

Thermogravimetric (TG) and Derivative Thermogravimetric (DTG) analysis have been used in the comprehension and in the study of the hydration reactions in cementitious pastes [1-4]. Through the quantitative determination of the main formed hydration products, TG and DTG data allow the study of the effects of different additives [5-9] including their pozzolanic activity when is the case [10-13].

Differential Thermal Analysis (DTA) has been used as a tool to analyze thermal effects, through the measurement of the temperature difference between a sample and an inert reference, when both are submitted to an external heating or cooling device [14]. In NCDTA, these external devices are not used, the system operates semi-adiabatically and the same difference is measured, due to the thermal effects promoted by the spontaneous cement hydration exothermal reactions [1].

The effect of the W/C ratio on cement hydration degree has been studied by backscattered electron imaging, showing a good relation with data obtained by thermogravimetry [15]. By nitrogen adsorption and mercury intrusion porosimetry of hydrated portland cement pastes, the pore structure of hydrated cements show that as W/C ratio is increased, the resulting porosity is increased [16]. As pastes with same porosity have same permeability, at a given hydration age and a given W/C ratio, pastes made from coarse-ground cements have higher permeability values than those from fine-ground cements which hydrated rapidly [17], as is the present cement case.

According to the literature data [18], and of a previous work of the authors [19] it was noticed by thermogravimetry that the increase of the W/C ratio, from 0.35 to 0.55, increases the hydration degree in the first 24 hours of high initial strength and sulphate resistant Portland cement (HS SR PC) hydration, due to the increase of the amount of total reacted water.

In this work, the hydration behavior of HS SR PC pastes during their first 24 hours of hydration was evaluated from NCDTA [1] and TG/DTG curves and the mechanical behavior, from Vicat Method measurements. W/C ratios equal to 0.35, 0.45, 0.55, 0.65, 0.75 and 0.85 were used to evaluate the influence of the W/C ratio on the cumulative energy evolved as a function of hydration time and on the initial and final setting times, as well as to investigate if a significant increase of the relative amount of water, keeps increasing the hydration degree as noticed for lower W/C ratios [19].

The results of the present paper can be applied for the HS SR PC. For other types of cement, specific studies must be performed. The aim of this paper was to complement part I with data referring to higher W/C conditions and to compare, at the early stages, the kinetics of the evolution of the mechanical resistance (by Vicat method) with that of the hydration process (by NCDTA) as a function of the increasing W/C ratio.
It is well known that the increase of the W/C decreases the mechanical resistance of cementitious materials. However, the motivation of this work was to obtain products with increased porosity of the matrix, through the increase of the water content, at maximized calcium hydroxide production conditions, to allow their future use for CO_2 absorption. For a same W/C ratio, the use of a high initial strength cement allows obtaining higher final mechanical properties than when using lower initial strength cements.

2. Materials

In this study, a Lafarge High Initial Strength and Sulphate Resistant Portland Cement (HS SR PC) [20] was used, which allows to reach high strengths at early hydration stages. The development of high initial strength is due to the use of a different proportion of limestone and clay in the production of the clinker than that used in usual Portland cement manufacture, as well as due to a higher milling degree of the cement, in order to accelerate its reactions with water, by the higher specific external area of the particles, reaching a higher strength in a shorter time.

This kind of cement may have a maximum of 5% of carbonates addition and aggregation of blast furnace slag or pozzolanic materials [21].

3. Methods

A simplified schematics of the NCDTA, is presented in Figure 1. It is a system that consists in two main cups, one containing an inert reference material, which in the present case is a hydrated HS SR PC cement paste, aged more than 3 months and the other one, containing the paste sample. Each cup is isolated by an external polystyrene cup and has a cover through which a thermistor with 0.03^{o}C resolution is introduced to measure the reference or sample temperature (T_{ref} or T_s). The temperature data acquisition is done by a controller and an interface, linked to a computer to measure the temperature difference between sample and reference on real time.

In NCDTA procedures, pastes with W/C from 0.35 to 0.85 were prepared as follows: the cement was inserted in each cup, previously containing the proper amount of deionized water where homogenization was manually done for 30 seconds. Then, the cup was covered and the thermistor was introduced in vertical position through a hole at the center of the cover of each cup. Before inserting the thermistor its external surface was protected by a very thin polyethylene film. Temperature data were collected during the first 24hours of hydration, every minute.

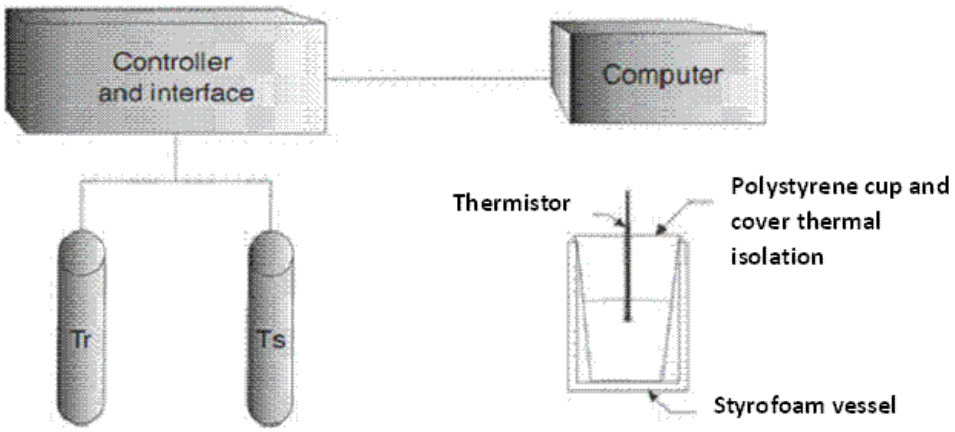

Fig 1– Simplified schematics of the NCDTA system.

The method to measure the consistency change of the pastes as a function of time was the Vicat Analysis, performed according to Brazilian Standard Method (NBR11581) [22], which measures the Vicat needle's penetration in a paste as it's setting process occurs. Pastes with W/C of 0.65 to 0.85 were also prepared for thermogravimetric analysis, to complete the previous work (part I) [19], in which details of the preparation of the pastes and of the sampling processes are described.

The thermal analyses were performed in a TA Instruments, SDT Q600 model TGA/DTA/DSC simultaneous apparatus with the same operating conditions than in part I: heating rate of 10 °C min^{-1}, from 35 to 1000°C, and using 100 mL min^{-1} of nitrogen flow. Before this, the samples were dried inside the equipment initially at 1°C min^{-1} from 30 to 35°C, followed by a drying isothermal step at 35°C for 1 h, to eliminate the residual non combined free water [12].

4. Results and Discussion

Figure 2 presents the NCDTA curves the pastes with W/C ratio from 0.35 to 0.85.

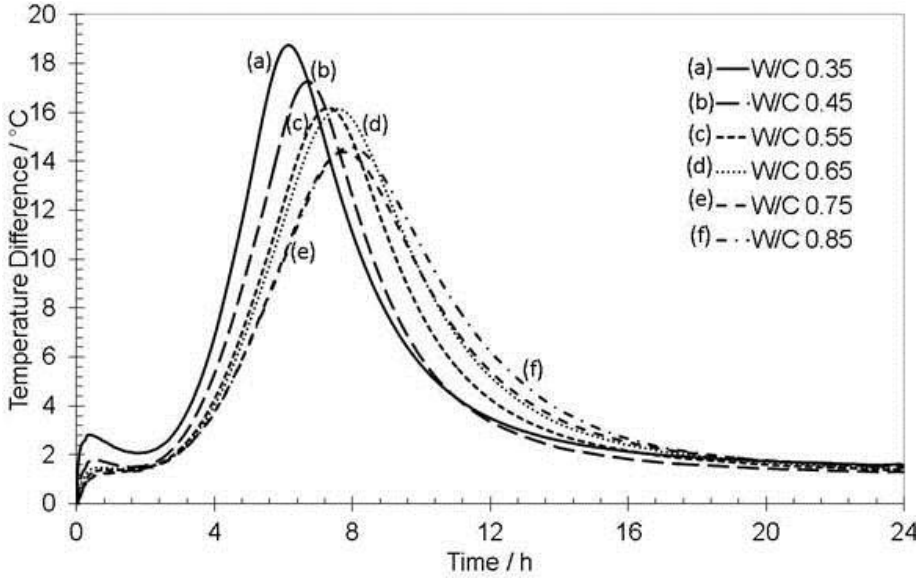

Fig 2–NCDTA curves for the pastes from 0.35 to 0.85 W/C ratio in the first 24h of hydration.

We can see from the NCDTA curves in Figure 2, that during the pre-induction and induction phases (first two hours), corresponding to the initial ettringite formation, the 0.35 W/C case shows the highest formation of this phase. During the acceleration period (from the 2nd to 7th hour), the highest tobermorite + calcium hydroxide initial formation occurs in 0.35 case, indicated by respective highest NCDTA peak in Fig.2. These two occurrences confirm respective results obtained by TG/DTG in Part I [19].

During the acceleration step, which is responsible mainly for the formation of tobermorite and $Ca(OH)_2$, the influence of the water content becomes visible. The higher is the W/C ratio, the lower is the maximum ($T_s - T_{ref}$) difference and the higher is the time when this maximum occurs. To distinguish correctly the behavior of the curves it would be necessary to normalize them. This is not possible in the 0.75 and 0.85 W/C ratio cases due to the fact that a separate aqueous phase appeared due to the significant excess of water added to hydrate the same cement mass in these cases.

For the pastes from 0.35 to 0.65 W/C ratio, where the pastes were homogeneous, it was possible to normalize the respective NCDTA curves, as detailed in a previous work [23] and by integration, to obtain the respective cumulative energy curves, in arbitrary units as presented in Figure 3.

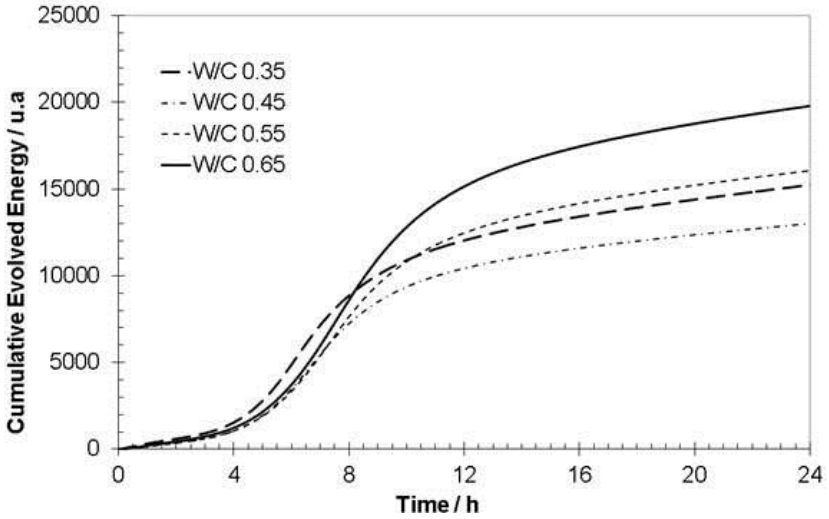

Fig 3–Cumulative evolved energy for the pastes with W/C ratios 0.35 to 0.65 in the first 24h of hydration.

We can see from the Figure 3 that from 0.45 to 0.65 W/C, which presents the highest total cumulative energy evolved from hydration reactions at 24 hours, the higher is the water content, the higher is the released energy from the hydration reactions. After 8h, (when the acceleration period was already occurring) the difference among the three cases is more evident, which can be seen from the increasing difference of cumulative energy for each case.

It must be noted that during the first 8 hours, as it was also noted by the total combined water content estimated by thermogravimetry in Part I, the total accumulated released energy was higher for the 0.35 case, because of its higher reacting mixture temperature in this period. This fact caused a higher final accumulated evolved energy at 24h for 0.35 case when compared to 0.45 case, although both cases apparently show in respective NCDTA curves a same total energy generated from respective hydration reactions within the 8 to 24 h period.

We can notice that for the 0.45 to 0.65 W/C cases, at 24 hours hydration, the increase of the cumulative energy is directly proportional to the increase of respective initial water content of the mixture, confirming our previous conclusion by thermogravimetry [19] that up to the W/C=0.65 case, the higher is the initial W/C ratio, the higher is the hydration degree, at 24hrs of hydration.

Thus, during the first hours of hydration, where the pastes are more fluid, the cement content is the regulating factor of the hydration kinetics, with limited released energy,

registered by the practically same difference temperature between each sample and reference, as indicated by the close NCDTA curves.

On the other hand, with further water consumption by the hydration reactions in the following period, the water becomes the main regulating factor of the hydration process, showing that more fluid pastes release more heat, which is expressed by the cumulative energy at the end of the first 24h of hydration, except for the 0.75 and 0.85 W/C ratio cases, which could not be compared, because they formed two phases. This will be done by thermogravimetry, as follows.

Considering that the thermogravimetric analysis of the original cement provides as final residues the cement oxides, the final residue of the pastes at 1000^{o}C, corresponds to the same resultant oxide composition of the original cement [12, 19].

The TG curves for the 0.65, 0.75 and 0.85 W/C ratio cases on initial cement mass basis of the 4h and 24h hydration samples are presented respectively in Figures 4 and 5.

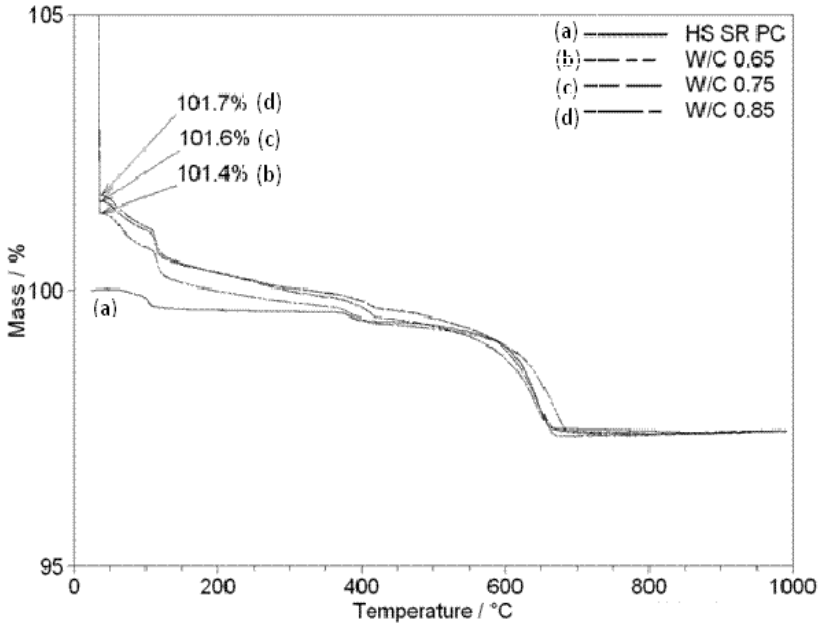

Fig 4– TG Curves of the unhydrated HS SR PC and of the 0.65, 0.75 and 0.85 W/C pastes at 4h of hydration on initial cement mass basis.

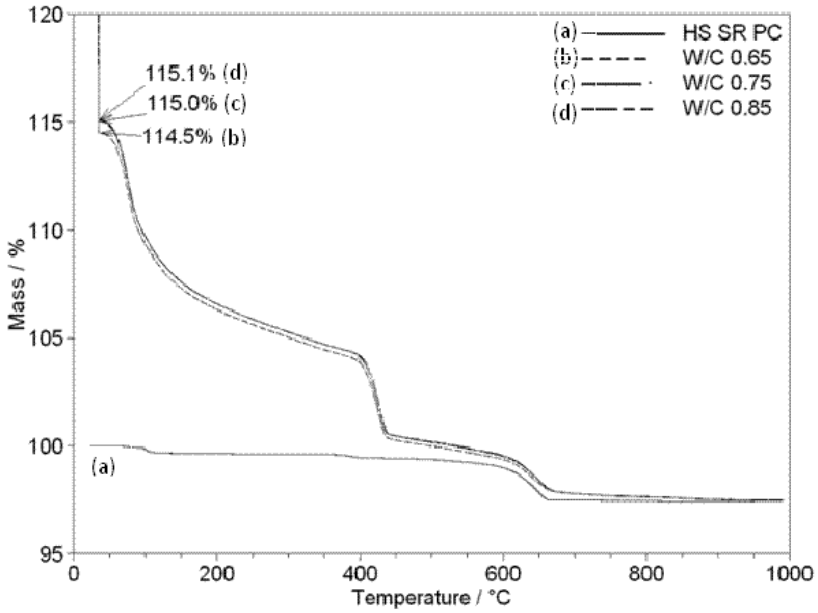

Fig 5–TG Curves of the unhydrated HS SR PC and the 0.65, 0.75 and 0.85 W/C pastes at 24h of hydration on initial cement mass basis.

We can see, on initial cement mass basis that the amount of hydrated products, continues to increase with the hydration time [19].

We notice that at 4h of hydration, there are some differences between the curves that completely disappear with 24h of hydration, showing that there is a limit on the hydration degree, expressed by the approximation of the three curves right after the drying step at 35°C. Thus, the amount of excess water, that forms another phase above the paste, does not practically contribute to an extra hydration.

From the DTG curves of Figures 6 and 7 we can see that the most fluid pastes tend to produce less hydrated products, in the earlier stages, but this restriction, caused by the water content, disappears at 24h, due to the water consumption through the hydration reaction [19].

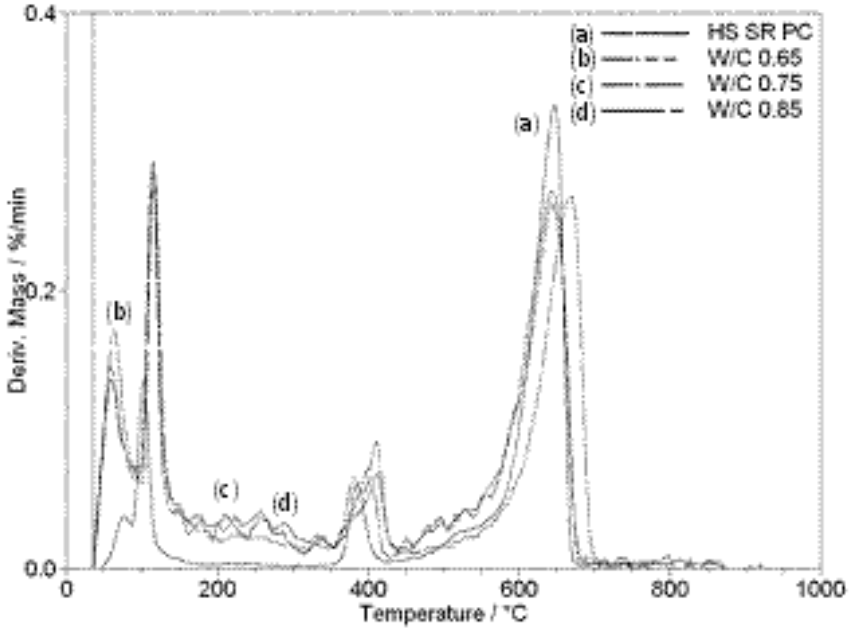

Fig 6– DTG Curves of the unhydrated HS SR PC and the 0.65, 0.75 and 0.85 W/C pastes at 4h of hydration on initial cement mass basis.

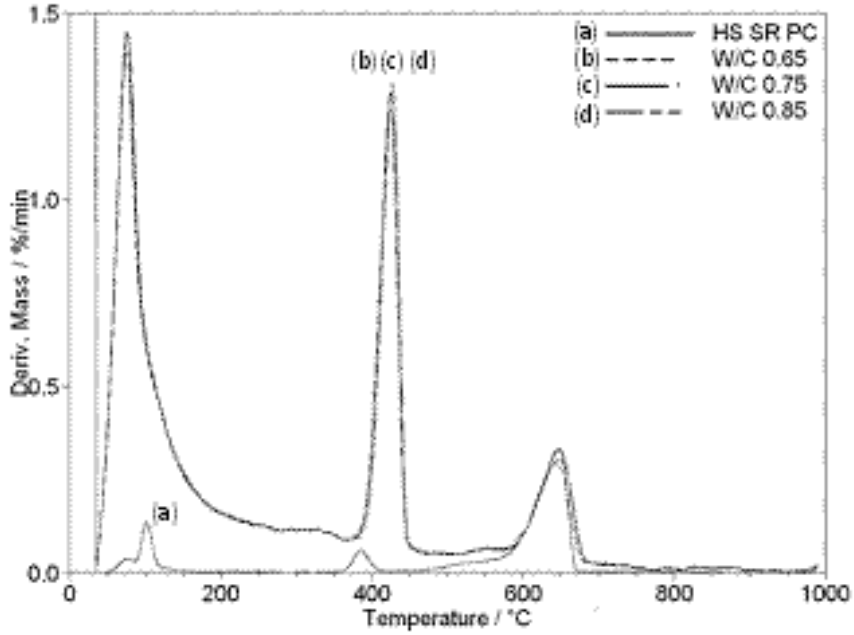

Fig 7– DTG Curves of the unhydrated HS SR PC and the 0.65, 0.75 and 0.85 W/C pastes at 24h of Hydration on initial cement mass basis.

Considering the temperature decomposition steps of the main hydrated phases [23], we can evaluate from TG curve with more accuracy the amount of hydrated phases, for 4 and 24h of hydration on initial cement mass basis. Thus, for the 0.65, 0.75 and 0.85 W/C ratio cases, the amount of total combined water, the amount of water released from

tobermorite and ettringite dehydration and the amount of $Ca(OH)_2$ on the initial cement mass basis at 4h and 24h of hydration, are presented respectively in Figures 8 and 9.

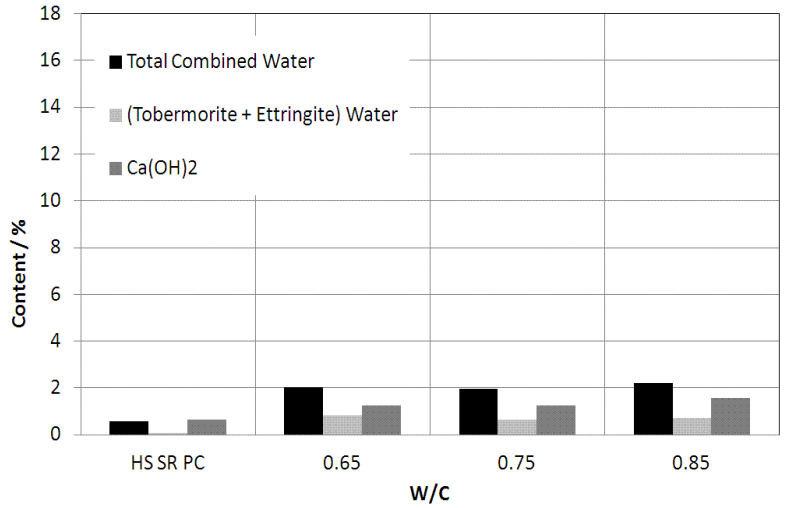

Fig 8– Content of hydrated products at 4h of hydration on initial cement mass basis and of unhydrated HS SR PC.

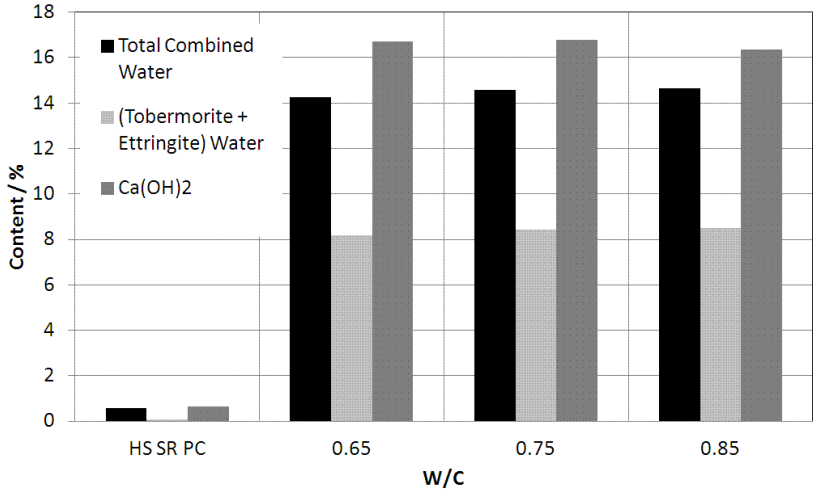

Fig 9– Content of hydrated products at 24h of hydration on initial cement mass basis and of unhydrated HS SR PC.

We can see an increase of the amount of hydrated products with the increase of the hydration time. For 24h of hydration, we notice that for the 0.75 and 0.85 W/C ratio cases, the amount of formed hydrated products is the same, confirming the tendency of a limit of the cement hydration degree for these pastes.

Figure 10 presents for the pastes with W/C ratio from 0.35 to 0.65 the results for the total combined water content. By extrapolation, it can be estimated that, the paste phases of the 0.75 and 0.85 W/C cases, which presented the same approximated 14.60%

of total combined water, actually, correspond to a W/C ratio equal to 0.66. This is the actual maximum W/C ratio of the 0.75 and 0.85 paste phases.

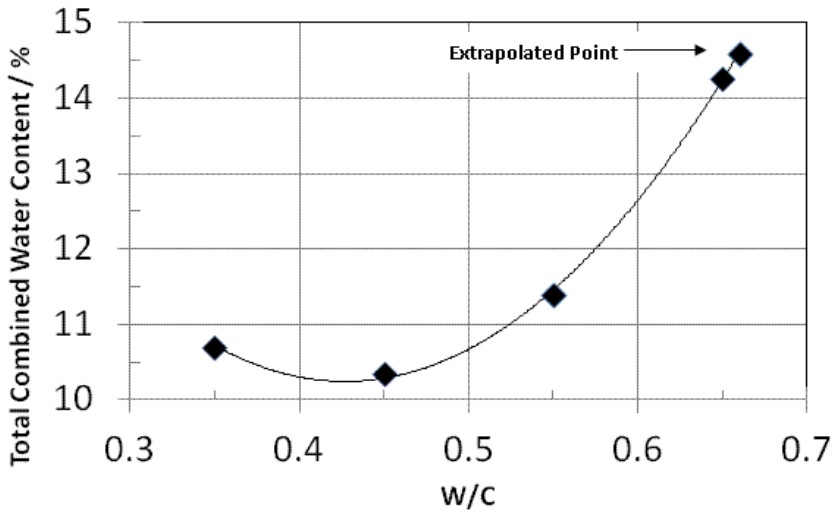

Fig 10– Content of total combined water at 24h of hydration on initial cement mass basis for W/C ratios 0.35 to 0.65 and for the extrapolated value for the limit case, which total combined water was measure by TG.

It becomes clear, through Figure 10, that the increase of the water content from 0.45 to 0.65 W/C ratio contributes effectively for the increase of hydrated phases. But there is a maximum limit of effective W/C ratio in the reacting medium, apparently at W/C=0.66, above which, the excess of water forms a separate aqueous phase, that does not interfere in the final results.

The higher value of the total combined water at 0.35 W/C case, when compared to the 0.45 W/C case, as previously discussed with NCDTA results, is due mainly to the fact that during the first 8 hours of hydration, the lower W/C ratio of the former case, caused a higher mean mixture temperature than in 0.45 W/C case, which in turn accelerated and enhanced hydration reactions, confirming that up to 8h, the relative cement content dictates the hydration reactions, whereas, between 8 and 24 hours, the relative water content influences more the hydration reactions.

Figure 11 presents, for the pastes with W/C ratio from 0.35 to 0.85 the results of the initial (IS) and final setting (FS) times by Vicat analysis.

We can see that, the higher is the W/C ratio, the higher are the initial and the final of setting times.

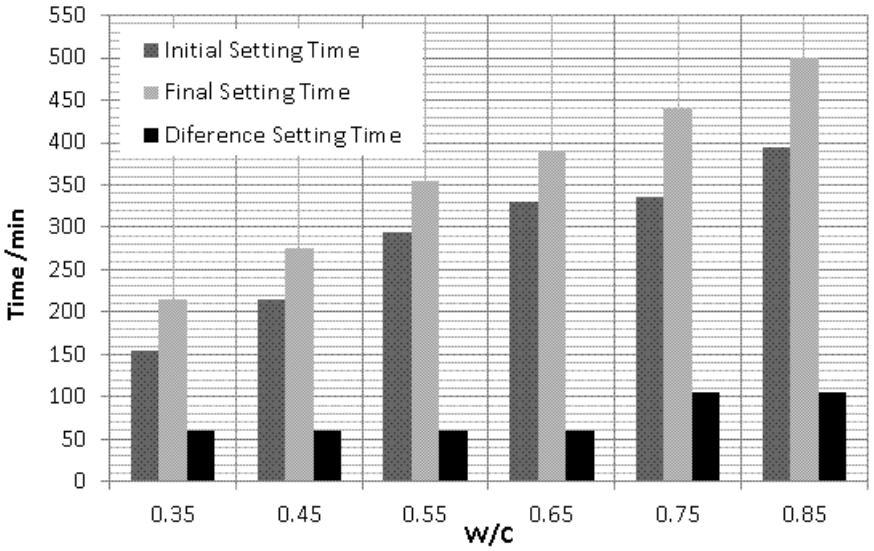

Fig 11–Vicat initial and final setting times curves and their difference as a function of W/C ratio in HS SR PC hydration.

The (IS – FS) difference is practically the same for 0.35 to 0.65 cases. However, this difference increases for 0.75 and 0.85 W/C cases, which present another same value. Figures 12 to 17 present three NCDTA curves, for the cases 0.35 (less fluid) to 0.85 (more fluid), with the indication of the points at their respective Vicat initial and final setting times.

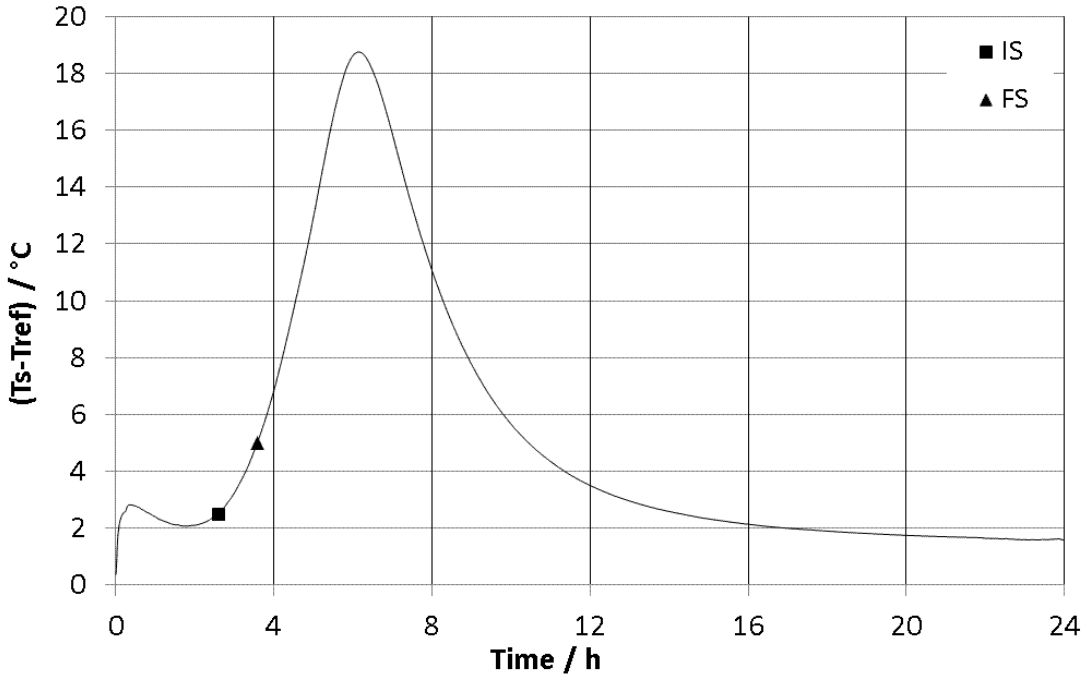

Fig 12–0.35 W/C ratio NCDTA curve with indication of the respective Vicat initial and final setting times.

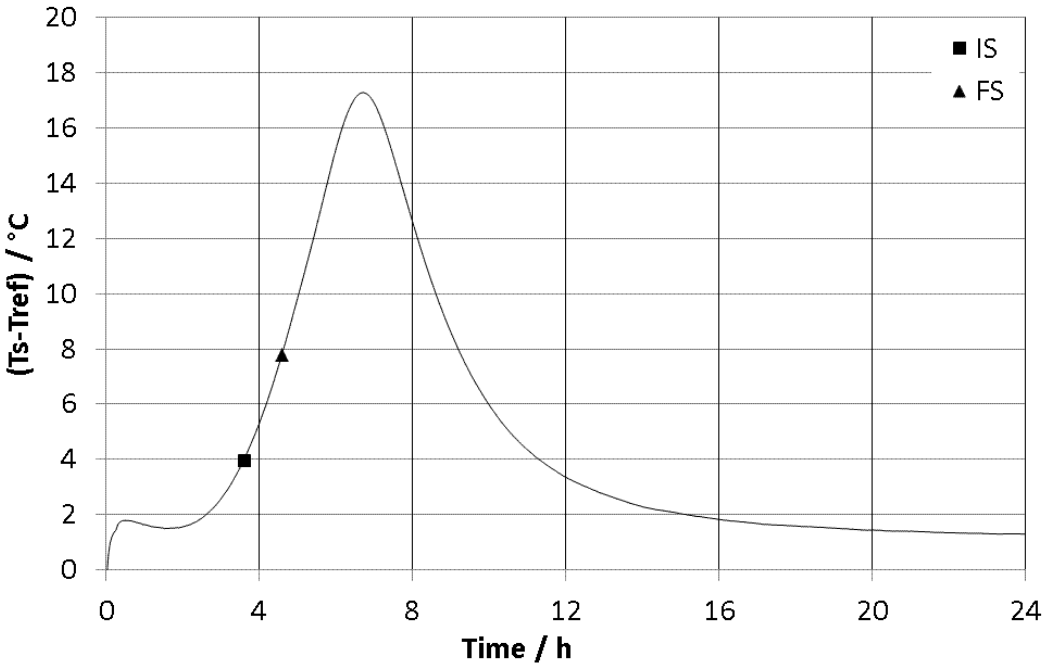

Fig 13– 0.45 W/C ratio NCDTA curve with indication of the respective Vicat initial and final setting times.

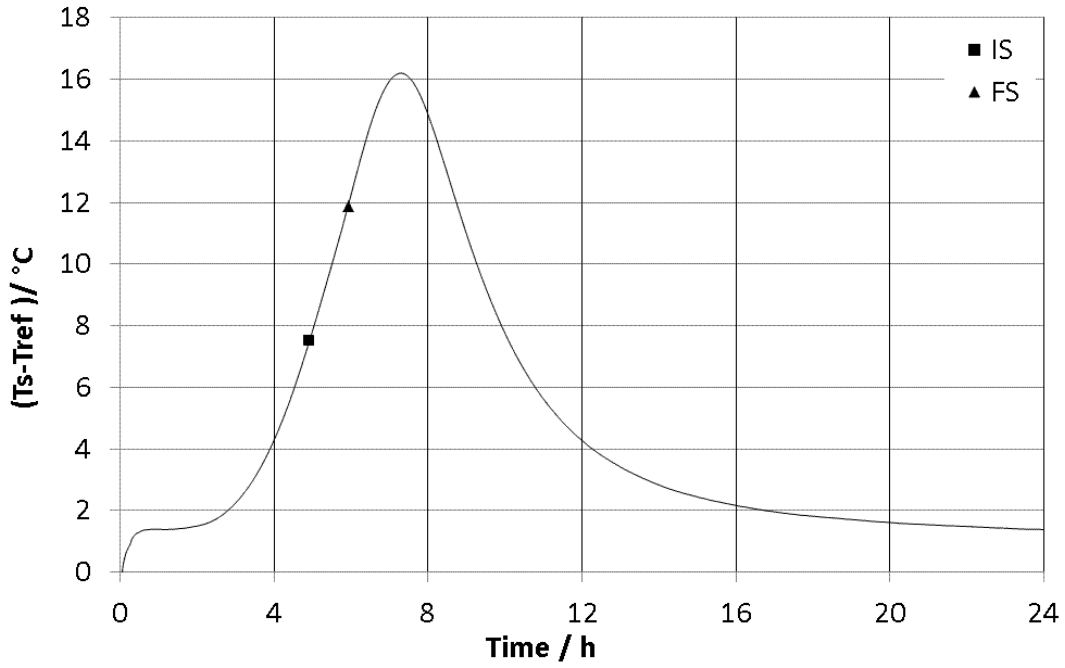

Fig 14– 0.55 W/C ratio NCDTA curve with indication of the respective Vicat initial and final setting times.

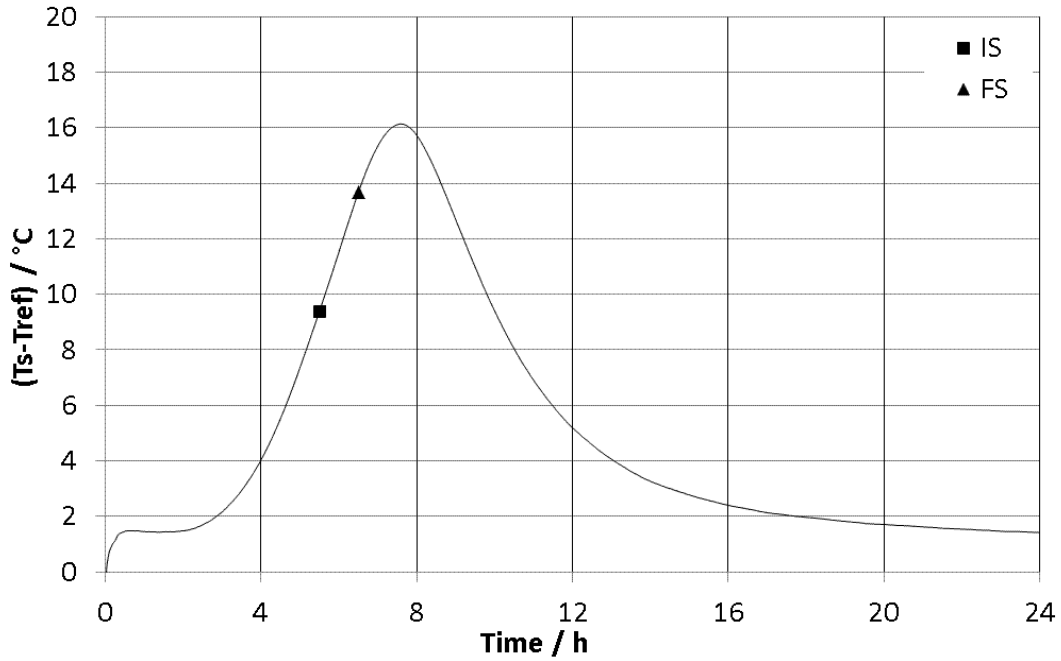

Fig 15– 0.65 W/C ratio NCDTA curve with indication of the respective Vicat initial and final setting times.

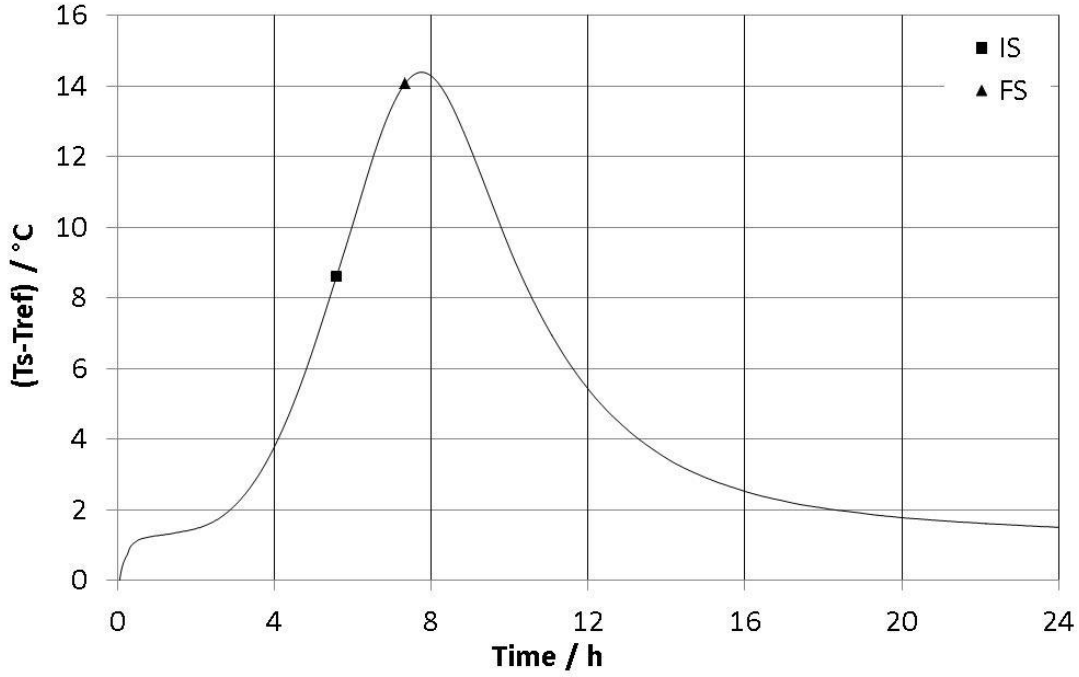

Fig 16– 0.75 W/C ratio NCDTA curve with indication of the respective Vicat initial and final setting times.

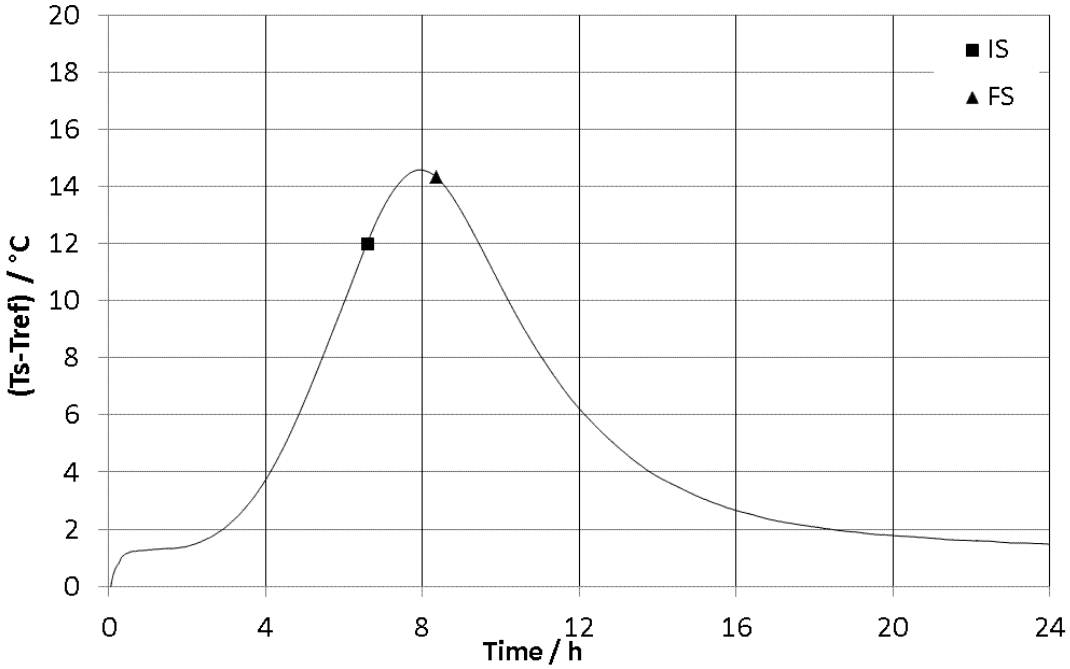

Fig 17– 0.85 W/C ratio NCDTA curve with indication of the respective Vicat initial and final setting times.

It can be noticed, from Figures 12, 13, 14, 15, 16 and 17, that independently of the fact that the increase of the water content in the mixture, provides or not an increase on the amount of the hydrated products, it always promotes an increase of Vicat initial and final setting times. In other words, the higher is the W/C ratio the longer will be the setting and solidification process of the pastes.

It can also conclude from Figures 12, 13, 14, 15, 16 and 17, that the higher is the W/C ratio, the higher must be the HS SR PC hydration degree to have a same mechanical resistance. As an example of this fact at the highest W/C ratio, the final of setting occurs during the deceleration period of the hydration process.

5.Conclusions

- From Non-Conventional Differential Thermal Analysis and Thermogravimetry on initial cement mass basis, it can be seen that in the range that was studied, at 24 hours of setting, the increase of the W/C ratio initially causes a little decrease on the hydration degree, after which only increases up to a limit, where there is a maximum calcium hydroxide formation.
- The hydration limit is due to the maximum miscibility of the water with cement,

above which, a separate aqueous phases is formed, which in turn does not interfere with the hydration process.

- By Vicat method it can be seen that for all cases, when W/C ratio increases, increasing the water content of the paste, both initial and final setting times increase. Thus a higher W/C ratio produces more fluid pastes at a same initial time of hydration, independently of having formed a separate aqueous phase.
- The final of setting time measured by Vicat method, which represents a same mechanical compressive resistance condition, occurs at higher hydration degrees, as the W/C ratio is increased. This indicates that the delay of the solidification process, which was also seen from NCDTA curves, is increased as the W/C ratio increases and does not present a limit as occurs for the hydration process.

Acknowledgments The authors acknowledge the experimental assistance of the Chemical School Thermal Analysis and Civil Engineering Structure Laboratories and the financial support of the National Research Council (CNPq).

References

1. Melchert MBM, Viana MM, Lemos MS, Dweck J, Büechler PM. Simultaneous solidification of two catalyst wastes and their effect on the early stages of cement hydration. J Therm Anal Calorim. 2011; 105(2):625-33.
2. Chaipanich A, Nochaiya T. Thermal analysis and microstructure of Portland cement-fly ash-silica fume pastes. J Therm Anal and Calorim. 2010; 99(2):487-93.
3. Dweck J, Buchler PM, Coelho ACV, Cartledge FK. Hydration of a Portland cement blended with calcium carbonate. Thermochim Acta. 2000; 346:105-13.
4. Gruyaert E, Robeyst N, De BN. Study of the hydration of Portland cement blended with blast-furnace slag by calorimetry and thermogravimetry. J Therm Anal Calorim. 2010; 102(3):941-51.
5. Dweck J, Silva, PFF, Buechler, PM, Cartledge FK. Study by thermogravimetry of the evolution of ettringite phase during type II Portland cement. J Therm Anal Calorim. 2002; 69(1):179-86.
6. Guirado F, Gali S, Chinchon JS. Thermal decomposition of hydrated alumina cement

(CAH10). Cem Concr Res. 1998; 28(3):381-90.

7. Parrott LJ, Geiker M, Gutteridge WA, Killoh, D. Monitoring portland cement hydration: comparison of methods. Cem Concr Res. 1990; 20(6):919-26.

8. De Weerdt K, Ben HahaM.; Le Saout G, Kjellsen KO, Justnes H, Lothenbach, B. Hydration mechanisms of ternary Portland cements containing limestone powder and fly ash. Cem Concr Res. 2011; 41(3):279-91.

9. Vessalas K, Thomas PS, Ray AS, Guerbois J-P, Joyce P, Haggman J. Pozzolanic reactivity of the supplementary cementitious material pitchstone fines by thermogravimetric analysis. J Therm Anal Calorim. 2009; 97(1):71-6

10. Trezza MA, Scian AN. Waste fuels: their effect on Portland cement clinker. Cem Concr Res. 2005; 35(3):438-44.

11. Pacewska B, Wilinska I, Bukowska M. Hydration of cement slurry in the presence of spent cracking catalyst. J Therm Anal Calorim. 2000; 60(1):71-8.

12. Dweck J, Cunha ALC, Pinto CA, Gonçalves JP, Büchler PM. Thermogravimetry on calcined mass basis – hydrated cement phases and pozzolanic activity quantitative analysis. J Therm Anal Calorim. 2009; 97: 85–9.

13. Escalante JI, Mendoza G, Mancha H, Lopez J, Vargas G. Pozzolanic properties of a geothermal silica waste material. Cem Concr Res. 1999; 29(4), 623-25.

14. Ramachandran VS, Phil DMSc. Applications of Differential Thermal Analysis in Cement Chemistry. New York 1969.

15. Gomes JC, Cabrera J, Jalali S. The degree of cement hydration determined by backscattered electron imaging. Materials Science of Concrete. Spec. Vol. (1998) 109-26

16. Almudaiheem JA. Nitrogen adsorption and mercury intrusion porosimetry of hydrated Portland cement pastes. Arabian Journal for Science and Engineering 17(3) (1992) 357-69.

17. Powers TC, Copeland LE, Hayes JC, Mann HM. Permeability of Portland cement paste. J Amer Conc Inst 26 (1954) 285-98

18. Hewlett PC. Lea's. Lea's Chemistry of cement and concrete. 4th ed. London: Arnold; 1998.

19. Neves Junior A, Filho RDT, Fairbairn EM, Dweck J. Early stages hydration of high initial strenght Portland cement – part I – thermogravimetric analysis on calcined cement mass basis. J Therm Anal Calorim. 108 (2012) 725-31.

20. Brazilian Association of Technical Standards. High initial strength Portland cement. Rio de Janeiro: NBR 5733;1991 (In Portuguese).

21. Brazilian Association of Technical Standards. Moderate sulphate resistance Portland cement and moderate hydration heat (MRS) and high slphate resistance. Rio de Janeiro: NBR 5737; 1986 (In Portuguese).

22. Brazilian Association of Technical Standards. Determination of setting process. Rio de Janeiro: NBR 11581; 1991 (In Portuguese).

23. Cunha ALC, Gonçalves JP, Büchler PM, Dweck J, Effect of metakaolin pozzolanic activity in the early stages of cement type II paste and mortar hydration. J Therm Anal Calorim. 2008; 92(1):115-9.

ARTIGO C - Neves Junior A, Toledo Filho R.D, Dweck J, Fairbairn E.M.R. CO_2 sequestration by high initial strength Portland cement pastes. Journal of Thermal Analysis and Calorimetry, v. 113, p.1577-1584, 2013.

CO_2 sequestration by high initial strength Portland cement pastes.

Alex Neves Junior[a], Romildo Dias Toledo Filho[a], Jo Dweck[b] and Eduardo de Moraes Rego Fairbairn[a]

[a] Civil Engineering Program – COPPE – Rio de Janeiro Federal University, Brazil

[b] School of Chemistry - Rio de Janeiro Federal University, Brazil.

Journal of Thermal Analysis and Calorimetry

2013

Abstract

During their formation, pastes, mortar and concretes have been used to capture CO_2. This work presents a methodology to estimate the carbon dioxide (CO_2) sequestered by high strength and sulphate resistant Portland cement pastes during their early stages of hydration, by Termogravimetry and Derivative Termogravimetry. Water to cement ratio equal to 0.50 and 0.70 were evaluated and the CO_2 captured amount was determined through TG/DTG curve data on initial cement mass basis, obtained during accelerated carbonation from the fluid state and accelerated carbonation after a first hydration process. The experiments were performed in a controlled chamber, maintaining the CO_2 content at 20-vol% and the temperature at 25°C, at different relative humidity (RH) (60 and 80%) ambient. The procedure allows one to estimate the amount of CO_2 sequestered by the initial cement mass of a given volume of paste, as well as to evaluate the RH and W/C ratio influence on the amount of hydrated formed products, mainly on the $Ca(OH)_2$, important to CO_2 fixation.

Keywords: Carbon dioxide sequestration, Carbonation, Early hydration, Thermogravimetry

1.Introduction

The CO_2 effects in the atmosphere and the efforts to mitigate the global warming caused by the greenhouse effect are well known [1]. Among the existing strategies, the sequestration of carbon dioxide by cementitious materials has proven to be efficient for this purpose [2-7].

Calcium carbonate thermal decomposition and its reverse reaction kinetics are still being studied by thermogravimetry and differential thermal analysis [8-9], as well as new CO_2 adsorptive products and respective sorption among these are advanced materials such as lithium ceramics, activated carbon and zeolites [10-12] and other low cost sorbents, such as waste tire char and chicken waste char [12].

Although the carbonation reaction may damage the adherence between the steel bars and the matrix in reinforced concrete, this does not happen in cementitious products with absence of steel, e.g., matrices reinforced with polymeric or natural fibers. In these

cases, the $Ca(OH)_2$ present in the cementitious matrix, as well as calcium silicate hydrates (C-S-H) react with CO_2, mainly on the early hydration stages [4] forming calcium carbonate ($CaCO_3$) and leading to benefits such as a higher early mechanical improvement, accelerating the curing process as well as improving durability [7]. Otherwise, the durability of a composite made with natural fibers improves within a $Ca(OH)_2$ free matrix [13].

The carbonation may occur simultaneously to cement hydration reaction on early stages. The major hydrated product that contributes to this reaction is $Ca(OH)_2$ by Eq. 1.

$$Ca(OH)_2 + CO_2 \longrightarrow CaCO_3 + H_2O \quad (1)$$

C-S-H phases can also react with CO_2 in mature matrixes forming $CaCO_3$ and silica gel [4], as exemplified per Eq. 2:

$$3CaO.2SiO_2.xH_2O + 3CO_2 \longrightarrow 2SiO_2xH_2O + 3CaCO_3 \quad (2)$$

Literature data also show that on the early stages the C-S-H phase becomes intermingled with carbonates, generating an amorphous calcium-silicate-hydrocarbonate binding phase [4], contributing to the carbonation reaction. The measurement of CO_2 absorption has been done by the mass gain on real time or through the sample mass difference registered before and after carbonation treatment [2]. According to literature data [4] there is about 8% of CO_2 absorption capacity in pastes on cement mass.

The current thermogravimetric study has the objective to contribute to an alternative environmental solution, and the enhancement of the paste solidification process for new civil engineering applications, through the better understanding and mastering the CO_2 chemisorption process by the hydrated components of a special cement paste. This work presents an evaluation of carbon dioxide sequestration on specimens of cementitious pastes through Termogravimetry (TG) and Derivative Termogravimetry (DTG) analysis. The pastes were subjected to 24h of carbonation, after being cured from the fluid state and from different initial hydration times.

2.Materials and Methods

For this study, a high-initial strength and sulphate resistant Portland cement (HS SR PC) was used to prepare the paste specimens, which allows to reach high strengths still at

early hydration stages [14, 15]. The chemical composition, determined by XRF and the TG and DTG curves of this cement were presented in a previous work by the authors [16].

The pastes were composed only by water and cement, in such a way that its behavior would not be affected by aggregates. The main characteristics of the present study were based on a previous experiment carried out by the authors with pastes carbonated during 8h from the fluid state:

- Water to cement ratio (W/C) of 0.5 and 0.7. The specimens produced with these ratios were referenced, in the present paper, as P_{50} and P_{70}.

- Relative humidity (RH) of 80 and 60%. The specimens submitted to these humidity conditions are referenced as H_{80} and H_{60}.

- Content of CO_2 inside the chamber of 20% in volume and 25^{o}C temperature

Views of controlled chamber and CO_2 controlling device are shown in Figures 1 and 2.

Fig 1 – Controlled climatic chamber

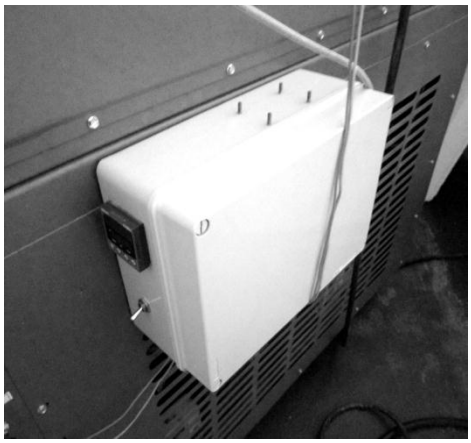

Fig 2 – CO_2 controlling device

Deionized water was used to prepare the pastes, which were mixed during 30s in a beaker in a humidity chamber with RH=99%. The weight was registered before and after their casting in a square iron mold (115 mm x 115 mm) with a height of 25 mm.

The initial cement masses of P_{50} and P_{70} specimens were respectively 421.95 and 342.14 g;

After different times of hydration at 25°C in sealed conditions to ambient and subsequent demolding and carbonation for 24h, the aliquots for thermal analysis were extracted at the end of the period of exposition to CO_2 atmosphere. For the reference specimens they were taken right after demolding. The aliquots were taken using a vertical drilling machine, as shown in Figure 3, from four different regions: top (*T*), top/middle (*TM*), middle (*M*) and bottom (*B*). The extracted powders were put immediately into a glass bottle containing 3 ml of acetone, to stop the hydration process at the sampling time.

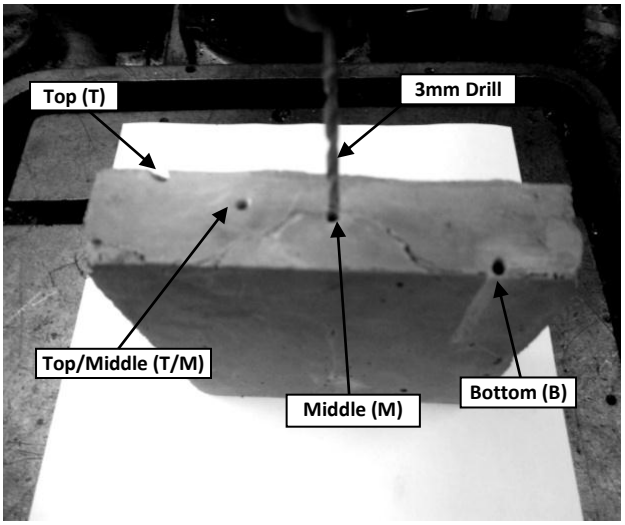

Fig 3 – Detail of the 3mm drill and the regions of analysis

The specimens were submitted to CO_2 atmosphere in different conditions:

1) Just after casting, for 24 hours. In this condition the sample remains inside the mold and the CO_2 could only penetrate by the exposed surface as depicted in Figure 4. In this case we collected aliquots from "*T*", "*TM*", "*M*" and "*B*" region. The specimens are referenced as $F_{0\text{-}24}$.

2) After demolding at casting times of 4, 12 and 24 hours for P_{50} pastes and 6, 12 and 24 hours for P_{70} pastes. Just after powring, the mold was sealed with a PVC film and silicone. In these conditions, the CO_2 can flow over all the surfaces of the specimens (Figure 5). For these specimens we collected aliquots from "*T*", "*TM*" and "*M*" region, because it was supposed that the same absorption phenomena would occur

in the other opposite half of the specimen. These specimens are referenced as F_{n-24} where "*n*" is the time at demolding.

3) Reference specimens were not submitted to CO_2 atmosphere. These specimens were sealed just after casting. P_{50} specimens were demolded at 4, 12, 24 and 48 hours and P_{70} demolded at 6, 12, 24 and 48 hours. In this case we collected aliquots from "*M*" region. These specimens are referenced as F_{p-0}, where "*p*" is the time at demolding.

Therefore we will use the following nomenclature to reference a specimen:

- **$\underline{P_mH_nF_{o-p}}$** , where "*m*" is the W/C ratio (in mass%), "*n*" is the relative humidity (in %), "*o*" is the demolding time and "*p*" is the time during which the specimen was submitted to CO_2 ambient.

When reference specimens results were obtained by linear interpolation between nearer time measured values they were referenced as **$\underline{P_mH_nREF_q}$**, where "*q*" is the reference age for which the values have been interpolated.

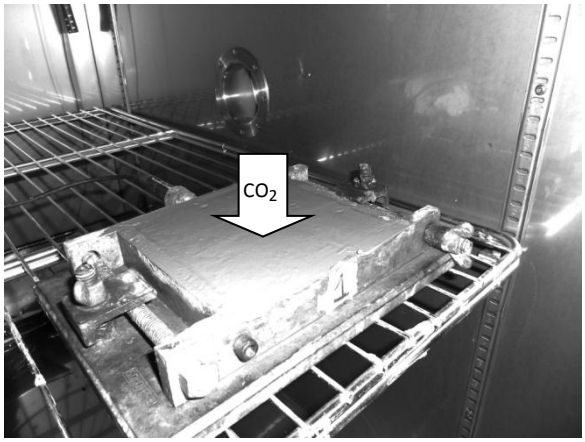

Fig 4 – Unidirectional Flow

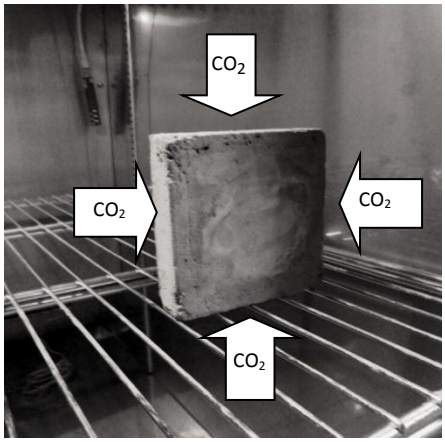

Fig 5 – Multidirectional Flow

Table 1 shows the experimental conditions used to investigate the CO_2 absorption.

Table 1 – Experiment conditions

Specimens	W/C (%)	RH (%)	Demolding time (h)	Exposition to CO_2 time (h)	Regions of sampling	Age at sampling
$P_{50}H_{80}F_{0\text{-}24}$	50	80	-	24	T/TM/M/B	24
$P_{70}H_{60}F_{0\text{-}24}$	70	60	-	24	T/TM/M/B	24
$P_{50}H_{80}F_{4\text{-}24}$	50	80	4	24	T/TM/M	28
$P_{70}H_{60}F_{6\text{-}24}$	70	60	6	24	T/TM/M	30
$P_{50}H_{80}F_{12\text{-}24}$	50	80	12	24	T/TM/M	36
$P_{70}H_{60}F_{12\text{-}24}$	70	60	12	24	T/TM/M	36
$P_{50}H_{80}F_{24\text{-}24}$	50	80	24	24	T/TM/M	48
$P_{70}H_{60}F_{24\text{-}24}$	70	60	24	24	T/TM/M	48
$P_{50}H_{80}F_{4\text{-}0}$	50	80	4	-	M	4
$P_{70}H_{60}F_{6\text{-}0}$	70	60	6	-	M	6
$P_{50}H_{80}F_{12\text{-}0}$	50	80	12	-	M	12
$P_{70}H_{60}F_{12\text{-}0}$	70	60	12	-	M	12
$P_{50}H_{80}F_{24\text{-}0}$	50	80	24	-	M	24
$P_{70}H_{60}F_{24\text{-}0}$	70	60	24	-	M	24
$P_{50}H_{80}F_{48\text{-}0}$	50	80	48	-	M	48
$P_{70}H_{60}F_{48\text{-}0}$	70	60	48	-	M	48

Thermal analyses were performed in a TA Instruments, SDT Q600 model TGA/DTA/DSC simultaneous apparatus at a 10 °C min^{-1} heating rate, from 35 to 1000 °C, by using 100 mL min^{-1} of nitrogen flow. Before this, they were dried inside the equipment initially at 1 °C min^{-1} from 25 to 35°C, followed by an isothermal step at 35°C for 1 h, to eliminate the residual non combined free water [17].

The contents of the products were calculated using the procedure described in previous works of the authors [16,18]. It uses the TG and DTG data on the initial cement mass basis for the determination of the hydration and carbonation products. On this basis were plotted all the TG and DTG curves from which the contents of the following products were determined, were plotted:

- The water released from the C-S-H and ettringite phases decomposition, between 50 and 200°C;
- The total combined water released during analysis, including the water lost from dehydroxylation of the $Ca(OH)_2$ between 35 and 450°C;

- The water lost during the dehydroxylation of $Ca(OH)_2$, between 380 and 450°C;
- The CO_2 lost during the decarbonation of $CaCO_3$, between 500 and 750°C;

Considering that there is an initial amount of $CaCO_3$ in the anhydrous cement, the additional amount of $CaCO_3$ within the pastes is exclusively due to the carbonation reaction, mainly with $Ca(OH)_2$ and calcium silicate hydrated phases as shown in Eq (1) and (2). Thus, the methodology used to determinate the CO_2 uptake was based in a comparison of the $CaCO_3$ data from the TG and DTG curves for the anhydrous cement and the carbonated paste. The difference between the two curve CO_2 contents is the CO_2 chemically absorbed during the carbonation reactions in each considered region.

Thus, the amount of $CaCO_3$ (%) effectively formed in the considered normal surface at sampled region is given by Eq. 3.

$$CaCO_{3ef} = \frac{ML_{CO_2} \cdot 100}{44} - [CaCO_3]_{cem} \quad (3)$$

Where:

ML_{CO_2} = % of total mass loss of CO_2 from $CaCO_3$ in the considered surface.

$[CaCO_3]_{cem}$ = % mass of $CaCO_3$ present in the original cement mass of the sample.

Assuming a homogeneous distribution of the cement mass for all regions, it is possible to determine the mass of CO_2 that formed $CaCO_3$ in each region by Eq.1.

Thus, the amount of CO_2 captured in the form of $CaCO_3$ in each considered surface is given by Eq. 4:

$$[CO_2]_{captured} = \frac{CaCO_{3ef} \cdot 44}{100} \quad (4)$$

Therefore, the mass percentage of CO_2 sequestered in the considered specimen can be obtained by Eq. 5:

$$[CO_2]_{total\_captured\_by\_the\_specimen} = \frac{\int_0^{ht} kf(h)Adh}{M_i} \quad (5)$$

Where:

$f(h)$ = function that represents the CO_2 mass captured in a volume dV, as a function of the deepness (h). (See Figure 6)

M_i = initial cement mass in the specimen.

$dV = Adh$

V_{tot} = total volume of the specimen = Ah_t

h_t = maximum deepness of the specimen.

k = initial cement mass per specimen volume for each case = M_i / V_{tot} ;

A = exposed surface, considering unidirectional CO_2 flow through the specimen.

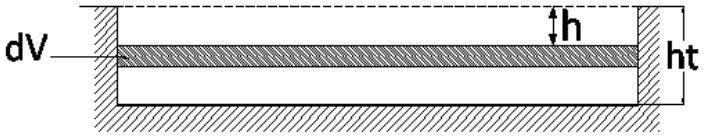

Fig 6 – Schematics of the lateral view cross section of the specimen and infinitesimal volume

An estimate of the total amount of $Ca(OH)_2$, after carbonation treatment, can be obtained by Eq. 6:

$$[Ca(OH)_2]_{Total} = [Ca(OH)_2]_{consumed} + [Ca(OH)_2]_{remaining} \quad (6)$$

Where, $[Ca(OH)_2]_{consumed}$ is given by Eq. 7:

$$[Ca(OH)_2]_{consumed} = \frac{[CO_2]_{captured} \cdot 168.18}{100} \quad (7)$$

$[Ca(OH)_2]_{remaining}$, corresponds to the $Ca(OH)_2$ remaining after carbonation process, obtained from Eq. 8:

$$[Ca(OH)_2]_{remaining} = [Ca(OH)_2]_{(TG)data} - [Ca(OH)_2]_{cement} \quad (8)$$

Here,

$[Ca(OH)_2]_{(TG)data}$ = $Ca(OH)_2$ estimated from TG data on initial cement basis after carbonation treatment.

$[Ca(OH)_2]_{cement}$ = Initial $Ca(OH)_2$ content in original unhydrated cement sample.

4.Results and Discussion

Figure 7 presents the CO_2 contents, for $P_{70}H_{60}F_{0\text{-}24}$ and $P_{50}H_{80}F_{0\text{-}24}$ specimens.

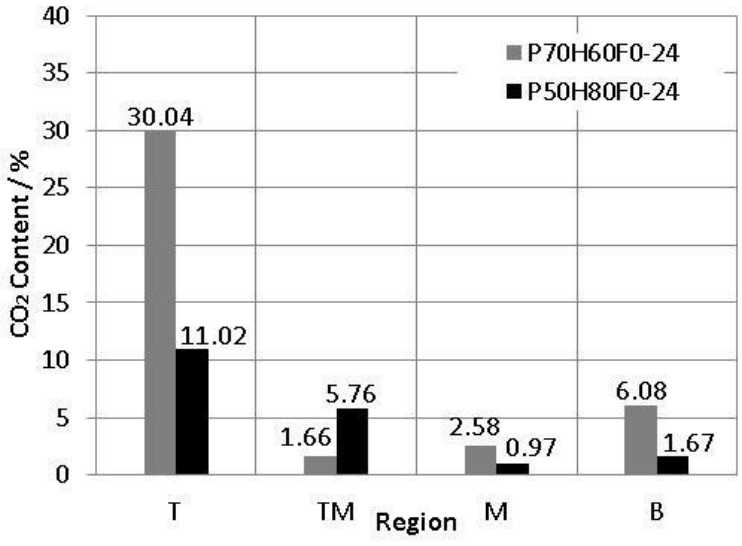

Fig.7 – CO_2 content for the carbonated specimens from the fluid state

It can be noticed that the top of the specimen absorbs more CO_2 than the bulk. For these specimens it was observed the formation of a carbonated coat that could obstruct the progress of carbonation within the bulk was observed. Figure 7 also shows that, despite of the higher endothermic effect caused by the evaporation of the free water, the higher relative amount of water content on P_{70} paste and its higher porosity in relation to the P_{50} paste, contributed to the production of more $Ca(OH)_2$ [16] and to the increase of CO_2 absorption, respectively.

A better and much higher distribution of the CO_2 content was observed in the specimens submitted to CO_2 atmosphere after solidification as depicted in Figure 8.

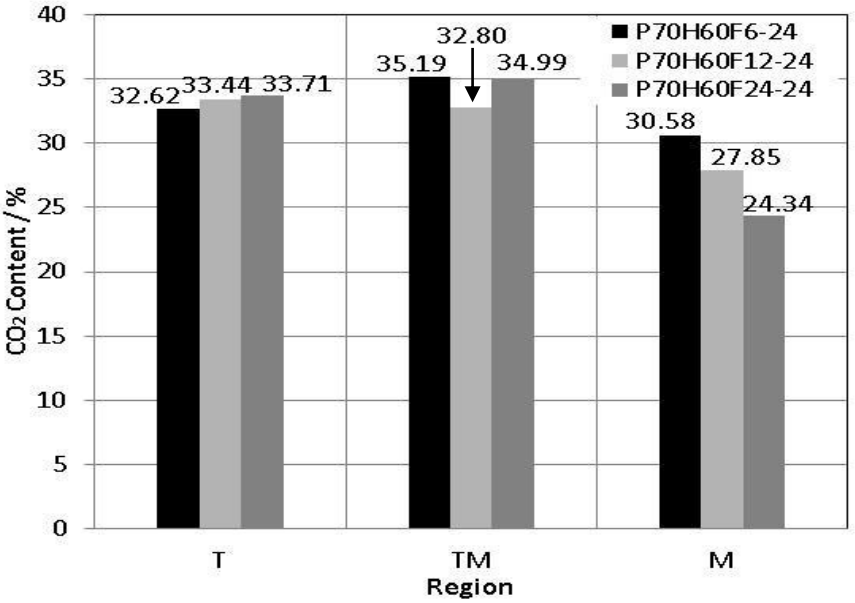

Fig.8 – CO_2 content for the carbonated $P_{70}H_{60}F_{6\text{-}24}$, $P_{70}H_{60}F_{12\text{-}24}$, $P_{70}H_{60}F_{24\text{-}24}$ specimens

Due to the better results on the CO_2 absorption, we choose the P70H60 pastes as an example to express the results of the main hydrated products.

The contents of C-S-H+Ettringite, total combined water and $Ca(OH)_2$ for the specimens $P_{70}H_{60}F_{6\text{-}24}$, $P_{70}H_{60}F_{12\text{-}24}$ and $P_{70}H_{60}F_{24\text{-}24}$ (ages of 30, 36 and 48 hours) compared to the reference specimens at the middle region at the same ages ($P_{70}H_{60}REF_{30}$, $P_{70}H_{60}REF_{36}$ and $P_{70}H_{60}F_{48\text{-}0}$) are presented in Figures 9, 10 and 11.

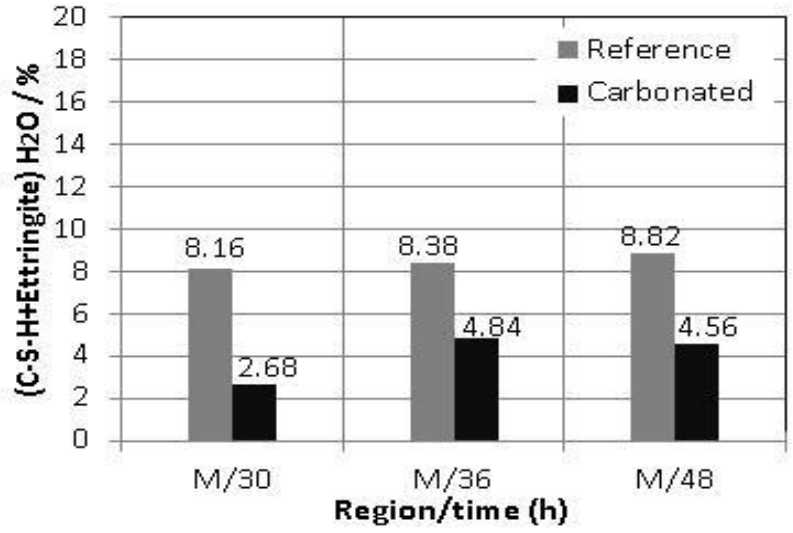

Fig.9 – (C-S-H + ettringite) combined H_2O content at the middle region of the paste, for 0.70 W/C ratio cases carbonated for 24h, after initial hydration times of 6, 12 and 24 hours

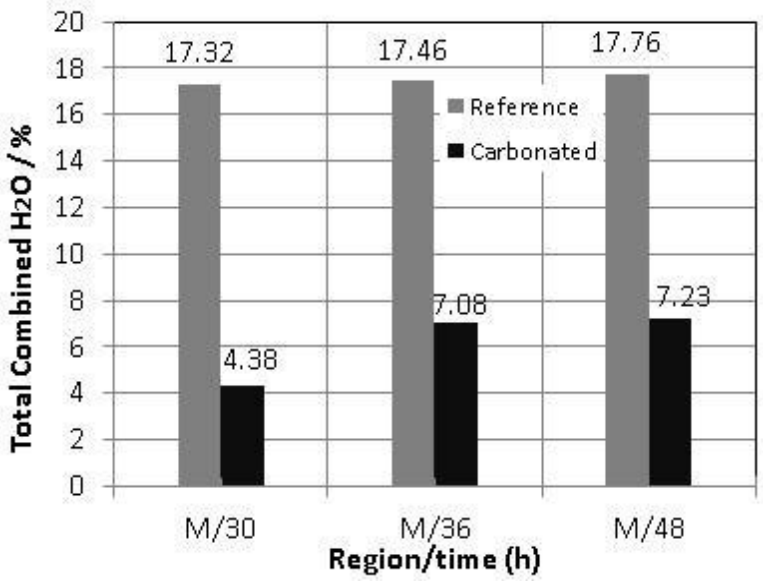

Fig.10 – Total combined H_2O content at the middle region of the paste for 0.70 W/C ratio cases, carbonated for 24 h after initial hydration times of 6, 12 and 24 hours.

Figure 9 indicate that for an early exposition to CO_2 at 6 hours the carbonation reaction consumes a larger amount of C-S-H and ettringite than for the ages.

This effect is also verified in Figure 10 where the water combined to C-S-H, ettringite and $Ca(OH)_2$ is plotted.

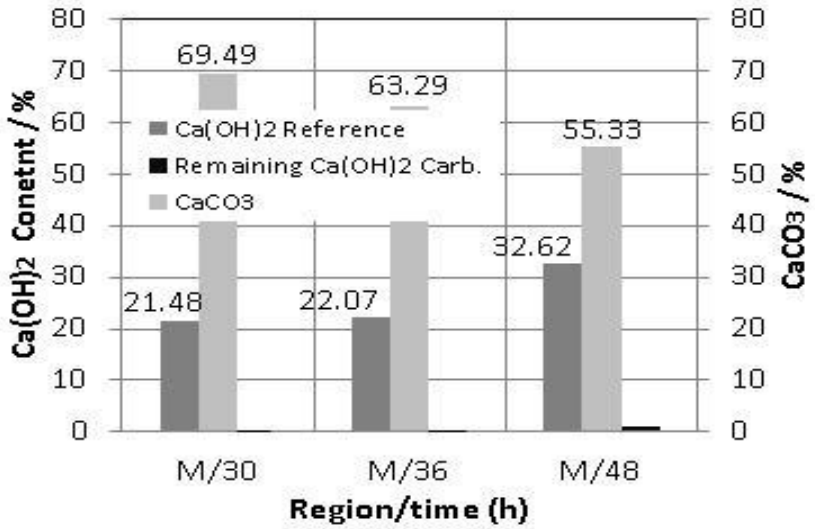

Fig.11 – $Ca(OH)_2$ and $CaCO_3$ contents at the middle region of the paste, for 0.70 W/C ratio cases carbonated for 24h, after initial hydration times of 6, 12 and 24 hours

Figure 11 shows that $Ca(OH)_2$ was totally consumed for $P_{70}H_{60}F_{6\text{-}24}$ and $P_{70}H_{60}F_{12\text{-}24}$ pastes. Figure 11 indicates the participation of the C-S-H phases in the carbonation, releasing more calcium to the aqueous phase and reducing their Ca/Si ratio [4,19]. The

highest consumption of $Ca(OH)_2$ occurred after 6h of initial hydration, reflecting the highest carbonation process at this condition.

Figures 12 and 13 show TG/DTG data at different regions for the best results of CO_2 capture at the applied conditions.

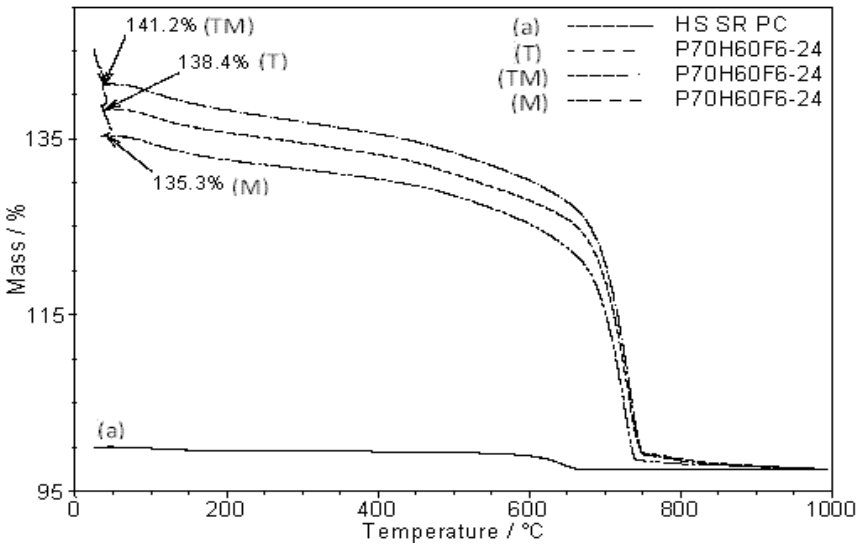

Fig.12 – TG curves of carbonated specimens for the HS SR PC with 0.70 W/C ratio, at different regions, after 6h of initial hydration.

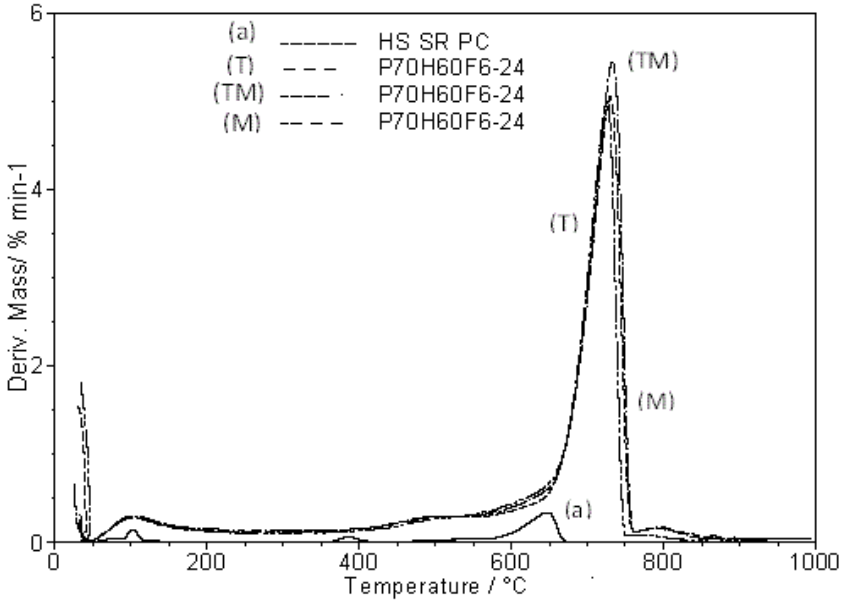

Fig.13 – DTG curves of carbonated specimens for the HS SR PC with 0.70 W/C ratio, at different regions, after 6h of initial hydration

Figures 12 and 13, show the respective TG and DTG data for the 0.70 W/C ratio pastes after 6h of initial hydration and RH=60%. It can be seen the complete depletion of $Ca(OH)_2$, due to the carbonation reaction in the three considered regions. There is no

remaining $Ca(OH)_2$ dehydroxilation DTG peak, confirming the efficiency of the carbonation process at this total hydration plus carbonation age (30h). Figure 14 and 15 shows with more details TG and DTG results for the reference and the 0.70 W/C ratio paste carbonated cases with the same total age of 48h at respective middle region of the specimens.

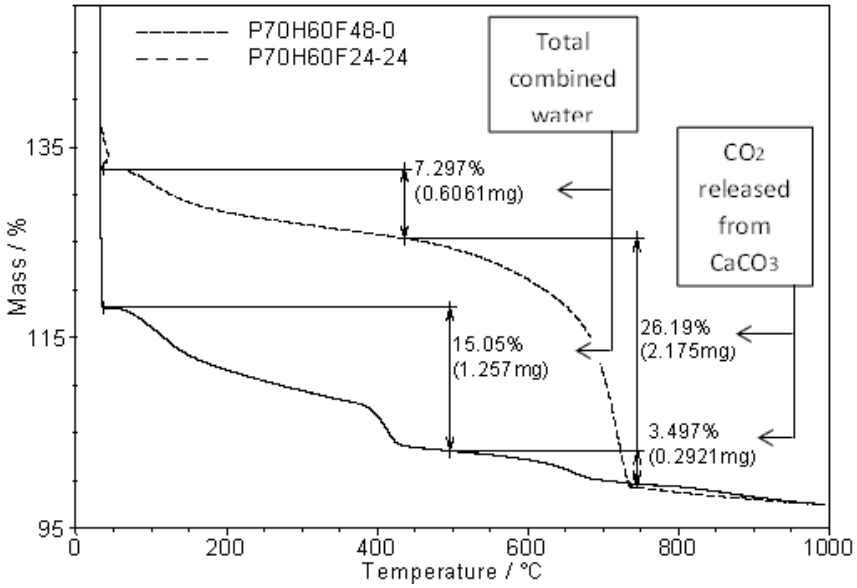

Fig.14 – Middle region sample TG curves of the 0.70 W/C reference paste hydrated for 48h and of same W/C sample paste hydrated for 24h, followed by 24 h of carbonation.

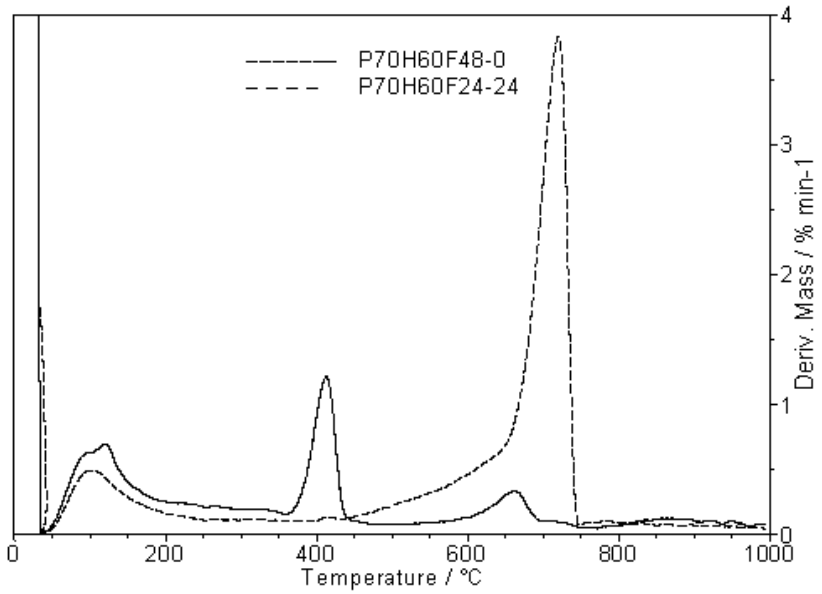

Fig.15 – Middle region sample DTG curves of the 0.70 W/C reference paste hydrated for 48h and of same W/C sample paste hydrated for 24h, followed by 24 h of carbonation.

We can see from Figure 15 the complete consumption of the $Ca(OH)_2$ and the respective high DTG peak of $CaCO_3$ indicating a high degree of carbonation of the previously 24h hydrated paste, when compared to the reference case at total same age. Comparing the total combined water, the reference paste presents a value two times higher than that of the carbonated paste. Also there is a decrease of the content of the hydrated products before the hydroxylation of $Ca(OH)_2$, indicating a significant carbonation of the original C-S-H phase, as shown in the Figures 9 and 10.

Figure 16 shows the profile of captured CO_2 content in the half part of the specimen thickness, for the 0.70 W/C ratio case specimens. The "*0*" thickness corresponds to the middle region and the "*1.25*" thickness refers to the top region.

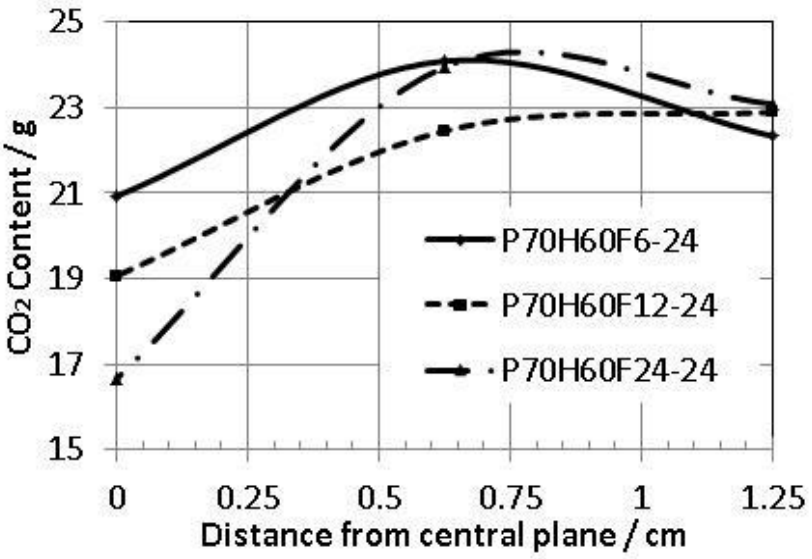

Fig.16 – CO_2 captured content profile for 0.70 W/C ratio specimens as a function of the distance from specimen central plane

From Figure 16, we can notice the increase on the amount of captured CO_2 in the top region, when compared to the respective specimen middle region. In the middle of the half part of the specimen, for 6h of initial hydration, the amount of CO_2 absorbed is higher than in the other parts. The CO_2 captured is practically the same for 6 and 24h of initial hydration at a plane 6.2mm from the middle of the specimen, as well as for top regions of specimens carbonated after 12 and 24 h. The carbonation was done by using a relative humidity of 0.6, which promotes water loss from the specimen to the ambient. This occurs during carbonation by water diffusion from the center of the specimen to the top and then, by vaporization from the top to the ambient. As a consequence, on the top region sample it was seen a higher free water content than in the central specimen.

This fact contributes to a lesser hydration degree at the center, with lower production of $Ca(OH)_2$, there contributing to the lowest absorption of CO_2 at the center of respective specimens, as can be seen in Figure 16.

Each curve of Figure 16 represents the function $f(h)$ from the center to the top of the specimen. Considering the initial used cement mass, we can obtain the total captured amount of CO_2, shown in Figure 17, considering time "*0*", when carbonation process starts from the fluid state. The total captured CO_2 in the specimens, will be the twice of these results.

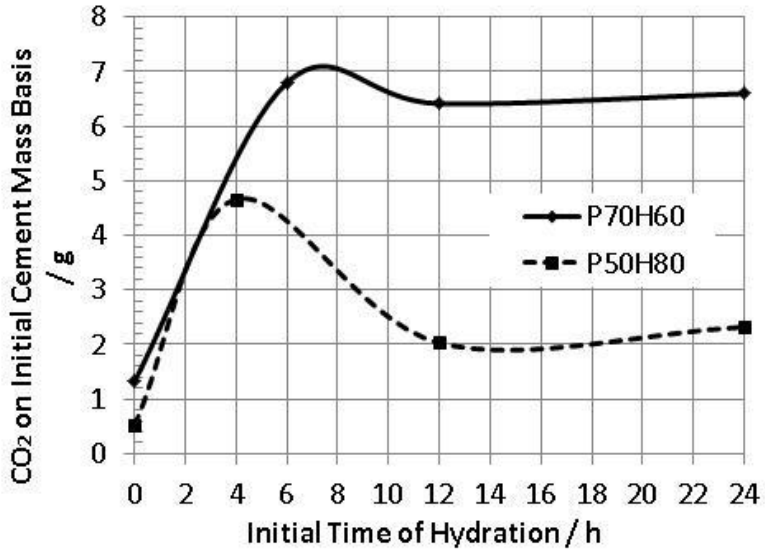

Fig.17 – Total CO_2 captured mass in the 0.70 and 0.5 W/C ratio specimens volume, when exposed to 24h carbonation, after different respective previous hydration times.

Figure 17 shows that after 24 hour carbonation a higher amount of CO_2, calculated by Eq 5, was captured by the 0.70 W/C ratio paste for most of the operating conditions, when compared to those of 0.50 W/C ratio case.

As we can see from the 0.70W/C case previously hydrated for 6h, after 24 h of carbonation, the CO_2 captured mass was equal to 6.8% of the initial cement mass, which corresponds to the condition of highest captured CO_2 mass per mass of cement. For the 0.50 W/C ratio paste, the highest CO_2 capture occurred after four hours of previous hydration.

The higher free water content and consequently, the higher porosity of the 0.70 paste, which promoted a higher CO_2 diffusivity, allowed a higher total absorption of CO_2.

Although the lower RH=60% increases the free water evaporation rate, the higher initial W/C ratio in the 0.70 W/C ratio case, allowed a higher residual water content during carbonation step, which contributes for the production of more hydrated products [16], specially $Ca(OH)_2$, enhancing the CO_2 absorption by during the carbonation step, producing more $CaCO_3$ in the specimen.

The higher occurrence of carbonation reactions in the 0.70 W/C ratio paste, forms more water (see Eq 1 and 2) compensating the higher free water evaporation rate and provides more additional water for the hydration reactions as well.

From the experimental results, it seems that, although the increase of RH for the 0.50 W/C ratio paste slows down the free water evaporation effect, its lower initial free water content decreases the formation rate of hydrated products [16], mainly of the C-S-H and $Ca(OH)_2$ and consequently, the CO_2 capture. It can also be noticed that after previous higher hydration time of these pastes, due to their lower and decreasing porosity, the CO_2 gas diffusion rate decreases and a lower capture of CO_2 occurs, as shown in Figure 17.

5.Conclusions

- TG and DTG on initial cement mass basis are efficient tools to estimate correctly the CO_2 absorption in a volume of hydrated cementitious material, knowing the amount of initial added cement.
- The paste prepared with 0.70 W/C ratio captures the highest amount of CO_2 after previous 6h of hydration, because carbonation reaction starts during its hydration accelerating period, during which a significant production of C-S-H phases and $Ca(OH)_2$ occurs.
- After 6h hydration the 0.70 W/C ratio paste still presents a high initial porosity and more free water content, which does not apparently saturate the pores, a fact that, in relation to the other previous hydration times (12 and 24h), enhances the gas diffusion, allowing to reach a higher CO_2 capture per initial cement mass.
- The carbonation reaction used for CO_2 absorption from the fluid state for cementitious pastes, has shown to be not so efficient due to the excess of free water, because, although it initially accelerates the CO_2 diffusion, it forms a high amount of

$CaCO_3$ at the solid/gas interface, in the shape of a solid plate that does not allow the CO_2 diffusion, to proceed into the paste after its formation.

- The use RH=60% has shown to be an optimum condition for the carbonation treatment, confirming previous data of the literature [4].
- Otherwise, although the RH=60% increases the loss of free water to the ambient, the higher initial relative water content of 0.70 W/C ratio paste, apparently compensates this loss, avoiding the decrease of the hydration reactions, as well as the carbonation ones.
- It seems that the carbonation reaction increases the amount of $Ca(OH)_2$ available to react with CO_2, mainly in the more fluid pastes, because it produces more water due to the carbonation reactions, which in turn enhances the hydration reactions, compensating the water loss from the evaporation induced by relative humidity conditions lower than 100%.
- As the carbonation reaction proceeds, during thermal analysis the amount of total combined water and the water released from C-S-H and ettringite decreases, indicating that besides calcium hydroxide, the C–S–H phases are being carbonated as well.
- The porosity and the content of available free water, regulated by the W/C ratio and relative humidity conditions, influences the hydration degree, the CO_2 diffusion capacity and the amount of hydrated products available to react with CO_2.

Acknowledgments The authors acknowledge the experimental assistance of the Rio de Janeiro Federal University Chemical School Thermal Analysis and Civil Engineering Structure Laboratories and the financial support of the National Research Council (CNPq).

References

1. In <http://unfccc.int/2860.php>
2. Shao Y, Mirza MS, Wu X. CO_2 Sequestration Using Calcium-Silicate Concrete. Can J of Civil Engin. 2006; 33:776.

3. Shao Y, Monkman S, Wang S. Market Analysis of CO_2 Sequestration in Concrete Building Products. Second International Conference on Sustainable Construction Materials and Technologies. 2010; Ancona, Italy, 28-30 June.

4. Rostami V, Shao Y, Boyd AJ. Microstructure of cement paste subject to early carbonation curing, Cem Concr Res. 2012; 183-93.

5. Shao Y, Monkman S, Boyd AJ. Recycling carbon dioxide into concrete: a feasibility study. Concrete Sustainability Conference. 2010; McGill University, Department of Civil Engineering, Canadá.

6. Habert G, Roussel N. Study of Two Concrete Mix-Design Strategies to Reach Carbon Mitigation Objectives. Cem Conc Comp. 2009;(31):397–402.

7. Shao Y, Zhou X, Monkman S. A New CO_2 Sequestration Process via Concrete Products Production. 2006; Department of Civil Engineering, McGill University. Montreal.

8. Galan I, Glasser FPJ, Andrade C. Calcium carbonate decomposition. J Therm Anal Calorim. 2013; (111):1197-1202.

9. Li Y, Liu H, Wu S, Sun R, Lu C. Sulfation behavior of CaO from long-term carbonation/calcination cycles for CO_2 capture at FBC temperatures. J Therm Anal Calorim. 2013; (111):1335-43.

10. Tejeda AR, Pfeiffer H. $\alpha \rightarrow \gamma$ Lithium borate phase transition produced during the CO_2 chemisorption chemisorption process. J Therm Anal Calorim. 2012; (110):807-11.

11. Landeros JO, Rendón TLA, Yáñez CG, Pfeiffer H. J Therm Anal Calorim. 2012; (108):647-55.

12. Zhao HY, Cao Y, Lineberry Q, Pan WP. Evaluation of CO_2 adsorption capacity of solid sorbents. J Therm Anal Calorim. 2011; (106):199-205.

13. Toledo Filho RD, Scrivener K, England GL, Ghavami K. Durability of alkali-sensitive sisal and coconut fibers in cement mortar composites. Cem Conc Comp. 2000; (2) 127-43.

14. BRAZILIAN ASSOCIATION OF TECHNICAL STANDARDS. High initial strenght Portland cement. NBR 5733, Rio de Janeiro, 1991 (In Portuguese).

15. BRAZILIAN ASSOCIATION OF TECHNICAL STANDARDS. Moderate sulphate resistance Portland cement and moderate hydration heat (MRS) and high sulphate resistance NBR 5737, Rio de Janeiro, 1986, (In Portuguese).

16. Neves Junior A, Dweck J, Toledo Filho RD. Early Stages Hydration of High Initial Strenght Portland Cement – Part I – Thermogravimetric Analysis on Calcined Mass Basis. J Therm Anal Calorim. 2012; (108):725-31.

17. Dweck J, Buchler PM, Coelho ACV. Hydration of a Portland cement blended with calcium carbonate. Therm Acta. 2000; (346):105-13.

18. Dweck J, Cunha ALC, Pinto CA. Thermogravimetry on Calcined Mass Basis – Hydrated Cement Phases and Pozzolanic Activity Quantitative Analysis. J Therm Anal Calorim. 2009; (97): 85-9.

19 Villain G, Thiery M, Platret G. Measurement Methods of Carbonation Profiles in Concrete: Thermogravimetry, Chemical Analysis and Gammadensimetry. Cem Concr Res. 2007; (37):1182-92.

ARTIGO D - Neves Junior A, Toledo Filho R.D, Dweck J, Fairbairn E.M.R. A study of the carbonation profile of cement pastes by thermogravimetry and its effect on the compressive strength. Journal of Thermal Analysis and Calorimetry. DOI 10.1007/s10973-013-3556-7.In press 2014

A study of the carbonation profile of cement pastes by thermogravimetry and its effect on the compressive strength.

Alex Neves Junior[a], Romildo Dias Toledo Filho[a], Jo Dweck[b] and Eduardo de Moraes Rego Fairbairn[a]

[a] Civil Engineering Program – COPPE – Rio de Janeiro Federal University, Brazil

[b] School of Chemistry - Rio de Janeiro Federal University, Brazil.

Journal of Thermal Analysis and Calorimetry

2014

Abstract

In a previous work the authors have carbonated totally high initial strength and sulfate-resistant Portland cement (HS SR PC) pastes. In order to solve the mechanical problems caused by the intense carbonation that occurred during those experiments, new carbonation conditions were applied in this study. The obtained products were analyzed with respect to the carbonation reactions by thermogravimetry and compressive mechanical strength. Comparative analysis with reference pastes obtained without carbonation at the same age shows that CO_2 capture increases with carbonation time. However there is an optimum time, up to which the carbonation treatment does not affect the mechanical properties of the paste. Below this time, the lower is the carbonation time the higher is the increase of compressive strength, when compared to that of the reference pastes processed at same operating conditions without carbonation.

Key Words: CO_2 capture, Early cement curing, Early stage hydration, Thermogravimetry.

1. Introduction

Carbonation has been used with cementitious materials to capture CO_2 in a stable form of calcite. The literature reports a 9% CO_2 capture capacity using 16% binder at 2h of carbonation [1] and at the same time, 16% capture is possible when the ambient is only CO_2 [2]. The carbonation presents an environmental feasibility of CO_2 sequestration when using cementitious materials. Considering the annual global concrete production, the capture can reach 1,8 million tonnes of CO_2 [3], which may increase if carbonation curing is performed adjacent to a CO_2 source location, as a cement industry [4-5]. Another advantage of the carbonation is the shortly achieved mechanical resistance. A cementitious material with short term carbonation creates a microstructure with more strength-contributing solids than conventional hydration, increasing the durability [2-6]. Actually, other ways of CO_2 capture have been developed, as occurs with SO_2 capture behaviour of the calcium oxide derived from dolomite and/or limestone [7] and with some different lithium ceramics, which are potential CO_2 captors [8].

In a previous work, [9] the authors concluded that, in a HS SR PC paste with water to cement ratio (W/C) of 0.7, after an initial hydration time of 6h, the exposition to

environmental conditions of relative humidity (RH) equal to 60% and 20mol% of CO_2 at 25°C, are optimum conditions to maximize the CO_2 capture in that paste, due to the high porosity and the available free water. All the samples were treated with CO_2 initially during 24h in the optimum conditions, to maximize the capture.

According to the literature, the calcite formation in cementitious materials as concrete, mortars and pastes, during the carbonation reaction, can reduce the porosity and improves the resistance [2,6] of materials that do not use reinforced steel. In a previous step of this study, to verify this tendency and to analyse the best conditions of capture with mechanical properties, 25mm diameter with 50mm height cylinders were prepared. Some were treated with CO_2 during 24h in the same cited optimum conditions of capture and others were not carbonated (only hydrated) to be comparative references. All were tested for compressive strength after being cured in a 100% RH environment for 28 days.

It was noticed that the compressive strength of the carbonated cylinders decreases considerably in relation to reference pastes obtained at same operating conditions without carbonation by ~51%, showing that the increase of the CO_2 exposition time increases the CO_2 capture, but the cementitious matrix is damaged, affecting its resistance.

Considering, the best conditions achieved by the authors to capture CO_2 in the cementitious pastes [9], this article presents a study by Thermogravimetry (TG) and Derivative Thermogravimetry (DTG), of the quantitative evolution of the main phases formed in the hydrated products in cylinders treated with CO_2 at different times of carbonation, within the 24h of carbonation initially proposed. The respective compressive strength was also measured as a function of time of carbonation, to see in which conditions the final resistance is not affected in relation to the reference pastes.

2. Materials and methods

The paste specimens were prepared using, a high initial strength and sulfate-resistant Portland cement (HS SR PC), [10, 11] which allows reaching high strengths still at early hydration stages. Its chemical composition determined by XRF is presented at

Table 1. Its specific mass is 3.11 g/cm³ and particle size distribution is shown in Fig 1. The TG and DTG curves of the cement are presented in Fig 2.

Table 1 – Composition of the cement

Compound	Content / %
CaO	66.92
SiO_2	16.45
Al_2O_3	5.00
SO_3	4.44
Fe_2O_3	3.3
TiO_2	0.4
K_2O	0.35
MnO	0.28
SrO	0.25
ZnO	0.03
ZrO_2	0.02
LOI	2.55
D_{80}	25.1µm
Especific mass	3.11 g/cm³

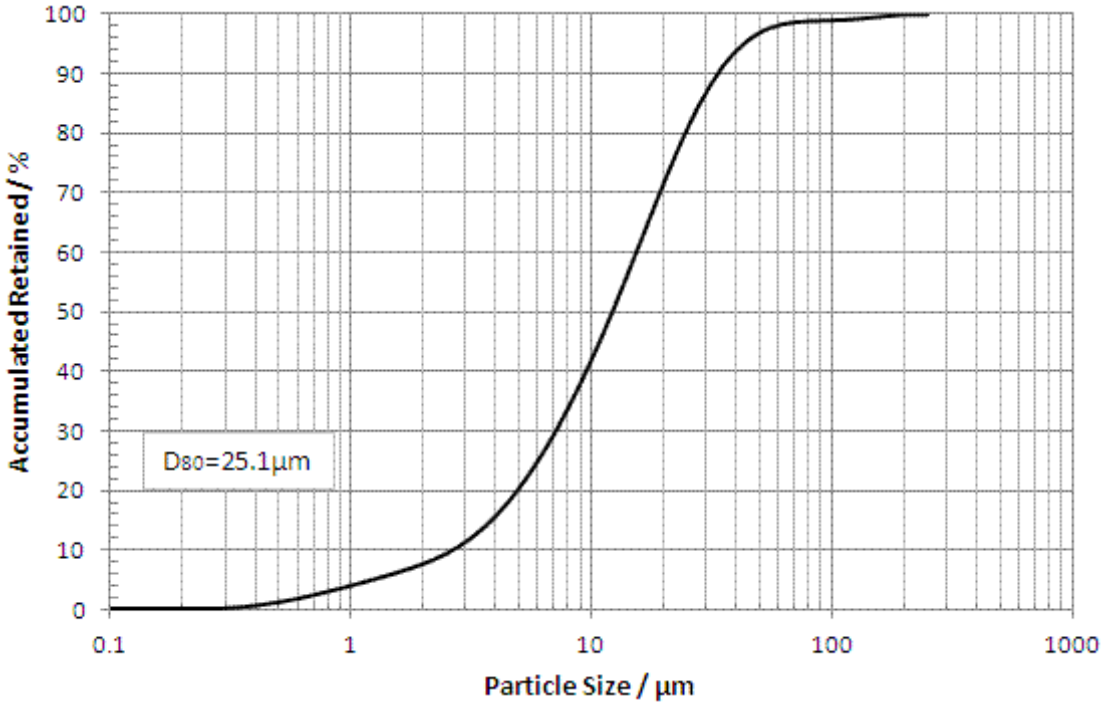

Fig.1- Cement particle size distribution

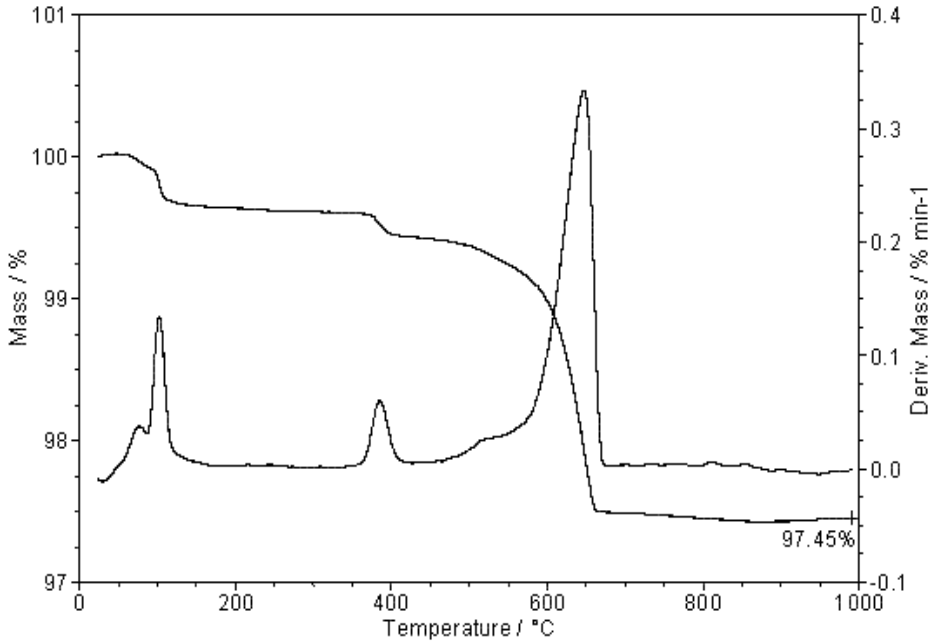

Fig.2- TG and DTG curves of the cement.

The best CO_2 capture conditions in cementitious paste, achieved by the authors [9] were maintained:

- water to cement ratio: 0.7
- initial hydration time: 6h
- relative humidity (RH): 60%
- temperature: 25°C
- CO_2 volume concentration : 20%

Deionized water was used to prepare the pastes, which were mixed during 30 s in a mechanical mixer in an environmental temperature of 23°C (±2°C).

The prepared paste was immediately cast in 25 cylinders with 25mm of diameter and 50mm of height, and were demolded after an initial hydration of 6h in an environment with RH=100%, followed by a treatment with CO_2 at 7 different times of carbonation: 1, 2, 4, 8 and 12h in a controlled climatic chamber maintained at RH of 60%. After the carbonation treatment in the chamber, 4 cylinders for each carbonation time, were cured in an environment with RH=100%, during 14 days for the compressive strength test, which was performed in a SHIMADZU machine, model UH – F1000kN with a loading speed of 0,01mm/min following the Brazilian standard methods [13]. A fifth specimen obtained after a same carbonation time was separated for thermal analysis, which was cut in two parts longitudinally, according to Fig. 3 after the carbonation treatment. From

the flat exposed surface of one of the parts, the aliquots for thermal analysis were taken from four different regions in the radial direction (r=0, r=0.42, r=0.84 and r=1.25) and put immediately into a little glass bottle containing 3 mL of acetone, to stop the hydration process. After they were conditioned in little sealed plastic bags until the test, which was performed in a TA Instruments, SDT Q600 model, TGA/DTA/DSC simultaneous apparatus at a heating rate of 10 °C min^{-1}, from 35 to 1000 °C, by using 100 $mL.min^{-1}$ of nitrogen flow. Before this, they were dried inside the equipment initially at 1 °C min^{-1} from 25 to 35°C, followed by an isothermal step at 35°C for 1 h, to eliminate any residual non combined free water.

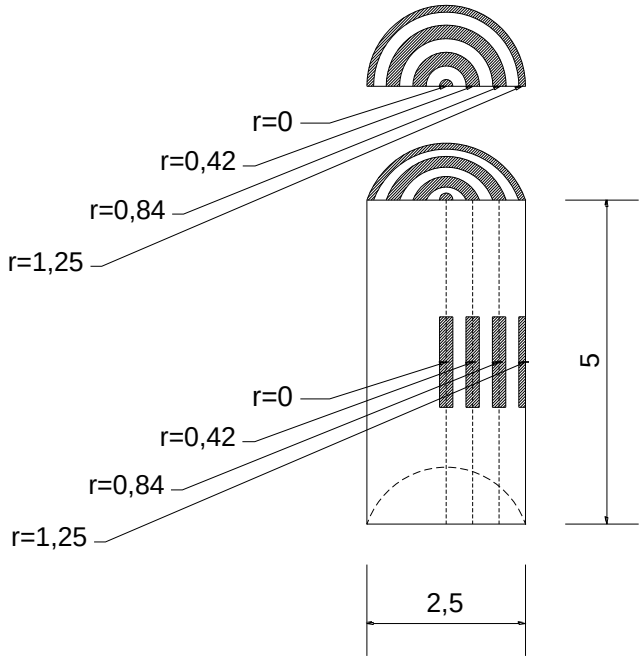

Fig. 3- Details of the cylinder's studied regions by thermal analysis (distances in cm)

The contents of the main phases were calculated using the procedure described in previous works of the authors [12,14,15]. It uses the TG and DTG curves data on the initial cement mass basis for the determination of the hydration and carbonation products. On this basis, the following data were determined from respective mass losses:

• The water released from the tobermorite and ettringite phases decomposition, between 50 and 200 °C;

• The total combined water is released between 35 and 450 °C during analysis, which also includes the water lost from dehydroxylation of the $Ca(OH)_2$;

• The $Ca(OH)_2$ content, calculated stoichiometrically from the water lost during its dehydroxylation, between 380 and 450 °C;

• The $CaCO_3$ content from the CO_2 lost during its decarbonation between 500 and 750 °C;

The compressive strength was determined at the 14th day of cure at RH=100%, after respective carbonation times.

Table 2 shows the experimental conditions of carbonation after the 6h hydration at which samples were taken for thermal analysis.

Table 2 – Experimental carbonation conditions and sampling for thermal analysis

Specimens	Expostion to CO2 / h	Region of sampling /"r" in cm	Age of sampling / h
PC1h	1	r=0/r=0.42/r=0.84/r=1.25	7
PC2h	2	r=0/r=0.42/r=0.84/r=1.25	8
PC4h	4	r=0/r=0.42/r=0.84/r=1.25	10
PC8h	8	r=0/r=0.42/r=0.84/r=1.25	14
PC12h	12	r=0/r=0.42/r=0.84/r=1.25	18

3.Results and discussion

Figures 4 and 5 present respectively, the total combined water and tobermorite+ettringite bound water contents.

Figure 6 shows the TG and DTG curves of the samples taken from each region after different carbonation times. From these curves the main phases were quantified as detailed in materials and methods. Results are shown in the next figures, with respective discussions. In the respective DTG curves appear two decarbonation steps. The first one is referred to the less crystalized $CaCO_3$ decarbonation and the second, to the more crystallized one [15].

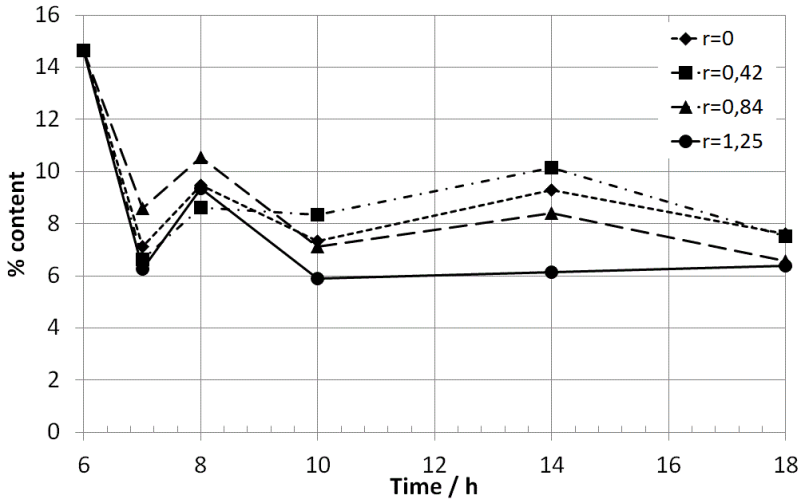

Fig.4 – Total combined water content on initial cement mass basis, at different times during carbonation.

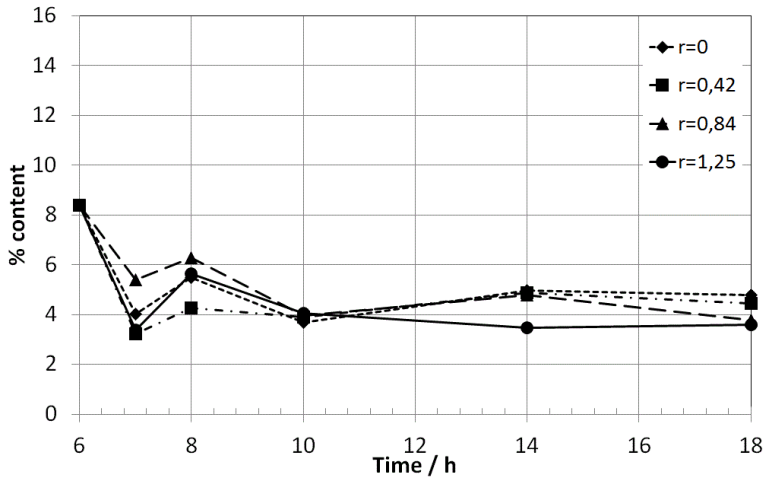

Fig.5 – Tobermorite+ettringite bound water content on initial cement mass basis, at different times during carbonation.

It can be noticed that the behavior of the curves representing the total combined water and that of tobermorite +ettringite bound water at each considered times of carbonation are similar. In the first hour of carbonation and exposition to the quite low relative humidity ambient (60%), there is a significant loss of water from all the hydrated phases which were present initially in the cement paste.

As occurred with the $Ca(OH)_2$ content (Fig.7), the content of total combined water and that of tobermorite +ettringite bound water increased between 1 and 2h of carbonation, due to the increase of the hydration degree and practically to a non-carbonation of the inner regions in this period.

During the next 2 hours of carbonation, inner regions begin to carbonate, as seen from Fig.8 and the combined water contents decrease, due probably to a higher porosity caused by the higher carbonation state of the specimen and the maintenance of the low relative humidity effect. This fact also indicates a modification of the tobermorite initial bound water content, as seen in Fig 4 [16].

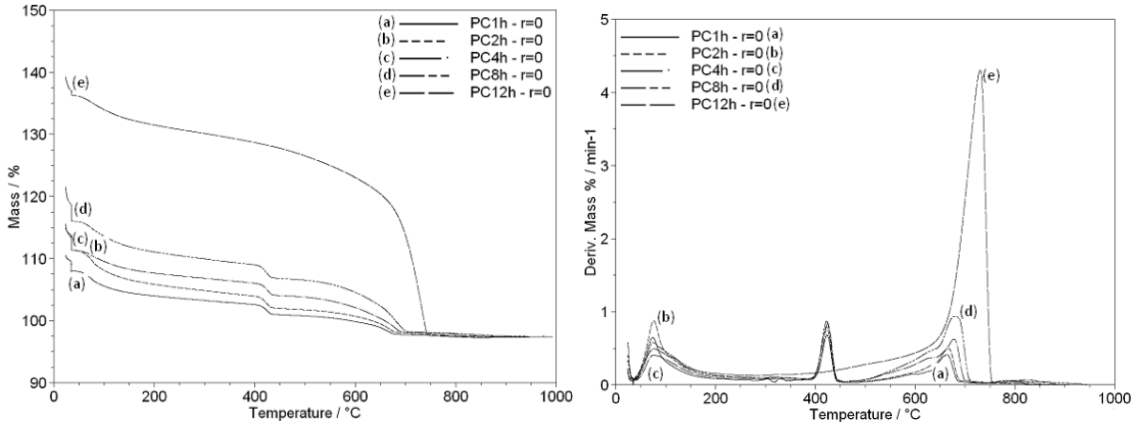

(a)

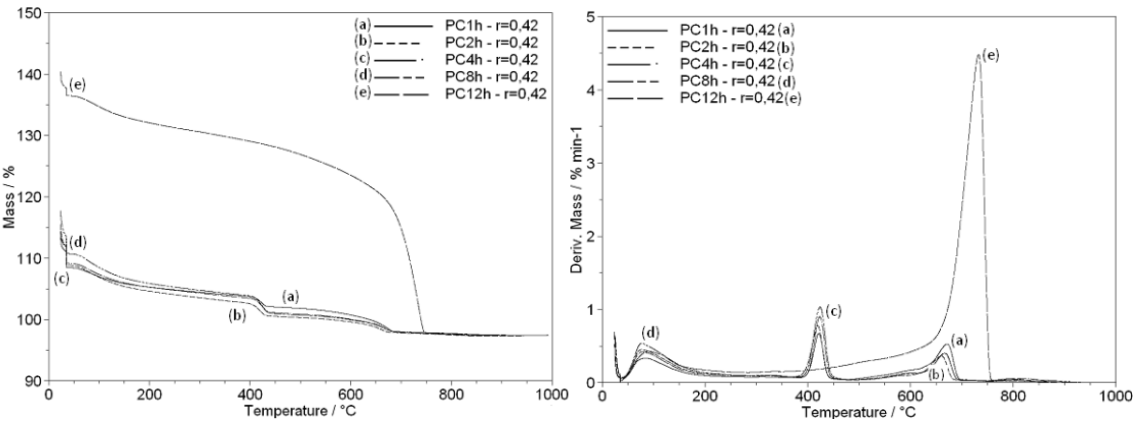

(b)

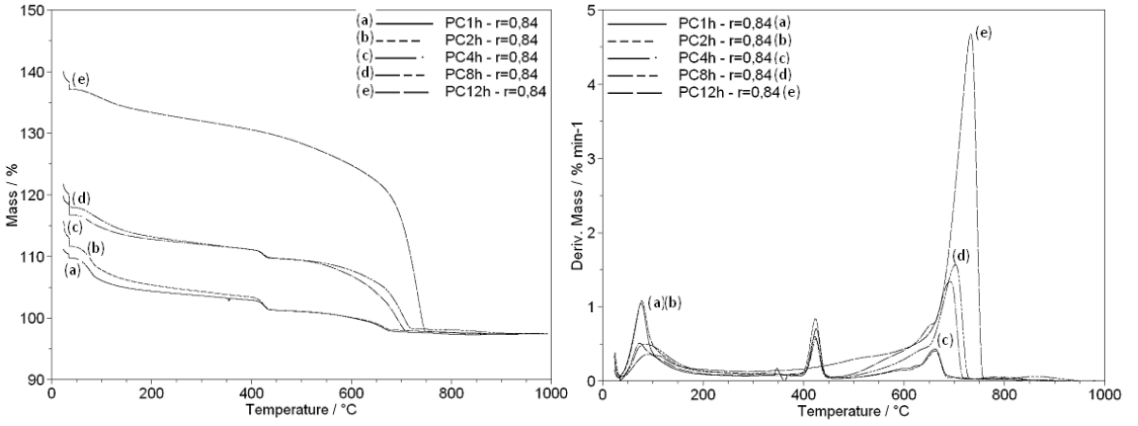

(c)

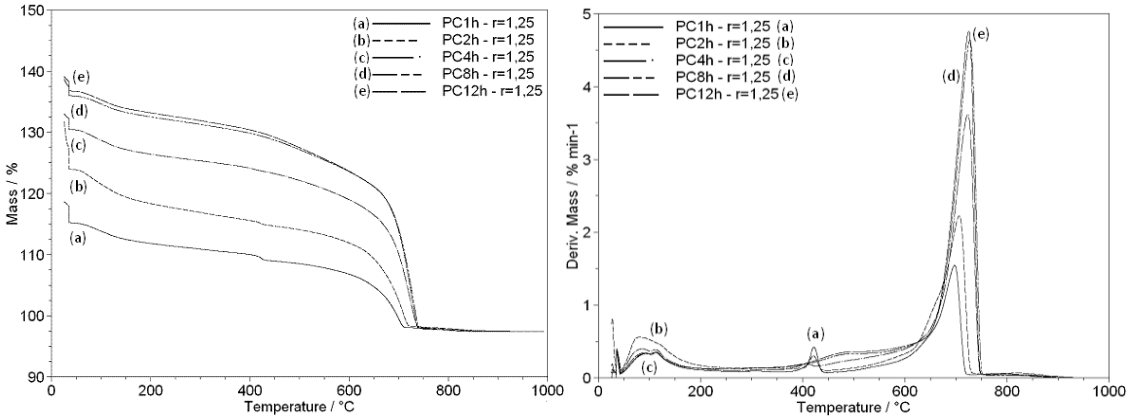

(d)

Fig.6 - TG/DTG results on initial cement mass basis

(a) for r=0 region, **(b)** for r=0.42 region, **(c)** for r=0.84 region **(d)** for r=1.25 region.

Between 4 and 8h of carbonation, an increase of the total combined water and that of the tobermorite+ettringite bound water occurs for the most inner regions at r = 0, 0.42 and 0.84. As the content of $CaCO_3$ keeps practically constant for the regions r = 0.42 and 0.84, their increase of total combined water and tobermorite +ettringite bound water occurs probably due to the water produced from the previous carbonation between 2 and 4h and the large content of weakly bound tobermorite water [16].

The $Ca(OH)_2$ was totally consumed at 4h of carbonation at r = 1.25, according to Fig.7 and its $CaCO_3$ content increased between 4 and 8h. The decrease of its total combined water and that of tobermorite+ettringite phases from 4h of carbonation, occurs probably due to the direct carbonation of some tobermorite phase at the external surface, and to the low relative humidity water vaporization effect. This causes a large modification of the matrix structure, which porosity also was increased by the higher carbonation state.

Between 8 and 12h of carbonation the content of total combined water for the regions at r = 0 and 0.42 decreases substantially, confirming a significant modification on the structure of the silicates produced by their carbonation according to Fig.8. The same decrease is observed for the tobermorite+ettringite bound water, but with a lower intensity.

Fig. 7 presents the $Ca(OH)_2$ content profile in the specimen during carbonation.

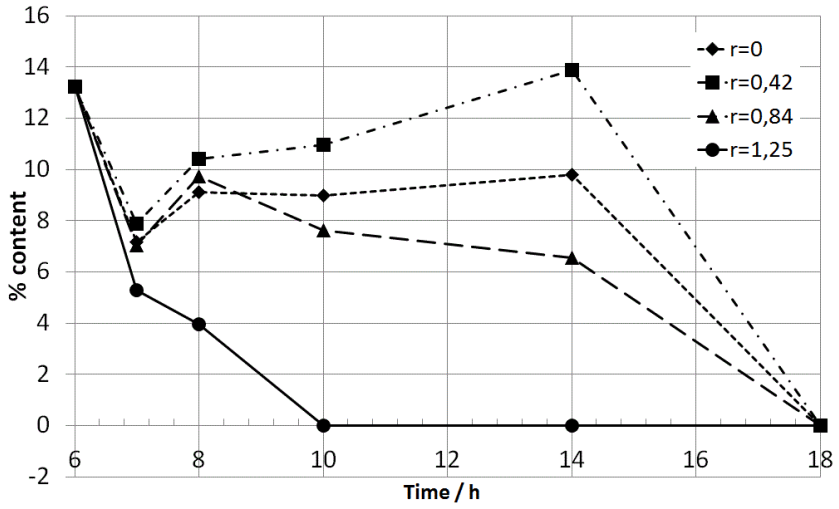

Fig.7 - $Ca(OH)_2$ content on initial cement mass basis at different times during carbonation.

There is a decrease in the $Ca(OH)_2$ content in the first hour of carbonation. During this period, as there is a significant water mass loss which diffuses from the center to the cylinder external surface, it probably dissolves some of the calcium hydroxide that is in inner regions, which when migrates to the outer regions is carbonated, decreasing in this period, the residual calcium hydroxide of the inner regions.

The content of $Ca(OH)_2$ from 1 to 2h of carbonation increases for the regions at r = 0, 0.42, 0.84, indicating the continuity of the hydration. In this period, apparently the CO_2 did not affect these regions according to Fig.8, which shows the calcium carbonate content profiles. However, at r = 1.25 a decrease of the $Ca(OH)_2$ content occurs, (Fig.7) due to the carbonation effect and at 4h of carbonation, a total consumption of the $Ca(OH)_2$ can be seen there, indicating, as expected, that the external surface is being carbonated much faster than the other regions.

Between 2 and 4h of carbonation occurs a decrease of the $Ca(OH)_2$ content at r = 0.84 and 1.25, accompanied by an increase of the $CaCO_3$ content, according to Fig.8. The content of $Ca(OH)_2$ for the region at r = 0 practically does not change and for r=0.42 increases slightly. The continuous loss of water from evaporation decreases the hydration rate at these regions and the slight carbonation that occurred in these period in the most central region (shown in Fig.8), consumed some of the additional formed $Ca(OH)_2$ during this period.

Between 4 and 8h of carbonation, for the region at r=0.84 a little decrease of the content of $Ca(OH)_2$ occurs (Fig.7), and for the regions at r = 0 and 0.42 occurs an increase, due to the hydration caused possibly by their higher water content.

At 12h of carbonation, all the inner regions of the specimen show total consumption of the $Ca(OH)_2$ according to Fig 7.

Fig. 8 presents the $CaCO_3$ content profiles in the specimen.

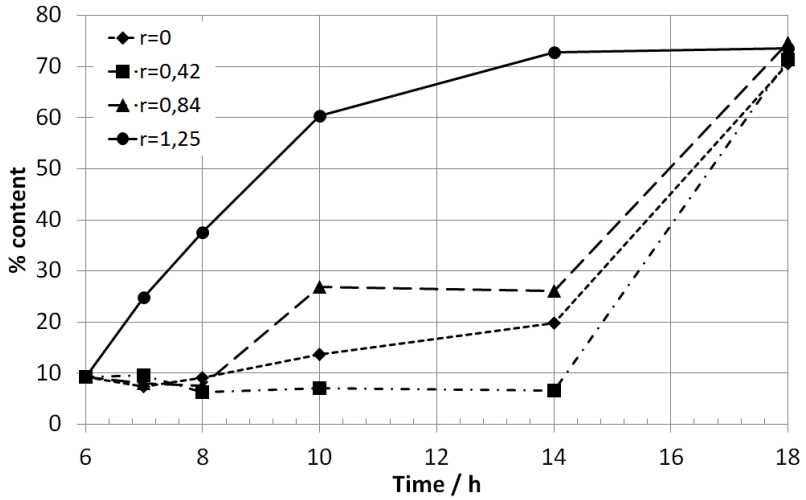

Fig.8 - $CaCO_3$ content on initial cement mass basis, at different times during carbonation.

In the first 2 hours of carbonation the $CaCO_3$ content was practically constant for the regions at r=0, 0.42 and 0.84, showing that the carbonation did not affect these regions, in this period.

From Figures 7 and 8 it can be seen that during the first two hours of carbonation at the external surface (r=1.25) the increase in $CaCO_3$ content was 28,32% while the decrease in $Ca(OH)_2$ content was 9,27% which is lower than the stoichiometrically consumption of 20,95% of $Ca(OH)_2$ that has actually occurred to produce that increase in $CaCO_3$ content. This indicates that somehow the water phase that is diffusing from the inner regions of the cylinder is lixiviating some of the $Ca(OH)_2$ formed in inner regions to the outer regions of the specimen, where it is carbonating.

Between 2 and 4h of carbonation, an increase of the $CaCO_3$ content at r=0, 0.84 and 1.25 regions is observed. At r=0.84 and 1.25 regions the carbonation is accompanied by a decrease of the $Ca(OH)_2$ according to the Fig. 7. As the $Ca(OH)_2$ content keeps constant for r=0 (Fig.7) this may indicate that the all the formed $Ca(OH)_2$ in this period

was carbonated. At r=0.42 the content of $CaCO_3$ keeps practically constant what explains the increase of the $Ca(OH)_2$ content due to the continuity of the hydration.

Between 4 and 8h of carbonation, the content of $CaCO_3$ at r=0 and 1.25 increased. At r=1.25, the $Ca(OH)_2$ was totally consumed (Fig.7) and the content of tobermorite+ettringite bound water has decreased (Fig.5). This confirms the intense carbonation of the silicates at r= 1.25 affecting its microstructure. At r= 0, the $Ca(OH)_2$ content (Fig.7) and that of total combined water and tobermorite+ettringite bound water (Fig.4 and 5) have increased. Considering a small diffusion of CO_2 from the external surface to the center during this period, the carbonation that has occurred slightly at r=0, and that did not occurred practically at r=0.42 and 0.84 can be explained by the much smaller mass of that region, as shown in Fig.1.

The external surface was totally carbonated up to 8h (Fig.8) and the other regions presented a large carbonation in this stage. Increasing the carbonation time to 12h, practically all the regions of the cylinder become carbonated, as expected from the consumption of all $Ca(OH)_2$ (Fig.7).

Fig. 9 presents the evolution of the compressive strength measured after 14 days of cure, after each carbonation time.

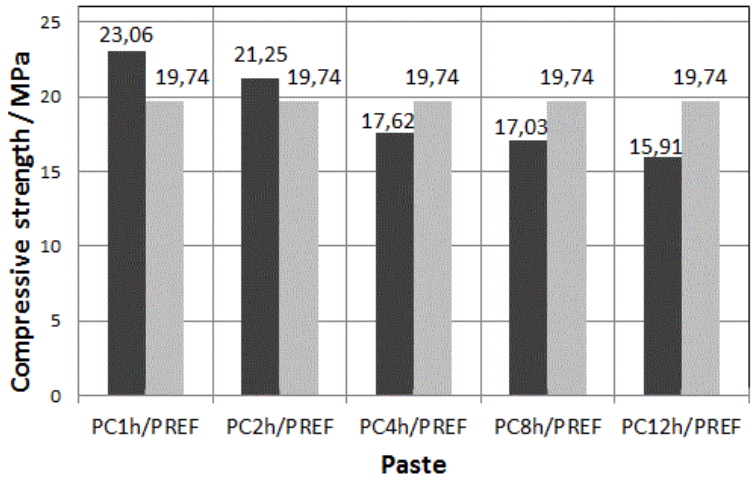

Fig. 9- Compressive strength as a function of CO_2 time exposure

It shows that at 1 and 2h of carbonation, the compressive strength of the paste is higher than that of the reference (PREF) and from 4h of carbonation, the resistance of the carbonated paste decreases, showing that increasing the time of exposure to CO_2, it affects the compressive mechanical resistance of the paste. According to Fig 6 and 7,

between 1 and 2h of carbonation, at the inner regions there is an increase of the $Ca(OH)_2$ content and the absence of carbonation seen by the maintenance of the $CaCO_3$ content. These facts indicate that the increase of the mechanical resistance probably occurs due to the low relative humidity effect and the consequent loss of bound water. This promotes a shrinkage on the tobermorite structure, reflected by a decrease of its basal distance, without changing its degree of polymerization [17], decreasing the porosity and increasing the resistance. From 4h of carbonation it was noticed from Figures 4 and 5, that the tobermorite phase, responsible for the resistance of the paste, starts to be affected structurally by the CO_2, explaining the decrease of the resistance with respect to the reference. Fig. 10 shows the pictures of the longitudinal cross sections of the cylinders at different carbonation times, after being immersed in water and dried at room temperature at 23°C (±2°C).

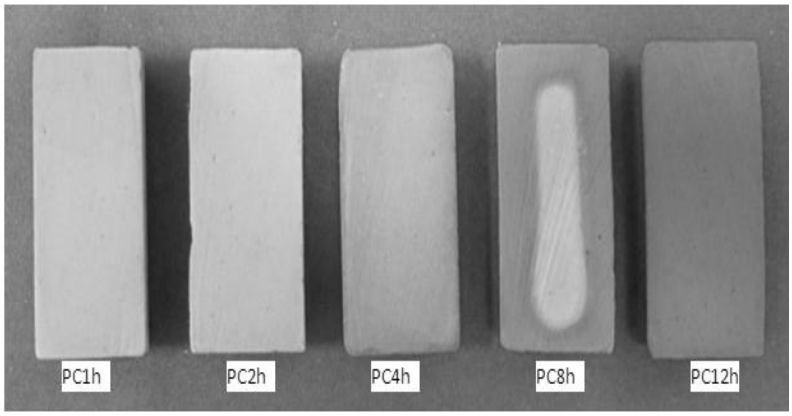

Fig. 10-Profile of the carbonated samples

From Fig.10, the evolution of the coloration of the longitudinal cross sections can be noticed. At 8h of carbonation, there is a gradient of carbonation with a noticeable carbonation front. At 1 and 2h of carbonation the coloration are practically equal. At 4h of carbonation the specimen begins to darken showing a transition behaviour. The specimen PC12h is more darken than the others due to the higher porosity than the other cases and consequent higher absorption of water.

For the PC8h there are two different coloured regions: the central part similar to PC1h, PC2h and PC4h and the other, more dark, equal to that of PC12h case, clearly showing the carbonation front.

4.Conclusions

- During carbonation the low relative humidity ambient causes the release of free water and some of the combined water from the hydrated phases, promoting an aqueous phase flow from the inner to the outer regions of the paste.
- This aqueous flow causes, by lixiviation, the migration of Ca^{++} ions from the inner to outer regions of the cylinder, which causes, during the first two hours of carbonation, a higher $CaCO_3$ content increase than that of the stoichiometrically expected, at the external surface.
- During this period, practically no carbonation was noticed at the inner regions of the cylindrical solidified paste, and the loss of part of the bound water causes the shrinkage of the crystalline structure, without affecting its degree of polymerization. This more densified structure promotes a total higher compressive mechanical resistance than that of the reference paste.
- After this initial period, the mechanical resistance begins to decrease due to the fact that the carbonation degree increases toward the inner regions of the cylindrical paste, by the carbonation of inner $Ca(OH)_2$ phases, as well as of the hydrated calcium silicate phases, for higher carbonation times.
- In spite of the CO_2 exposure time increases its capture, which may completely carbonate the paste, a practical time limit must be chosen, to avoid affecting negatively the resulting mechanical resistance of the paste.

Acknowledgments The authors acknowledge the experimental assistance of the Rio de Janeiro Federal University Chemical School Thermal Analysis and Civil Engineering Structure Laboratories and the financial support of the National Research Council (CNPq).

References

1. Shao Y, Mirza MS, Wu X. CO_2 sequestration using calcium–silicate concrete. Can J Civ Eng. 2006;33:776.

2. Shao Y, Zhou X, Monkman S. A new CO_2 sequestration process via concrete products production. Montreal: Department of Civil Engineering, McGill University; 2006.
3. Shao Y, Monkman S, Wang S. Market analysis of CO_2 sequestration in concrete building products. Second international conference on sustainable construction materials and technologies. Italy: Ancona; 2010. p. 28–30 June.
4. Shao Y, Monkman S, Boyd AJ. Recycling carbon dioxide into concrete: a feasibility study. Concrete sustainability conference. Canada´: McGill University, Department of Civil Engineering; 2010.
5. Habert G, Roussel N. Study of two concrete mix-design strategies to reach carbon mitigation objectives. Cem Conc Comp.2009;31:397–402
6. Rostami V, Shao Y, Boyd AJ. Microstructure of cement paste subject to early carbonation curing. Cem Concr Res. 2012;42(1): 186–93.
7. Li Y, Liu H, Wu S, Sun R, Lu C. Sulfation behavior of CaO from long-term carbonation/calcination cycles for CO_2 capture at FBC temperatures. J Therm Anal Calorim. 2013;111:1335–43.
8. Tejeda AR, Pfeiffer H. α-γ Lithium borate phase transition produced during the CO_2 chemisorption process. J Therm Anal Calorim. 2012;110:807–11.
9. Neves Junior A, Dweck J, Toledo Filho RD, FairBairn EMR. CO_2 sequestration by high initial strength Portland cement pastes J Therm Anal Calorim. 2013; 113:1577-84.
10. Brazilian Association of Technical Standards. High initial strength Portland cement. NBR 5733. Rio de Janeiro. 1991.
11. Brazilian Association of Technical Standards. Moderate sulphate resistance Portland cement and moderate hydration heat (MRS) and high sulphate resistance NBR 5737. Rio de Janeiro. 1986.
12. Neves Junior A, Dweck J, Toledo Filho RD, FairBairn EMR. Early stages hydration of high initial strength Portland cement—Part I—thermogravimetric analysis on calcined mass basis. J Therm Anal Calorim. 2012;108:725–31.
13. Brazilian Association of Technical Standards. Concrete – compressive testing of cylindrical specimens. Rio de Janeiro. 1994
14. Dweck J, Buchler PM, Coelho ACV. Hydration of a Portland cement blended with calcium carbonate. Therm Acta. 2000;346:105–13.

15. Dweck J, Cunha ALC, Pinto CA. Thermogravimetry on calcined mass basis—hydrated cement phases and pozzolanic activity quantitative analysis. J Therm Anal Calorim. 2009;97:85–9.
16. Dweck J, Silva PFF, Buchler PM, Cartledge FK.Study by thermogravimetry of the evolution of ettringite phase during type II Portland cement hydration. J Therm Anal Calorim. 2002;69:179–186.
17. Cong X, Kirkpatrick RJ. Effects of the temperature and relative humidity on the structure of C-S-H gel. Cem Concr Res. 1995;25(6): 1237–45.

ARTIGO E - Neves Junior A, Toledo Filho R.D, Dweck J, Fairbairn E.M.R. A study of CO_2 capture by high initial strength Portland cement pastes at early curing stages by non conventional thermogravimetry and differential thermal analysis. To be submitted 2014.

A study of CO_2 capture by high initial strength Portland cement pastes at early curing stages by non conventional thermogravimetry and differential thermal analysis.

Alex Neves Junior[a], Romildo Dias Toledo Filho[a], Jo Dweck[b] and Eduardo de Moraes Rego Fairbairn[a]

[a] Civil Engineering Program – COPPE – Rio de Janeiro Federal University, Brazil

[b] School of Chemistry - Rio de Janeiro Federal University, Brazil.

To be submitted to an international journal

2014

Abstract

In a previous work, the authors monitored by non-conventional differential thermal analysis (NCDTA), the evolution of the hydration reactions in the first 24h of high initial strength sulphate resistant Portland cement (HSSRPC) pastes prepared at different water to cement ratios (W/C). This study was done to understand the influence of the W/C ratio on the simultaneous hydration and setting process, in a higher mass scale, which orientated to choose the best conditions of CO_2 capture by the paste.

Although the literature presents intensive studies based on monitoring cement hydration in adiabatical and semi adiabatical environments, studies of cement hydration in controlled climatic chambers are very rare. Using three W/C ratios (0.5, 0.6 and 0.7) and three relative humidities (60, 80 and 100%) at 25°C, the authors analyzed in real time the evolution of cement hydration reaction during the first 24h in an environmental controlled chamber. Using the best conditions of CO_2 capture achieved in a previous work by the authors, a new non-conventional DTA (NCDTA) system was developed to analyze hydration and conditions of HS SR PC paste, as well as a non-conventional TG system (NCTG) and mass changes on real time. The experiments with the NCDTA and NCTG systems allowed to correlate the thermal effects with the mass changes that occur during carbonation conditions.

Key Words: NCDTA, NCTG,early stage hydration, early carbonation curing, CO_2 capture.

1.Introduction

Differential thermal analysis (DTA) has been used as a tool to study thermal effects, by the measurement of temperature difference between a sample and an inert reference, when both are submitted to an external heating or cooling device. In cement and concrete research, experiments using isothermal calorimetry have been used to study pre-screen concrete materials, to identify incompatibility of cementitious materials; to forecast setting time, to evaluate early-age strength by thermal effects [1], to investigate the early stage hydration of different classes of oilweel cement at various temperatures [2], and to study the hydration kinetics [3].

In non-conventional differential thermal analysis (NCDTA) these external heating or cooling devices are not used and the system operates semi-adiabatically measuring the same temperature difference than DTA, due to the thermal effects promoted by the spontaneous cement hydration exothermal reactions. The NCDTA apparatus has been used by the authors for the comprehension and study of the cement hydration reactions, pozzolanic activity and influence of W/C ratio on the hydration kinetics [4-7].

Mass changes to calculate the CO_2 capture have been used by some authors [8-10]. They usually are based in a measurement of mass before and after carbonation, considering the mass of water released from the carbonation reaction.

However, examples of NCDTA applications used to study cement hydration reactions, allowing direct influence of the environment in the thermal effects, is scarce. In this work, the authors propose a new NCDTA system used in a controlled chamber to study the thermal effects of the hydration and carbonation reactions of a paste on real time. W/C ratios equal to 0.5, 0.6 and 0.7 were used, based on a previous work by the authors about CO_2 capturing by cementitious pastes [10]. Relative humidities equal to 60, 80 and 100% were used keeping the temperature constant at 25°C.

Using the best CO_2 capture conditions by a high initial strength and sulfate resistant Portland cement (HS SR PC) paste in a previous work [10], the thermal effects caused by the carbonation treatment were monitored in the first 24h by the new NCDTA system. Considering the same established conditions of CO_2 capture, a non-conventional thermogravimetric system was used inside the chamber to measure, the mass change caused by the CO_2 action in cylinders of HS SR PC paste, during their setting with $CaCO_3$ formation. The performed experiments allowed to identify the several steps that have occurred before and during carbonation and to establish a relationship between the measured thermal effects and the mass gain due to the carbonation reaction.

2.Materials and methods

In this study, a high initial strength and sulfate-resistant Portland cement (HS SR PC) [11] was used to prepare the paste specimens, which allow reaching high strengths at early hydration stages. This kind of cement may have a maximum of 5% of carbonate addition and aggregation of blast furnace slag or pozzolanic materials [12]. The

chemical composition, determined by XRF was presented in a previous work by the authors [13].

For this study the following operating conditions were used:

- Water to cement ratio (W/C) of 0.5, 0.6 and 0.7. The specimens produced with these rations were referenced in the present paper as P_{50}, P_{60} and P_{70};
- Relative humidity (RH) 60, 80 and 100%. The specimens submitted to these humidity conditions were referenced as H60, H80 and H100;
- The CO_2 content inside the controlled was equal to 20% in volume and the temperature was 25°C.

The details of the controlled chamber and CO_2 controlling device were shown in a previous work [10]. Deionized water was used to prepare the pastes. A simplified schematics of the NCDTA, was presented in previous work by the authors [14], which motivated the new NCDTA proposed system. It consists of two main squared iron molds of (115 x 115 mm usually used for concrete mechanical strength measurements) with a height of 25mm, one containing an inert reference material, which is a hydrated HS SR PC cement paste, aged more than 3 months and the other one, containing the paste sample.

Each iron mold was totally isolated from the environment of the controlled chamber by an external styrofoam mold, through which a thermistor with 0.03°C resolution was introduced through a hole at the half height of the iron mold, until the center of the square to measure the reference or sample temperatures (T_{ref} or T_s), according to Figs 1(a) and (b).

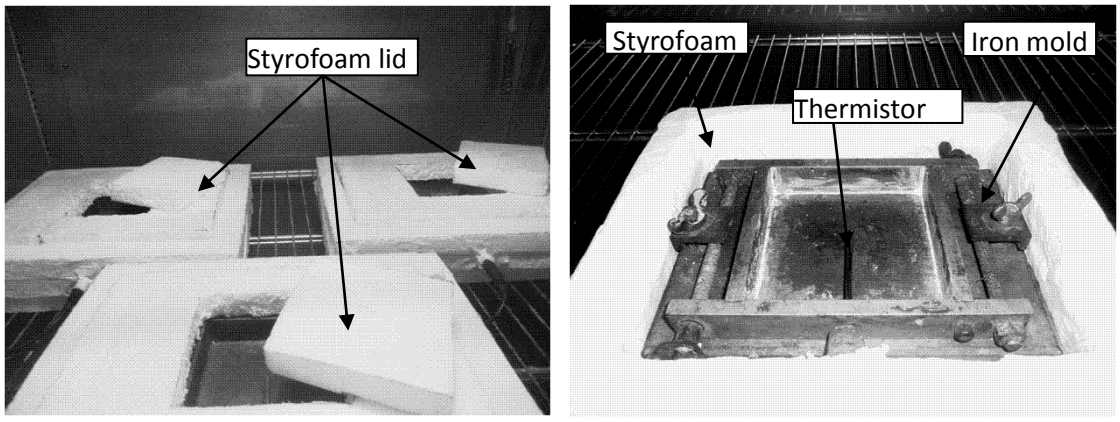

(a).....(b)

Fig 1 – (a) Detail of the styrofoam mold insulation with respective lid (b) Detail of the iron mold and the thermistor maintained inside it.

For the data acquisition at sealed conditions, according to Fig 3, the upper exposed surfaces of the reference and sample were covered with a styrofoam lid.

The temperature data acquisition was done by an interface, linked to a computer to measure sample and reference temperatures and their difference on real time according to Fig 4.

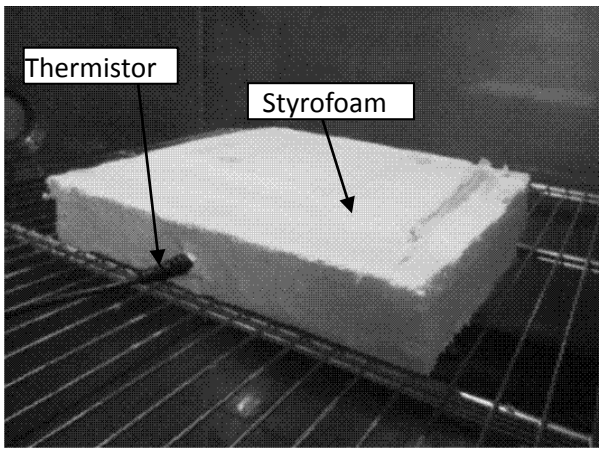

Fig 3 –Detail of the sealed system with Styrofoam insulation and the entrance of the thermistor.

The pastes were casted into the iron mold immediately after being prepared in a beaker during 30s in a relative humidity chamber at RH=99%. The temperatures were measured during 24h of hydration, from its beginning at fluid state.

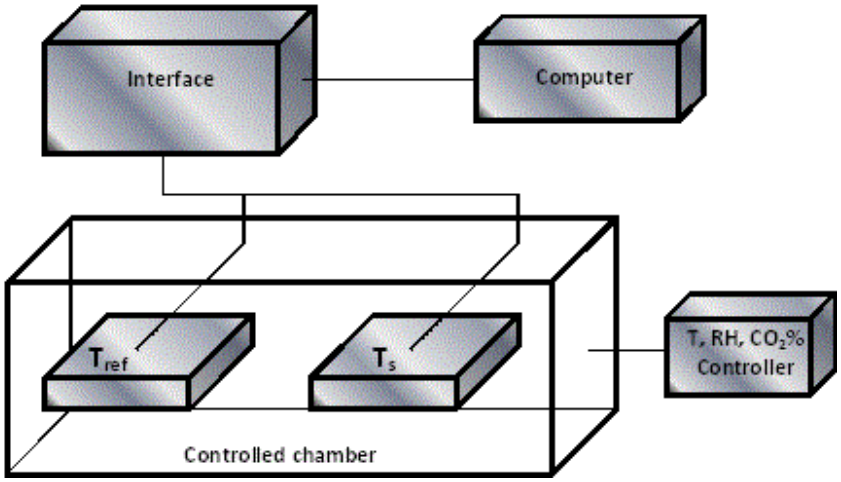

Fig 4 –Simplified schematics of the new NCDTA system

The following nomenclature was used to reference the specimens analyzed in the new NCDTA system:

- $P_mH_nF_o$, refers to the specimens exposed to the controlled chamber environment, where "*m*" is the W/C ratio (in mass *%*), "*n*" is the relative humidity (in *%*) and "*o*" is the time at which the temperature measurements have started.
- P_mREF, refers to the reference specimens analyzed in sealed conditions, where "*m*" is the W/C ratio (in mass *%*).

The carbonation treatment was performed with the new NCDTA system, only for the P_{70} case, using the following nomenclature:

- $P_mH_nF_{o\text{-}p}$, refers to the specimens exposed to the controlled chamber environment, where "*m*" is the W/C ratio (in mass *%*), "*n*" is the relative humidity (in *%*), "*o*" is the time at which the CO_2 treatment was started and "*p*" is the time (in hours) during which the specimen was exposed to CO_2 ambient.
- The specimen produced after an initial hydration of 6h in sealed conditions, 1h of carbonation in the best conditions of capturing (60%) and then more 17h of hydration in sealed conditions (100%), was referenced as $P_{70}H_{60\text{-}100}F_{6\text{-}1\text{-}17}$.

For the experiments done with mass data acquisition on real time, the cement and the water were mixed using an electronic mixer during 30s. After that, the paste was casted in a cylindric mold of polyvinyl chloride (PVC) of 25mm of diameter and 50mm of height. The specimens were cured in a chamber with 100% relative humidity for 6h of hydration at sealed conditions.

Then, the pre-cured cylinder was demolded and immediately placed on an Ohaus Scout Pro Balance 400g (Fig 5) located inside the controlled chamber, where the experiments were performed.

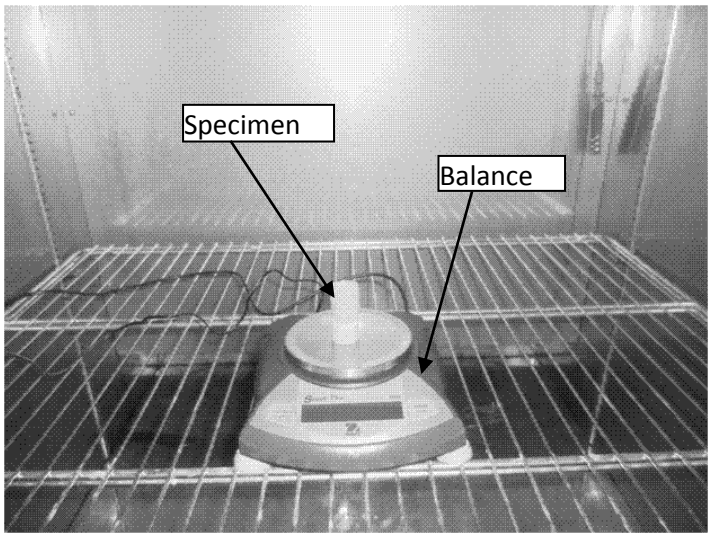

Fig 5 – Details of the NCTG system with the sample

Conventional thermogravimetric systems are composed by separate balance and heating chamber furnace, in which the sample is located on a holder, This holder stays on a device that comes from the external and separate balance [15-17]. As can be seen in Fig.5, the authors developed a new non-conventional thermo-gravimetric (NCTG) system, which has the balance located in a controlled ambient chamber as shown in Fig.6. The mass data acquisition on real time is done by an interface external to the chamber, which transforms and sends the output mass signal of the balance to a computer, where a file with the acquired data is saved for each run. The temperature (T), the relative humidity (RH) and CO_2 content inside the chamber are controlled by respective controlling devices of the chamber.

The following nomenclature was used to reference specimens in the mass measurements experiments:

$P_mH_nM_o$, where "*m*" is the W/C ratio (in mass *%*), "*n*" is the relative humidity (in *%*) and "*o*" is the time during which the specimen was submitted to CO_2 ambient.

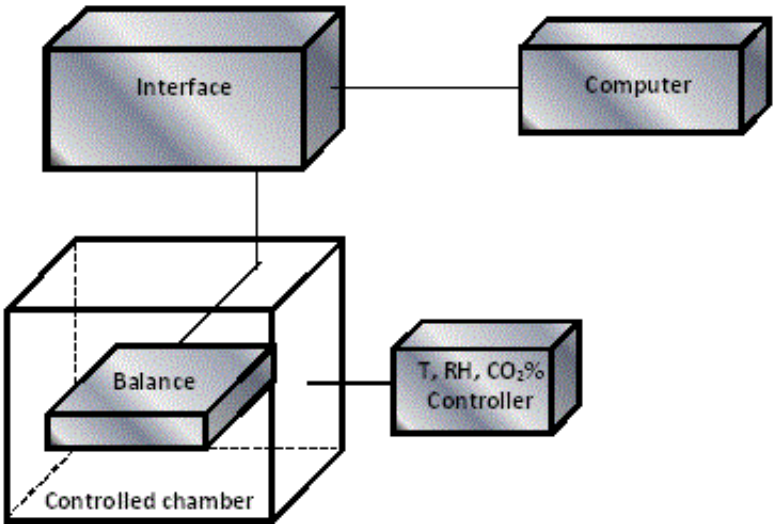

Fig 6 – Simplified schematics of the NCTG system

- The specimen produced with 1h of CO_2 treatment at a relative humidity of 60% and for 23h at a relative humidity of 100%, was referenced as $P_{70}H_{60\text{-}100}M_{1\text{-}23}$;

Table 1 shows the main experimental conditions of the studied specimens.

Table 1 – Experimental conditions

Specimens	W/C %	RH %	Begginig of the CO2 exposure/h	Exposition to CO2 time/h
$P_{50}REF$	50	-	-	-
$P_{60}REF$	60	-	-	-
$P_{70}REF$	70	-	-	-
$P_{50}H_{60}F_0$	50	60	-	-
$P_{60}H_{60}F_0$	60	80	-	-
$P_{70}H_{60}F_0$	70	100	-	-
$P_{50}H_{80}F_0$	50	60	-	-
$P_{60}H_{80}F_0$	60	80	-	-
$P_{70}H_{80}F_0$	70	100	-	-
$P_{50}H_{100}F_0$	50	60	-	-
$P_{60}H_{100}F_0$	60	80	-	-
$P_{70}H_{100}F_0$	70	100	-	-
$P_{70}H_{60}F_{0\text{-}0}$	70	60	-	-
$P_{70}H_{60}F_{6\text{-}18}$	70	60	6	18
$P_{70}H_{60\text{-}100}F_{6\text{-}1\text{-}17}$	70	60/100	6	1
$P_{70}H_{100}M_0$	70	100	-	-
$P_{70}H_{60}M_0$	70	60	-	-
$P_{70}H_{60}M_{24}$	70	60	6	24
$P_{70}H_{60\text{-}100}M_{1\text{-}23}$	70	60/100	6	1

3.Results and discussion

Figures 7(a) 7(b) and 7(c) show, respectively the NCDTA curves for the P_{50}, P_{60} and P_{70} pastes at different RH and sealed conditions (reference cases).

According to the Figures 7(a) 7(b) and 7(c), all the reference pastes presented at the initial time of hydration, the characteristic exothermic peak of the ettringite formation followed by a short induction time. The highest exothermic peak begins right after, during which the acceleration period occurs. At the RH=60% environment, during the induction period, where the hydration reactions slow down, the P_{50} pastes present a higher endothermic effect than the other cases.

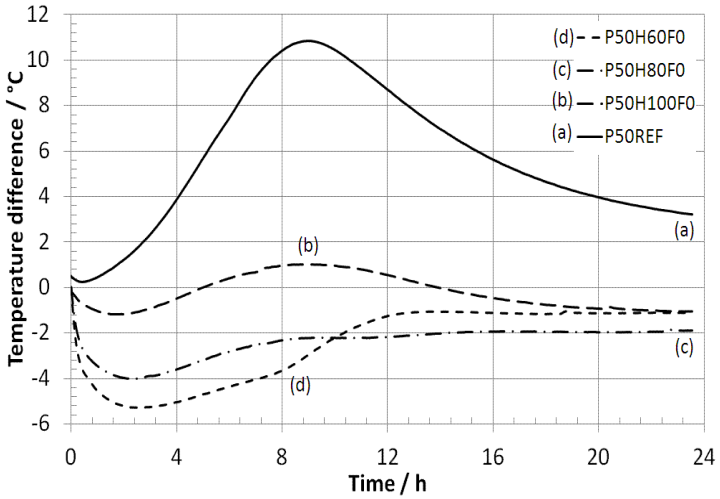

(a)

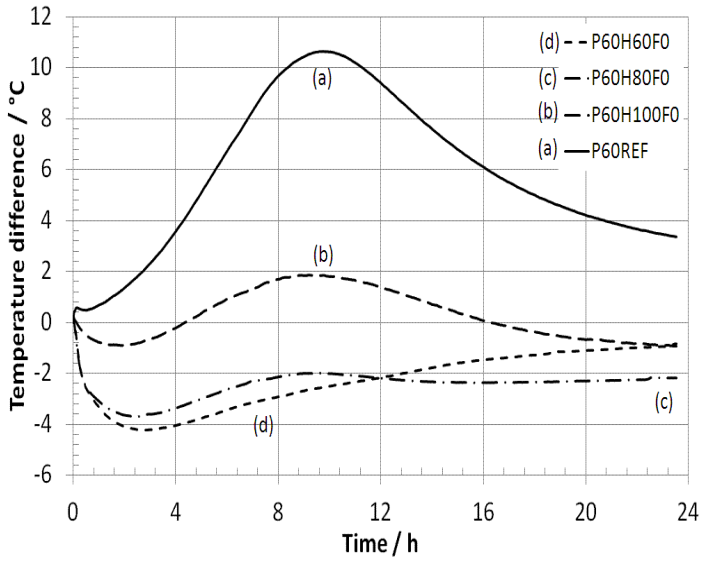

(b)

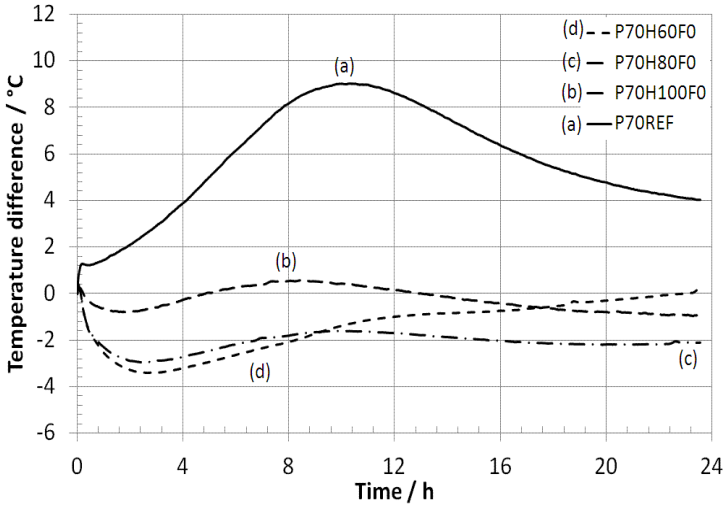

(c)

Fig 7 –NCDTA curves of the pastes: (a) P_{50}, (b) P_{60} and (c) P_{70}

This fact is due to the higher endothermic effect of water evaporation at RH=60%, than the smaller simultaneous exothermic effect due to hydration reactions at this initial smallest W/C ratio. During the acceleration period, from 8h of hydration, occurs an abrupt increase of the recorded temperature difference until its stabilization at 13h of hydration, after which the measured temperature difference keeps practically constant, due to the occurrence of equal simultaneous endothermic and exothermic effects and slightly increasing, when the latter are slightly higher than the former effects. The pastes P_{60} and P_{70}, continue to loose free water, because they present higher contents of water and porosity than the P_{50} pastes. Increasing the RH to 80 and 100%, the endothermic effect caused by the evaporation of the free water decreases during the induction period.

Even at relative humidity of 100%, the pastes presented losses of free water by evaporation during the pre-induction and induction periods; indicated by the lower temperature difference than those of the respective P_{50}REF, P_{60}REF and P_{70}REF maintained at sealed conditions. With the increase of the mechanical resistance of the paste at higher hydration times, due to the decrease of the porosity, a decrease of the releasing rate of the free water occurs, reflected by the increase of the NCDTA temperature difference signal during the acceleration step. The P_{50} pastes presented an increase of the temperature difference higher than the pastes P_{60} and P_{70}, due to their higher amount of cement per volume than the other cases.

Figure 8 shows the NCDTA curves for the P_{70} pastes at different conditions of CO_2 treatment, after 6 hours of hydration at sealed conditions

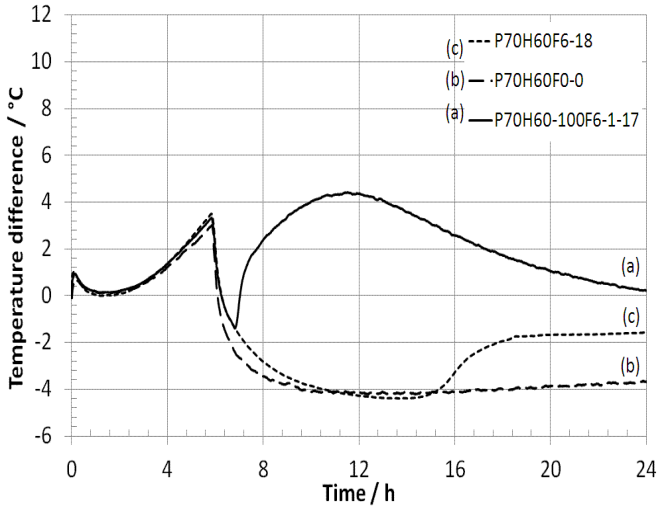

Fig 8 –NCDTA curves for the P70 pastes at different conditions of CO_2 treatment

According to Fig 8, until 6h of hydration, when the pastes were cured thermally isolated from the environment by the styrofoam mold, the pre-induction, induction and initial acceleration periods can be clearly noticed. When the styrofoam lid is removed, which was isolating the upper surface of the paste from the external environment of the controlled chamber at RH=60%, occurs a fast decrease of the temperature difference, caused by the significant loss of free water by evaporation. For the $P_{70}H_{60}F_{6\text{-}18}$ paste, which remained in contact with the CO_2 atmosphere of the chamber for 18h, we can notice an increase of the temperature difference for the paste treated with CO_2, between 15 and 18h of hydration, which was not observed for the $P_{70}H_{60}F_{0\text{-}0}$ paste, which was only submitted to the 60% RH ambient for the same time. This increase of temperature difference was caused by the exothermic effect of the carbonation reaction during the time at which it was more pronounced. For the $P_{70}H_{60\text{-}100}F_{6\text{-}1\text{-}17}$, with 1h of CO_2 exposition, only the expected loss of free water by evaporation has occurred in this period. Closing the system during the next 17 hours with the styrofoam mold lid, the NCDTA curve shows the increase of temperature difference of the acceleration period, reaching the maximum hydration rate at practically 12h. As the maximum hydration rate of the P70REF occurred at practically 10h, this indicates that the high endothermic effect that occurred during the 1h exposition to 60% RH and CO_2 ambient retards the hydration process.

Figure 9 shows the NCTG curves obtained for the P_{70} pastes at different conditions of CO_2 treatment.

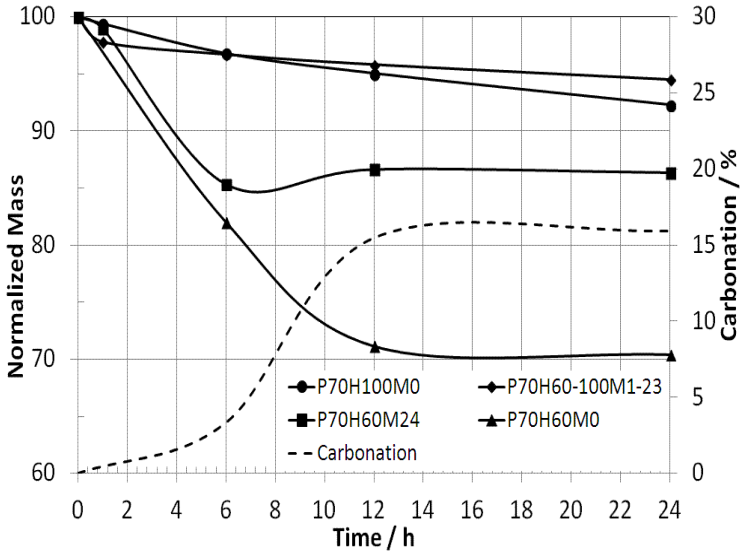

Fig 9 –NCTG curves for P70 pastes at different conditions of CO_2 treatment.

According to Fig 9, we can notice from the NCTG curves of the $P_{70}H_{100}M_0$ and $P_{70}H_{60\text{-}100}M_{1\text{-}23}$ cases until 6h, that the mass loss of the paste $P_{70}H_{60\text{-}100}M_{1\text{-}23}$ was higher than the paste $P_{70}H_{100}M_0$, due to the effect of the RH=60% ambient to which it was exposed during the unique hour of carbonation treatment. We can even see that at the RH=100% case in the controlled chamber, the paste $P_{70}H_{100}M_0$ shows a little mass decrease at the beginning of respective NCTG curve. This fact is due to an initial transient period, during which the controlled chamber attains the RH set point value from the initial lower ambient room RH condition within the chamber, caused when it must be opened between runs. From the 6^{th} to the 24^{th} hour, Fig 9 shows that the mass loss of the paste $P_{70}H_{60\text{-}100}M_{1\text{-}23}$ is lower than the case $P_{70}H_{100}M_0$. This fact occurred because of the carbonation effect that happened during one hour exposition to CO_2 in former case, which reduced the hydrated and carbonated paste porosity, reducing the water evaporation rate. For the NCTG curves of the pastes $P_{70}H_{60}M_0$ and $P_{70}H_{60}M_{24}$, we can notice that up to 6h, the paste $P_{70}H_{60}M_0$ presented a higher mass loss than the case $P_{70}H_{60}M_{24}$, because although both cases were being treated in a RH=60%, some calcite formation in the $P_{70}H_{60}M_{24}$ paste, decreased the water diffusivity for evaporation and consequently its resulting mass loss. From 6 to 12h, the $P_{70}H_{60}M_{24}$ paste, presented a mass gain, due to the effect of the carbonation of the paste in this stage, when compared to the case $P_{70}H_{60}M_0$ at the same conditions of RH. Thus, a carbonation curve was obtained from the difference between the NCTG curves of $P_{70}H_{60}M_0$ and $P_{70}H_{60}M_{24}$ cases, which shows the significant mass increase between 6 and 12h of hydration, due to the intense carbonation rate in this stage. From 12h, when all the free water was depleted and the carbonation stopped, the mass practically has not changed. Comparing the carbonation curve of Fig 9 with the NCDTA curve of the $P_{70}H_{60}M_{6\text{-}24}$ case in Fig 8, it can be noticed that, the high mass increase between 6 and 12h of carbonation in Fig 9 occurred approximately between the 8^{th} and 12^{th} hours of carbonation, shown in Fig 8 by the respective temperature difference increase step. Considering the different shapes and masses of the analyzed specimens in each case, this confirms that the mass increase has occurred during the exothermic carbonation reaction.

4.Conclusions

- The new Non-Conventional Differential Thermal Analysis (new NCDTA) system proposed by the authors assembled in a controlled ambient chamber is an

effective tool to study simultaneously, on real time, the hydration and carbonation reactions that may occur in cementitious pastes, from respective thermal effects.

- The non-conventional TG (NCTG) system assembled in a controlled ambient chamber allows one to study the mass changes due to the same reactions in cementitious pastes on real time.
- These two kinds of analysis can show the correspondence between the increase of the temperature difference due to the exothermic effect and the simultaneous increase of the mass due to the calcite formation during carbonation reactions.
- The new NCTG system shows that even when using 100% RH control inside the chamber, a small loss of water may occur from the pastes at the beginning transient step, due to the inevitable lower initial RH conditions of chamber, when the samples are inserted there.

Acknowledgments The authors acknowledge the experimental assistance of the Rio de Janeiro Federal University Chemical School Thermal Analysis and Civil Engineering Structure Laboratories and the financial support of the National Research Council (CNPq).

References

1. Ge Z, Wang K, Sandberg PJ, Ruiz JM. Characterization and performance prediction of cement-based materials using a simple isothermal calorimeter. J Adv Conc Tech. 2009;7(3);355-66.
2. Pang X, Bentz DP, Meyer C, Funkhouser GP, Darbe R. A comparison study of Portland cement hydration kinetics as measured by chemical shrinkage and isothermal calorimetry. Cem Con Comp 2013;39,23-32.
3. Garcia LI, Fernandez JA, Paloma A. Hydration kinetics in hydrid binders:Early reaction stages. Cem Conc Comp 2013; 39, 82-92.
4. Melchert MBM, Viana MM, Lemos MS, Dweck J, Büechler PM. Simultaneous solidification of two catalyst wastes and their effect on the early stages of cement hydration. J Therm Anal Calorim. 2011; 105(2):625-33.

5. Chaipanich A, Nochaiya T. Thermal analysis and microstructure of Portland cement-fly ash-silica fume pastes. J Therm Anal and Calorim. 2010; 99(2):487-93.
6. Dweck J, Buchler PM, Coelho ACV, Cartledge FK. Hydration of a Portland cement blended with calcium carbonate. Thermochim Acta. 2000; 346:105-13.
7. Gruyaert E, Robeyst N, De BN. Study of the hydration of Portland cement blended with blast-furnace slag by calorimetry and thermogravimetry. J Therm Anal Calorim. 2010; 102(3):941-51.
8. Shao Y, Mirza MS, Wu X. CO_2 Sequestration Using Calcium-Silicate Concrete. Can J of Civil Engin. 2006; 33:776.
9. Shao Y, Monkman S, Boyd AJ. Recycling carbon dioxide into concrete: a feasibility study. Concrete Sustainability Conference. 2010; McGill University, Department of Civil Engineering, Canadá.
10. Neves Junior A, Dweck J, Toledo Filho RD, FairBairn EMR. CO_2 sequestration by high initial strength Portland cement pastes J Therm Anal Calorim. 2013; DOI 10.1007/s10973-013-3117-0.
11. Brazilian Association of Technical Standards. High initial strength Portland cement. NBR 5733. Rio de Janeiro. 1991.
12. Brazilian Association of Technical Standards. Moderate sulphate resistance Portland cement and moderate hydration heat (MRS) and high sulphate resistance NBR 5737. Rio de Janeiro. 1986.
13. Neves Junior A, Dweck J, Toledo Filho RD, FairBairn EMR. Early stages hydration of high initial strength Portland cement—Part I—thermogravimetric analysis on calcined mass basis. J Therm Anal Calorim. 2012;108:725–31.
14. Neves Junior A, Dweck J, Toledo Filho RD, FairBairn EMR. Early stages hydration of high initial strength Portland cement—Part II—NCDTA and Vicat analysis. J Therm Anal Calorim. 2013;113:659–65.
15. TA Instruments – TGA 500 Thermogravimetric analyzer, 2013. http://www.egr.msu.edu/cmsc/equipment/ta-instruments-tga-500, downloaded on 20/10/2013.
16. TA Instruments – Symultaneous Q600 TGA/DSC equipment,2013. http://eqdb.nrf.ac.za/equipment/ta-instruments-sdt-q600-thermogravimetric-analyser-differential-scanning-calorimeter-tga, downloaded on 20/10/2013.

17. Mettler Toledo – Symultaneous TGA/DSC1 analyzer, 2013, http://www.azom.com/equipament-detais.aspx?EquipID=642, downloaded on 20/10/2013.

ARTIGO F - Neves Junior A, Toledo Filho R.D, Dweck J, Fairbairn E.M.R. The effects of the early carbonation curing on the mechanical and porosity properties of high initial strength Portland cement pastes. To be submitted 2014.

The effects of the early carbonation curing on the mechanical and porosity properties of high initial strength Portland cement pastes.

Alex Neves Junior[a], Romildo Dias Toledo Filho[a], Jo Dweck[b] and Eduardo de Moraes Rego Fairbairn[a]

[a] Civil Engineering Program – COPPE – Rio de Janeiro Federal University, Brazil

[b] School of Chemistry - Rio de Janeiro Federal University, Brazil.

To be submitted to an international journal

2014

Abstract

Mechanical and porosity related properties of high initial strength sulfate resistant Portland cement (HS SR PC) pastes subjected to early age carbonation curing were investigated. This work presents the characterization through mechanical properties, of carbonated HS SR PC pastes and of non-carbonated references. They were treated at two different times of carbonation (1h and 24h), at the best conditions of capturing, previously determined by the authors. The mechanical properties were characterized by compressive strength, tensile strength by diametrical compression, elastic modulus and poissons coefficient. It was found that 1h of carbonation improved the mechanical properties, while the increase of carbonation time to 24h, decreased significantly the same properties in relation to the reference specimens. The porosity related properties were characterized by total absorption, absorption by capillarity, gas permeability, and mercury intrusion porosity. It was noticed that the increase of the carbonation time from 1h to 24h, increased substantially the absorption properties. Despite the mechanical properties of the 1h carbonated paste were better than those of the reference, the absorbed water content of the carbonated specimen was slightly higher than that of the reference.

Key Words: early carbonation curing, compressive strength, total absorption, absorption from capillarity, gas permeability, mercury intrusion porosity.

1.Introduction

In a previous work the authors concluded that the CO_2 capture by an early high strength and sulfate resistant Portland cement (HS SR PC) paste should be done only after a brief hydration period [1]. This was proved by thermogravimetry, comparing samples treated with and without CO_2 [2]. Considering the same issue, the literature shows that the carbonation curing of cementitious materials can improve the mechanical and durability properties in some operating conditions [3,4].

The importance of the CO_2 treatment of cementitious materials as concrete, mortar and paste is the possibility to develop materials with a better performance than when using conventional curing, besides considering the environmental and economic benefits to capture CO_2 from the atmosphere [5-7].

According to the mechanical results obtained by the authors for cylinders of HS SR PC pastes, with 14 days of hydration, treated with CO_2 in two different times of carbonation (1 and 24h), it was noticed that the time of exposure to CO_2 is crucial for its capture capacity without damaging the cementitious matrix [8].

The aim of this work is to characterize, by mechanical property, porosity and permeability measurements after 28 days of conventional curing, the HS SR PC pastes subjected to CO_2 curing in the two carbonation times (1 and 24h) previously studied by the authors [8]. Carbonated cement pastes are compared with a conventionally hydrated reference paste by mechanical properties as compressive strength (elastic modulus, and poisson coefficient) and tensile strength by diametrical compression, as well as by porosity properties as total absorption, absorption by capillarity, gas permeability and mercury intrusion porosity.

2.Materials and methods

In this study, a high initial strength and sulfate-resistant Portland cement (HS SR PC) [9] was used to prepare the paste specimens, which allows to reach high strengths at early hydration stages. This kind of cement may have a maximum of 5% of carbonates addition and aggregation of blast furnace slag or pozzolanic materials [10]. The chemical composition, determined by XRF was presented in a previous work by the authors [11].

Deionized water was used to prepare the pastes, which were mixed during 30 s in a mechanical mixer in an environmental temperature of 23°C (±2°C).

The pastes, which were prepared using a water to cement ratio (W/C) of 0.7, were immediately cast in two types of molds:

- 36 cylinders with 25mm of diameter and 50mm of height for the compressive strength, absorption by capillarity and mercury intrusion porosity experiments.

- 36 discs with 50mm of diameter and 25mm of height for the tensile strength by diametrical compression, total absorption and gas permeability experiments.

For each experiment 12 specimens were separated, where:

- 4 specimens were conventionally hydrated during 28 days in an ambient of relative humidity of 100%. These specimens are referenced as P_{REF}.

- 8 specimens were hydrated during 6h in an environment of RH=100%, then they were demolded and immediately placed in a controlled climatic chamber maintaining the best conditions of capture established by the authors [1], which are RH=60%, 25°C and a volumetric concentration of 20% of CO_2 in the chamber. The specimens were treated with CO_2 during 2 different times of carbonation: 4 specimens treated during 1h of carbonation being referenced as P_{C1h} and 4 specimens treated during 24h of carbonation being referenced as P_{C24h}. After each carbonation treatment, the specimens were cured in an ambient with RH=100% until 28 days after respective preparation.

The mechanical tests of compressive strength and tensile strength by diametrical compression, were performed in a SHIMADZU machine, model UH – F1000kN with a loading speed of 0,01mm/min, following the respective Brazilian NBR 5739 and NBR 9778 standard methods [12, 13].

The tests of total absorption and absorption by capillarity, were performed according to the Brazilian NBR 9778 and NBR9779 standard methods [14,15] respectively.

The nitrogen gas permeability test was performed in a nitrogen gas permeameter used at LABEST/COPPE/UFRJ [16] with a controlled pressure of 0.2 MPa, which simplified schematics is shown in Figure 1. To perform this experiment, the cylindrical specimen is wrapped by an aluminum tape at all its lateral area, after which is positioned in a silicone rubber cylindrical ring, before being placed in the test chamber. The experiment consists on measuring the time during which a drop of water entrained by the nitrogen flow passes through the 5 ml volume height of a pipette. The drop of water is injected at the bottom of the pipette as shown in Figure 1 after attained a stable nitrogen flow. The gas permeability was calculated using the modified Darcy's law for compressible fluids.

$k = \frac{2\eta Qh.P_2}{A\left(P_1^2 - P_2^2\right)}$, where:

k =permeability (m²)

η =viscosity of the nitrogen at the temperature of the test (Ns/m²).

Q = nitrogen gas flow (m³/s)

h =height of the specimen (m)

P_1= pressure applied at the test chamber entrance (N/m²)

P_2= pressure at the exit of the test chamber (N/m²)

A= cross section area of the specimen (m²)

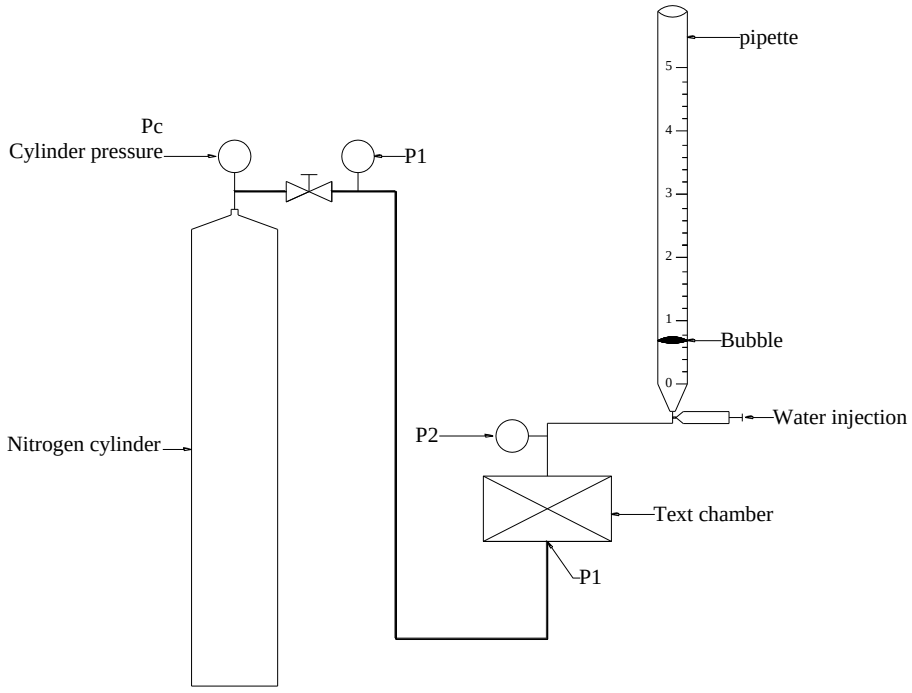

Fig. 1 – Nitrogen gas permeability set up

The mercury intrusion porosity test was performed in an AutoPore IV Micromeritics according to the ISO 15901/2005 standard method [17] with a contact angle of 130°.

3. Results

Figure 2 shows the compressive strength curves for the pastes P_{REF}, P_{C1h} and P_{C24h}.

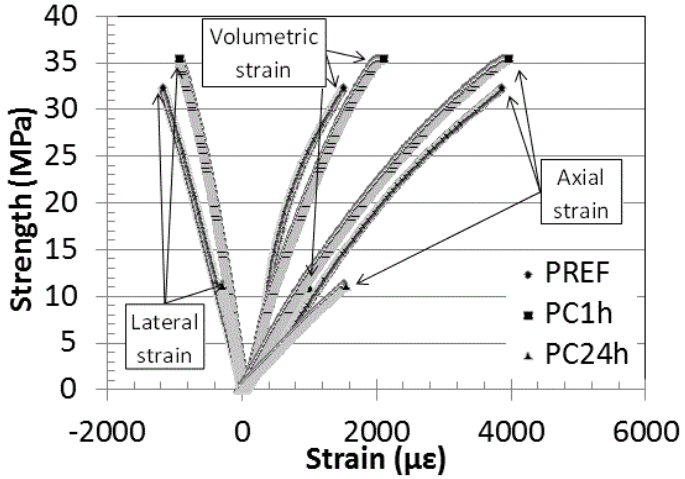

Fig. 2 – Compressive strength curves of P_{REF}, P_{C1h} and P_{C24h} pastes.

It can be noticed that the compressive strength of the paste P_{C1h} is higher than the P_{REF} and P_{C24h}, confirming the results obtained previously by the authors [8] for 14 days. From the non linear shapes of the curves shown in Figure 2, it's also verified that before rupture micro cracking occurs, which causes elastic and plastic deformation. The carbonation time of 24h damaged the matrix decreasing the resistance. However, the short carbonation time of 1h affects the cementitious matrix structure in a way that promotes a slight increase of the mechanical resistance, when compared to that of the reference paste, as also observed by others [8, 18] in similar operating conditions. This fact can be explained by two reasons. The first is the decrease of the interlayer porosity due to the desorption of the water promoted by the action of the low relative humidity ambient, which shrinks the crystalline structure of the C-S-H solid phase and turns it more dense than that of the reference paste without changing the degree of polymerisation [18]. The second reason is the formation, as stated by Rostami et al [8], for short carbonation times, of a calcium–silicate–hydrate phase intermingled with calcium carbonate, generating a microstructure with more strength-contributing solids than conventional hydration of a new binding amorphous phase of calcium–silicate–hydrocarbonate. These authors also state, as occurred in present case, that the re-hydration procedure applied after carbonation was essential in increasing late strength and durability

Table 1, shows the results obtained for the mechanical properties of the pastes P_{REF}, P_{C1h} and P_{C24h}.

Table 1 – Mechanical properties of the pastes P_{REF}, P_{C1h} and P_{C24h}

Properties	Age	Pastes		
		P_{REF}	P_{C1h}	P_{C24h}
Elastic modulus (MPa)	28	10.03 (±3.70%)	12.89 (±6.83%)	7.02 (±5.56%)
Poisson's coefficient		0.34 (±2.76%)	0.34 (±2.79%)	0.18 (±2.09%)
Tensile strength by diametrical compression (kN)		2.8 (±1.01%)	2.8 (±1.89%)	0.7 (±1.11%)

It can be seen that the elastic modulus of the paste P_{C24h} is lower than the pastes P_{REF} and P_{C1h}. Otherwise the paste P_{C1h} presents an elastic modulus higher than P_{REF}, corroborating the results of the Fig.2. The Poisson's coefficient and the tensile strength by diametrical compression of the pastes P_{REF} and P_{C1h} are the same, decreasing for the paste P_{C24h} due to the higher carbonation effects on the change of the structural composition and properties of the cementitious matrix.

The mechanical results follow the expected results of the literature [2], where a small loss of water for the paste P_{C1h} occurs due its initial operating conditions during the early carbonation curing. The subsequent hydration with the total remaining water content is apparently enough and higher than the stoichiometrically content needed to complete the hydration reactions as occurs in the reference paste at the end of 28days. The slightly higher elastic modulus can also be explained due to the fact that the total water/cement mass ratio after 1 hour carbonation in P_{C1h} case is lower than that of the reference paste case, but still enough to proceed the hydration reactions in a similar way of that of the reference paste case. The practically equal values obtained for the Poisson coefficient as well as for the tensile strength by diametrical compression of P_{REF} and P_{C1h} pastes, can also be explained by the same reasons.

For the P_{C24h} paste, the much higher water loss during the higher water desorption time, due to the much higher and intense carbonation time and simultaneous low relative humidity conditions, changes considerably the structure composition of the paste, as well as decreases significantly the remaining water content and water/cement mass ratio below the stoichiometrically needed amount of water, avoiding to complete the hydration reactions as occurred in the other two cases, which in turn also limited and

decreased significantly the final achieved its compressive mechanical resistance at the end of 28 days.

Table 2, shows the voids index, specific mass and total water absorption results of the pastes P_{REF}, P_{C1h} and P_{C24h}.

Table 2 – Voids index, specific mass and total water absorption of the pastes P_{REF}, P_{C1h} and P_{C24h}

Properties	Age	Pastes		
		P_{REF}	P_{C1h}	P_{C24h}
Voids index (%)	28	26.33 (±2.33%)	28.72 (±1.45%)	43,23 (±1,48%)
Specific mass (g/cm^3)		1.46 (±0.62%)	1.44 (±0.50%)	1.43 (±1.13%)
Total absorption (%)		18.09 (±2.93%)	19.93 (±1.93%)	30.30 (±2.56%)

The mechanical results shown in the Figure 2 and Table 1, indicate that with 1h of carbonation the mechanical resistance of P_{C1h} paste improved in relation to the P_{REF}, which apparently are not compatible with the results of Table 2, which show that the mean porosity level of the P_{REF} paste is slightly lower than that of P_{C1h} paste, indicated by the respective mean values of the voids index and total absorption.

These results may be explained by the thermogravimetric analysis results (TG/DTG) of samples taken from external surface and central parts of cylindrical specimens obtained after each carbonation time shown in Figure 3. As can be seen, in the P_{C1h} paste case, the CO_2 capture affected negatively only the surface of the cylinder, where carbonation was occurring, turning it more porous than the other regions and contributing to the increase of the superficially adsorbed water. However, in P_{C24h} paste case both external surface and central samples show practically the same carbonation, and consequent decrease of the mechanical resistance.

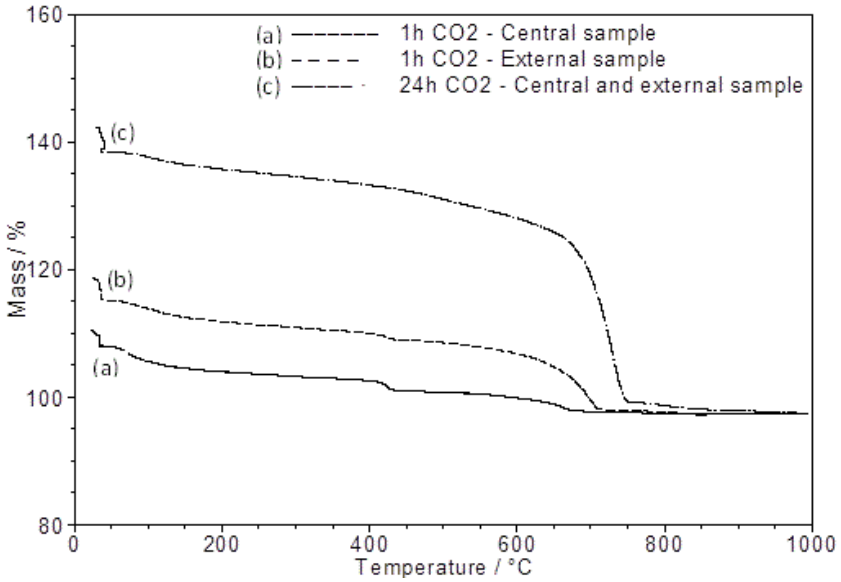

(a)

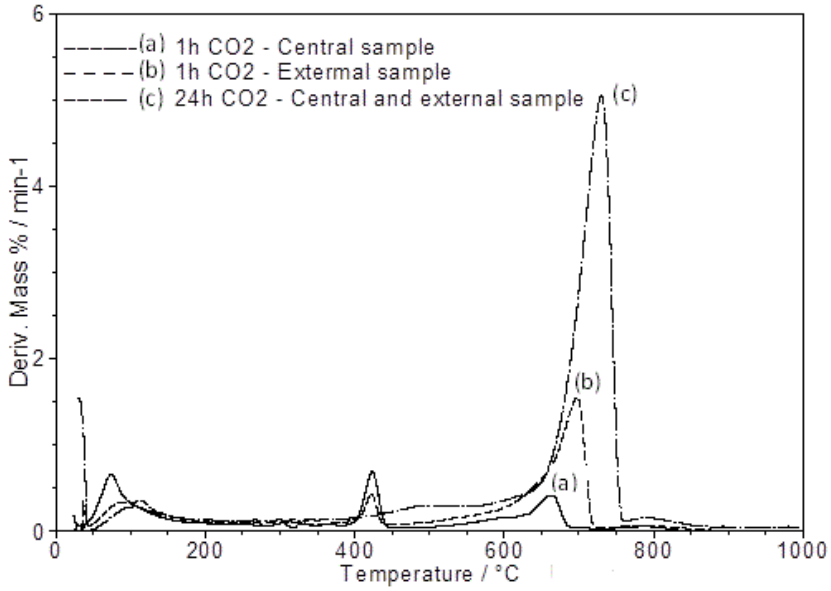

(b)

Fig. 3 – TG (a) and DTG (b) curves on initial cement mass basis of the pastes with 1h and 24h carbonation from central and external regions of the samples

The specific mass of the P_{C1h} is lower than that of the P_{REF} paste, because it's slightly higher porosity. However, it is important to note that, although the porosity of the P_{C24h} is higher than that of P_{C1h}, it's specific mass is only slightly lower than that of P_{C1h}. This occurs because in P_{C24h} much more $CaCO_3$ is produced, which has a higher specific mass [20].

Figure 4, shows the absorption of water by capillarity curves for the pastes P_{REF}, P_{C1h} and P_{C24h}.

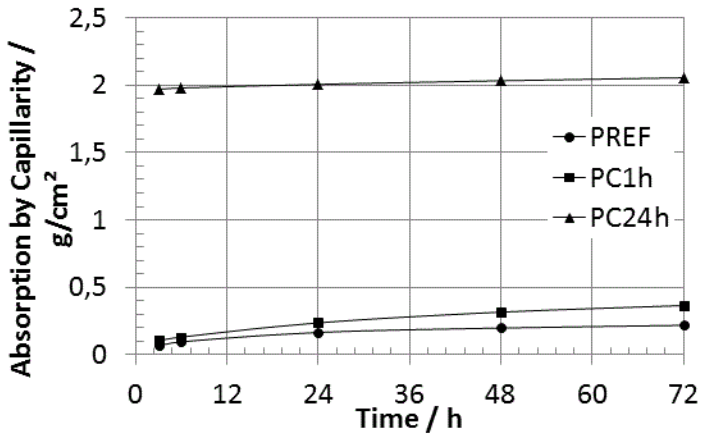

Fig.4 – Curves of absorption by capillarity from the first 72h for the pastes P_{REF}, P_{C1h} and P_{C24h}

As expected, it can be noticed from Figure 4 that the absorption water by capillarity for the paste P_{C24h} is much higher than those of P_{REF} and P_{C1h} pastes. Corroborating the results presented in the Table 2, the water absorbed of the paste P_{C1h} is slightly higher than of the P_{REF} paste.

Figure.5, shows the gas permeability results for the pastes P_{REF}, P_{C1h} and P_{C24h}.

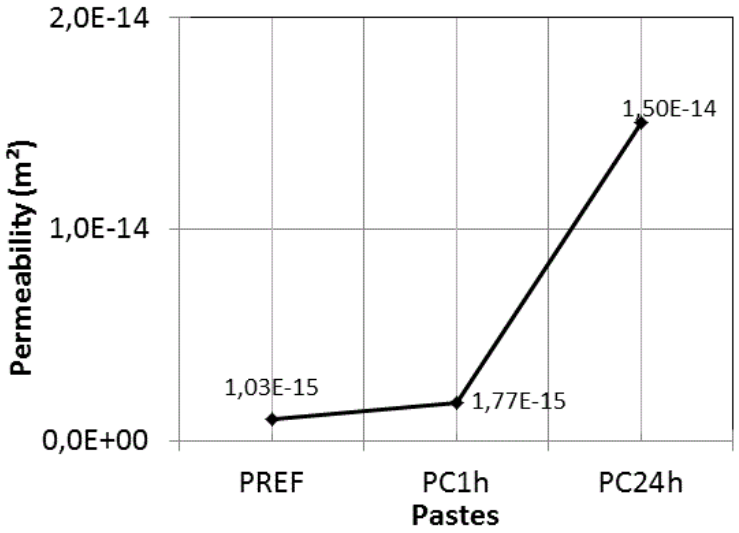

Fig.5 – Permeability results of the pastes P_{REF}, P_{C1h} and P_{C24h}

It can be seen from Figure 5, that the higher gas permeability of P_{C24h} paste, indicates its higher porosity. The P_{REF} and P_{C1h} pastes present the similar behaviour as their absorption by capillarity results in Fig.4.

Figure.6, shows the mercury intrusion porosity results for the pastes P_{REF}, P_{C1h} and P_{C24h}.

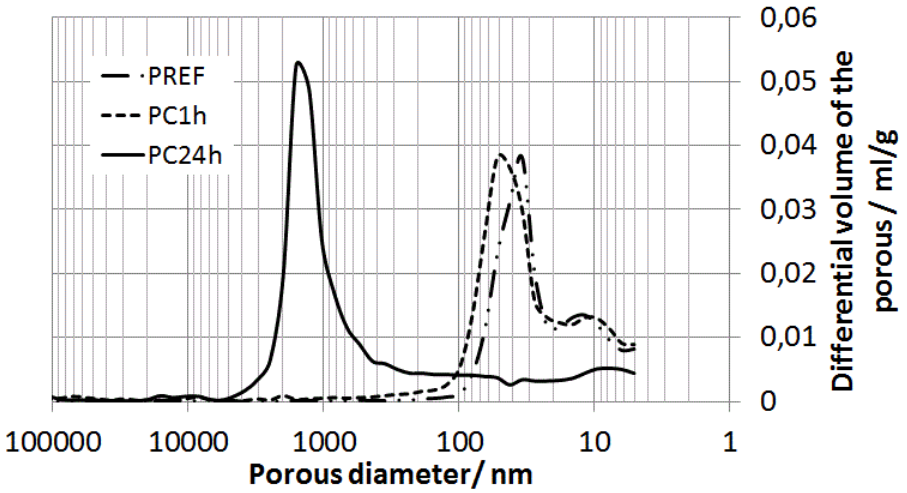

Fig.6– Mercury intrusion porosity curves of P_{REF}, P_{C1h} and P_{C24h} pastes.

From Figure 6, it can be seen that P_{C24h} presents higher pore sizes than the other pastes, which corroborate the previous discussed results and explain the absorption results presented previously. At the same time, from Fig. 6 up to porous diameters of 30nm, the pore size distribution of P_{C1h} paste, is practically equal to that of P_{REF}, and for higher pore diameters the shape of the distribution curve is similar, but slightly broader than that of the reference paste, caused very probably by the carbonation of more external parts of the P_{C1h} specimen as can be seen in Fig. 4.

Table 3, summarizes the results of the mercury intrusion porosity test for the pastes P_{REF}, P_{C1h} and P_{C24h}.

Table 3 – Mercury intrusion porosity results of the pastes P_{REF}, P_{C1h} and P_{C24h}

Properties	Age	Pastes		
		P_{REF}	P_{C1h}	P_{C24h}
Medium porosity (%)	28	31.27	36.5	41.66
Average pore diameter (nm)		18.65	21.55	63.8
Apparent density (g/cm³)		1.41	1.31	1.41
Specific surface area (m²/g)		47.5	51.8	18.6

The results presented on the Table 3, confirm the behaviour expected for the studied pastes. The specific surface area is related to the lateral surface area of the porous, which increases when the size of the porous decreases. Thus, the specific surface area result for the paste P_{C24h} is lower than the other cases.

The apparent density results for the pastes P_{REF} and P_{C24h} is equal, because in spite of the P_{C24h} being more porous than the P_{REF}, the $CaCO_3$ content and its respective density affects the apparent density.

As seen so far P_{C1h} when compared with P_{REF}, presents slightly higher values of porous diameter distribution and size, porosity, permeability and absorption by capillarity, as well as a slightly lower specific mass and apparent density pastes. The short carbonation does not change the original C-S-H gel structure [8] which indicates that the gel pore volume is maintained. However, during this carbonation time in the reference non carbonated paste, the C-S-H gel water decreases with time [19], indicating that the gel pore volume of this sample decreases in this period. This explains why the 1 hr carbonated paste presents a little higher porosity than that of the reference at the end of 28 days of hydration.

Thus, the fact that the P_{C1h} paste presents a slightly higher mechanical resistance to compression than P_{REF} paste, can be explained by its slightly higher content of calcium carbonate, which has a high hardness [20], as well as by the shrinkage of the C-S-H structure and the formation of a new binding amorphous phase, as discussed previously.

4. Conclusions

- The mechanical results after 28 days of hydration indicate that, at the used operating conditions, one hour of carbonation improves the mechanical resistance of a HS SR PC paste.
- These results also indicate that apparently 1h of carbonation does not affect the degree of polymerization of the C-S-H responsible for the resistance of the cementitious matrix, while 24 hours of carbonation at low relative humidity conditions significantly affects and may stop the hydration process due to a high water volatilization, limiting the achieved final mechanical resistance.
- The slight higher porosity of the P_{C1h} paste occurs due to a superficial structural change caused by the carbonation, forming calcium carbonate which having a higher density and hardness, contributes positively to the overall mechanical resistance of one hour carbonated paste.
- Increasing the carbonation time 1h to 24h also increases significantly the porosity and the pore sizes of the paste P_{C24h}, caused by the intense carbonation, as confirmed

by water absorption and mercury intrusion porosity results respectively, affecting significantly the final mechanical resistance of the paste.

- The porosity related property results indicate that the 1h carbonated paste have a structure that may promote a good durability.

Acknowledgments The authors acknowledge the experimental assistance of the Rio de Janeiro Federal University Chemical School Thermal Analysis and Civil Engineering Structure Laboratories and the financial support of the National Research Council (CNPq).

References

1. Neves Junior A, Dweck J, Toledo Filho RD, FairBairn EMR. CO_2 sequestration by high initial strength Portland cement pastes. J Therm Anal Calorim. 2013; 113: 1577-1584.
2. Rostami V, Shao Y, Boyd AJ. Microstructure of cement paste subject to early carbonation curing. Cem Concr Res. 2012;42(1): 186–93.
3. Shao Y, Mirza MS, Wu X. CO_2 sequestration using calcium–silicate concrete. Can J Civ Eng. 2006;33:776.
4. Shao Y, Zhou X, Monkman S. A new CO_2 sequestration process via concrete products production. Montreal: Department of Civil Engineering, McGill University; 2006.
5. Shao Y, Monkman S, Wang S. Market analysis of CO_2 sequestration in concrete building products. Second international conference on sustainable construction materials and technologies. Italy: Ancona; 2010. p. 28–30 June.
6. Shao Y, Monkman S, Boyd AJ. Recycling carbon dioxide into concrete: a feasibility study. Concrete sustainability conference. Canada´: McGill University, Department of Civil Engineering; 2010.
7. Habert G, Roussel N. Study of two concrete mix-design strategies to reach carbon mitigation objectives. Cem Conc Comp.2009;31:397–402.
8. Neves Junior A, Dweck J, Toledo Filho RD, FairBairn EMR. A study of the carbonation profile of cement pastes by thermogravimetry and its effect on the compressive strength. J Therm Anal Calorim. In Press 2014.

9. Brazilian Association of Technical Standards. High initial strength Portland cement. NBR 5733. Rio de Janeiro. 1991.
10. Brazilian Association of Technical Standards. Moderate sulphate resistance Portland cement and moderate hydration heat (MRS) and high sulphate resistance NBR 5737. Rio de Janeiro. 1986.
11. Neves Junior A, Dweck J, Toledo Filho RD, FairBairn EMR. Early stages hydration of high initial strength Portland cement—Part I—thermogravimetric analysis on calcined mass basis. J Therm Anal Calorim. 2012;108:725–31.
12. Brazilian Association of Technical Standards. Concrete – compressive testing of cylindrical specimens NBR 5739. Rio de Janeiro. 1994.
13. Brazilian Association of Technical Standards. Mortar and concrete – tensile strength by diametrical compression testing of cylindrical specimens NBR 7222. Rio de Janeiro. 1994
14. Brazilian Association of Technical Standards. Mortar and concrete hardened– water absorption, voids index and specific mass NBR 9778. Rio de Janeiro. 2006
15. Brazilian Association of Technical Standards. Mortar and concrete hardened– water absorption by capillarity NBR 9779. Rio de Janeiro. 1995
16. Cabrera JG, Lynsdale CJ. A new gas permeameter for measuring the permeability of mortar and concrete. Mag Conc Res. 1998;114,v40.
17. International Standards. Pore size distribution and porosity of solid materials by mercury porosimetry and gas adsorption Part 1 Mercury porosimetry. ISO 15901:2005
18. Cong X, Kirkpatrick RJ. Effects of the temperature and relative humidity on the structure of C-S-H gel. Cem Concr Res. 1995;25(6): 1237–45.
19. Dweck J, Silva PFF, Buchler PM, Cartledge FK. Study by thermogravimetry of the evolution of ettringite phase during type II Portland cement hydration. J Therm Anal Calorim. 2002;69:179–186.
20. Han J, Pan G, Sun W. Elastic modulus change investigation of cement paste before and after using nanoindentation technique. Proc Eng 2012:27;341-47.

ARTIGO G - Neves Junior A, Toledo Filho R.D, Dweck J, Cartledge F.K, Fairbairn E.M.R.Early carbonation curing effects on the microstructure of high initial strength Portland cement pastes. To be submitted 2014.

Early carbonation curing effects on the microstructure of high initial strength Portland cement pastes

Alex Neves Junior[a], Romildo Dias Toledo Filho[a], Jo Dweck[b]

Frank, K. Cartledge[c], Eduardo de Moraes Rego Fairbairn[a]

[a] Civil Engineering Program – COPPE – Rio de Janeiro Federal University, Brazil

[b] School of Chemistry - Rio de Janeiro Federal University, Brazil.

[c] Chemistry Department – Louisiana State University, USA

To be submitted to an international journal

2014

Abstract

In this work, the microstructure of high early strength and sulphate-resistant Portland cement (HS SR PC) carbonated pastes at two different times of carbonation (1h and 24h) was analysed at the best conditions for CO_2 capture as indicated by previous studies of the authors. The aim was to determine by X-Ray diffraction analysis (XRD), nuclear magnetic resonance spectroscopy (^{29}Si NMR) and scanning electron spectroscopy (SEM), how these different carbonation times affect the microstructure of the pastes, to better explain their respective mechanical and porosity related properties discussed in a previous paper.

The microstructure of the non-carbonated reference is homogeneous. The one hour carbonated paste shows a more porous region near its external exposed surface, surrounding a much higher inner non-porous homogeneous phase, while the 24 hour carbonated specimen shows a single and much more porous phase. The higher the carbonation time, the higher is the microstructure porosity of the carbonated regions and the higher is the condensation state of the respective solid matrix phases. The chemical composition changes resulting from the two different carbonation times differently affect the resulting mechanical and physical properties of the pastes.

Key Words: early carbonation curing, XRD, ^{29}Si NMR, and SEM.

1.Introduction

The microstructure of cementitious pastes has been extensively studied. The presence of the $CaCO_3$ in a carbonated cementitious matrix can be easily identified by instrumental analysis techniques such as FT-IR spectroscopy , XRD , ^{29}Si NMR and SEM [1-4].

By thermogravimetry and derivative thermogravimetry the authors found the best conditions of carbonation of HS SR PC pastes to improve their mechanical resistance [5]. They also have shown the influence of the duration of early carbonation curing on the mechanical and porosity related properties [6]. It was shown that 1h of carbonation improved the mechanical resistance of the paste after 28 days, when compared to a non carbonated reference paste, while 24h of carbonation significantly decreased the resistance. In the former case, the porosity was slightly higher than the reference paste,

but its denser structure with newly formed binding products caused greater compressive strength.

Continuing the characterization of the carbonated products, two of them (1h and 24h carbonation), have now been subjected to microstructural analysis, along with a conventionally hydrated reference paste after 28 days of cure. This paper will try to correlate the microstructural differences with the mechanical and porosity results of the previous article [6].

In this work XRD, ^{29}Si NMR and SEM techniques were used in the microstructure characterization.

2. Materials and methods

The paste specimens were prepared using a high initial strength and sulphate-resistant Portland cement (HS SR PC), [7,8] which allows high strengths to be reached even at early hydration stages. The chemical composition of this cement determined by XRF, andTG and DTG curves was presented in previous work of the authors [9].

Deionized water was used to prepare the pastes, which were mixed during 30 s in a mechanical mixer in an environmental temperature of 23°C (±2°C).

For each type of cylindrical 28 day hydrated paste labelled P_{REF}, P_{C1h}, and P_{C24h} (respectively non carbonated reference, 1 and 24h carbonated pastes) the XRD and ^{29}Si NMR analysis samples were taken out from the same central region of the cylinders and were put immediately into a glass bottle containing 3 mL of acetone, to stop the hydration process, after which they were milled.

For the SEM analysis, the samples were extracted after 28 days, from the same central region, as two discs for each analysis, with 50mm of diameter and 8mm of height. These analyses were performed after 28 days.

The crystalline phases of the carbonated and hydrated cement pastes were identified by a D8 focus Bruker XRD equipment using Cu Kα radiation, at 40kV and 40mA AC, 10°-60° 2θ scan interval, 0.05° and 1s per step. The smooth plane and fractured surfaces of

the samples were examined using FEI QUANTA SEM equipment with a coupled EDS mode to have a semi quantitative composition analysis of the specimen surfaces.

To analyse the structural modifications of the C-S-H phase, the Solid-state ^{29}Si NMR experiments were performed on a Bruker Avance III 400 spectrometer (9.4T), operating at a Larmor frequency of 79.46 MHz, and equipped with a 4mm Bruker CPMAS probe and ZrO_2 rotors, spinning at 5 kHz. ^{29}Si MAS NMR spectra were acquired by using direct polarization with high power 1H dipolar decoupling (HPDD) pulse sequence, with a pulse width of $\pi/2$ (4.38 µs) and repetition times of 60s to obtain quantitative data, with enough signal/noise ratio to integrate the spectra. The external reference used for chemical shifts was the Q_3 Si site of kaolinite at 91.5 ppm.

3.Results

Figure.1 shows the XRD spectra of the pastes P_{REF}, P_{C1h} and P_{C24h}.

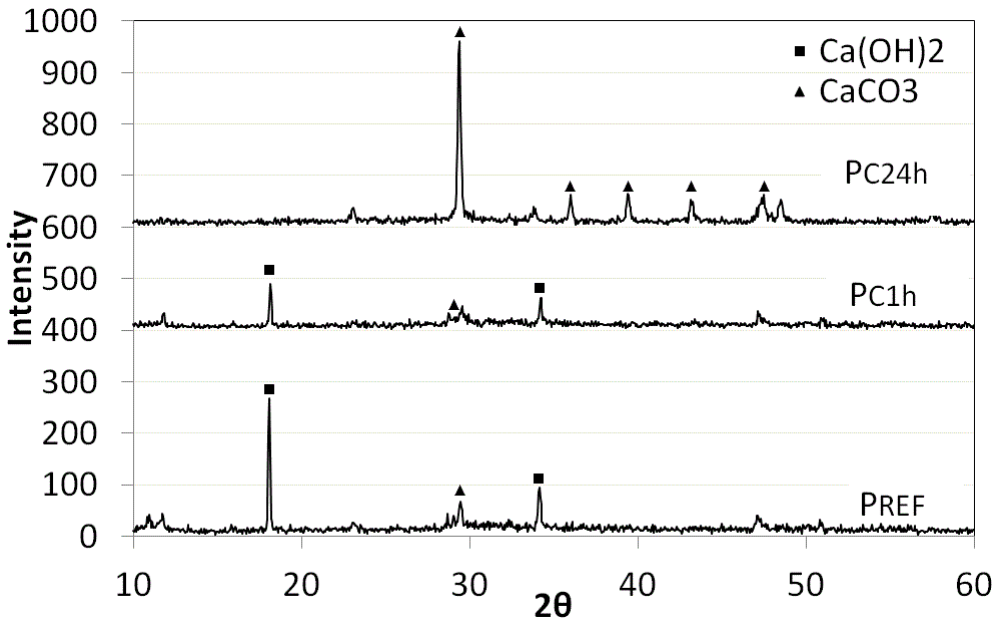

Figure 1 –XRD spectra of the pastes P_{REF}, P_{C1h} and P_{C24h}

It can be noticed that P_{REF} paste presents a high characteristic peak of $Ca(OH)_2$, which decreases with 1h of carbonation for P_{C1h}. In the case of P_{C24h} with 24h of carbonation, its XRD pattern confirms the complete consumption of the $Ca(OH)_2$, due to the absence of its characteristic XRD peaks, according to the previous TG/DTG results presented by

the authors [10]. As expected, the P_{C24h} pattern shows only the characteristic peaks of $CaCO_3$, indicating its high degree of carbonation.

Fig.2, shows the ^{29}Si NMR spectra of the pastes P_{REF}, P_{C1h} and P_{C24h}.

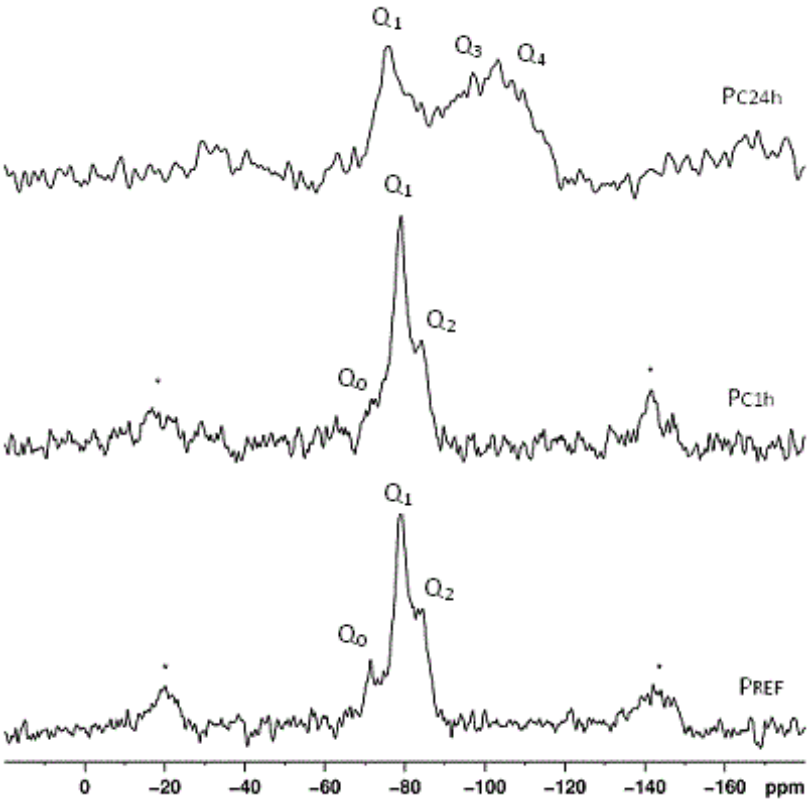

Figure 2 –^{29}SiNMR spectra of the pastes P_{REF}, P_{C1h} and P_{C24h}

The peaks of chemical shift are designated as Q_0,Q_1,Q_2,Q_3 and Q_4. Q_0 represents the unreacted calcium silicates, SiO_4^{4-}, while Q_1 and Q_2 show the dimeric silicate units, $[O_3SiOSiO_3]^{6-}$, and linear or cyclic polymeric silicate units, $\{O_3SiO[Si(O_2)O]_nSiO_3\}^{(6+2n)-}$ or $[Si(O_2)O]_n^{2n-}$ [1,2].

The appearance of the Q_3 and Q_4 in the P_{C24h} spectra indicates crosslinking between silicate chains and the presence of a modified C-S-H phase [2] with a higher degree of condensation compared to the P_{REF} and P_{C1h} specimens. In addition there is peak broadening in the Q_1 and Q_2 regions of the P_{C24h} spectrum, indicating that the Si atoms being observed are in a broader range of magnetic (and therefore also chemical) environments than in the P_{REF} and P_{C1h} samples. It is clear from these changes in spectral properties that carbonation has an intense effect on this paste. As shown in our

earlier work [6], the P_{C24h} sample has much greater porosity than the samples with shorter carbonation times. We interpret this to be the result of the combination of higher quantities of $CaCO_3$ along with a much higher degree of condensation in the C-S-H silicate units.

The decreasing proportion of Q_0 silicates units and the appearance of Q_3 and Q_4 when comparing the NMR spectra of P_{REF}, P_{C1h}, then P_{C24h} is the result of chemical condensation of the silicate units, i.e. more chain lengthening and crosslinking. The combination of increasing chemical condensation and increasing $CaCO_3$ content may actually result in a physical contraction of the C-S-H phase. Other reports [11,12] state that during early curing with a fast period of carbonation and low ambient humidity, the interlayer space of C-S-H phases may shrink, increasing C-S-H crystalline phase density and consequently contributing to the increase of the resulting mechanical resistance, when compared to that of a non carbonated reference paste, as noticed previously by the present authors for the same kind of pastes discussed in the present article [6]. That may be what is happening in our P_{C1h} sample. But the P_{C24h} sample in the present work shows extreme silicate condensation. If this leads to extreme C-S-H phase shrinking and is accompanied by large increases in $CaCO_3$ content, then the matrix becomes more porous and loses mechanical strength.

It must also be noted that the Q_0 peak, which denotes the presence of non reacted calcium silicate phases, is a little higher in the P_{REF} case than in P_{C1h}. This indicates that in the 1h carbonated paste, in addition to having denser hydrated calcium silicate phases, also has a higher degree of cement hydration than the P_{REF} sample, which contributes to its higher mechanical resistance, as previously reported [6].

The much lower Q_0 peak in the P_{C24h} paste indicates a higher degree of consumption of the original calcium silicate (CS) phases. However, as discussed above, the NMR spectral changes from P_{REF} to P_{C1h} to P_{C24h} indicate a highly modified C-S-H structure. CO_2 is acidic and will lower the pH of pore waters, resulting in greater degrees of silicate polymerization. It is also likely that the added CO_2 will not only increase the $CaCO_3$ content, but also lead to mixed silicate/carbonate products. The latter effect is suggested also by the thermogravimetric results presented in an earlier paper [5].

Thus, the much lower mechanical resistance of P_{C24h} paste, when compared to those of P_{REF}, P_{C1h} pastes [6], can be due to the significant presence of polymeric silicate phases and also carbonated silicate phases, both of which may contribute to the much higher porosity of the P_{C24h} paste than the non carbonated C-S-H phases present in P_{REF} and P_{C1h} pastes.

There is still another effect that may be contributing to the changes in C-S-H structure (and thus also in porosity and compressive strength) in the P_{C24h} paste. After an initial 6 h of cure at 100% humidity, each of the samples is demolded, then subjected to carbonation in an atmosphere that is only 60% relative humidity. The other two samples discussed in this paper had 0 h (P_{REF}) and 1 h only (P_{C1h}) at the lower humidity. The 24 h of cure at 60% humidity for the P_{C24h} sample may mean that appreciable pore water is lost, and thus is not available for silicate hydration. This effect can be seen in the thermogravimetric and non-conventional differential thermal analysis studies [5,13]

Figures 3 to 5 present typical SEM photomicrographs of the P_{REF}, P_{C24h} and P_{C1h} pastes.

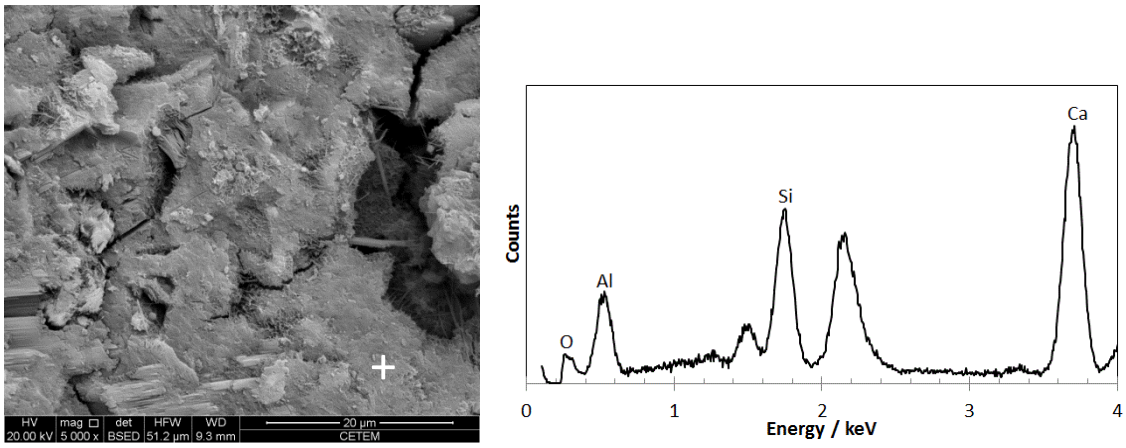

(a) (b)

Fig.3- P_{REF} paste: (a) SEM photomicrograph (b) EDS analysis of crossed point phase

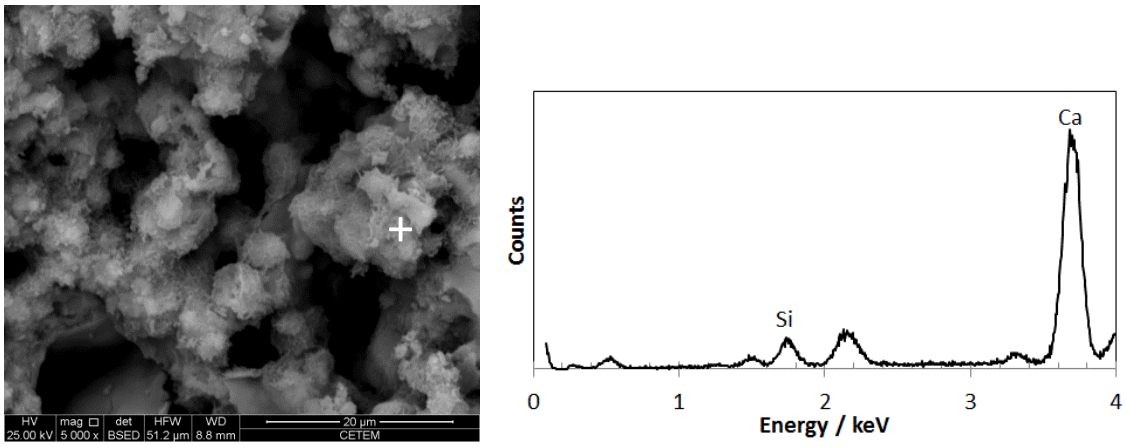

(a) (b)

Fig.4-P_{C24h} paste: (a) SEM photomicrograph (b) EDS analysis of crossed point phase

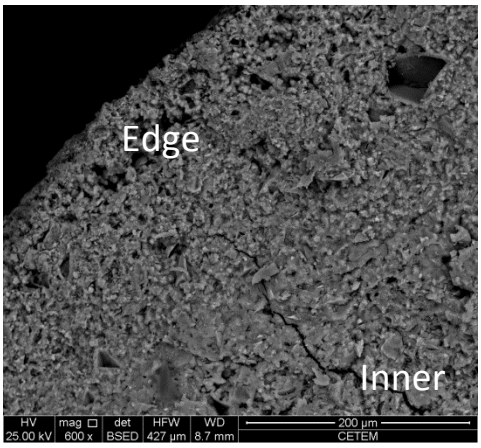

Fig.5-P_{C1h} paste: (a) SEM photomicrograph

Fig 3 shows the densified microstructure of the P_{REF} paste, and EDS analysis shows strong typical peaks of *Ca*, *Si*, *Al* and *O*. The high content of the designated elements indicates the presence of calcium silicate hydrates.

Fig.4 shows the much more porous microstructure of the P_{C24h} paste and different morphology for the solid phase than in the other two cases. EDS analysis of the main present phase in Figure 4(b), shows high *Ca* peaks and a decrease of the Si peak, with a very weak *O* peak, where, because of the intense free water loss, much lesser amounts of $Ca(OH)_2$ and tobermorite phases were formed from the original C_3S and C_2S phases. Instead, as was indicated by the respective NMR spectrum, the intense carbonation in these conditions, promoted the formation of a new and condensed solid carbonated calcium silicate phase, in agreement with other literature results [1]. It is clear in Figure

4(a) that the material has much higher porosity and bulk morphology quite different from that of the two other pastes.

Fig 5 shows the micrograph of a transverse section of P_{C1h}, where the morphological transition of the microstructure of the paste from the edge to the inner region of the paste is very clear, showing the expected modifications caused by the carbonation front near the surface, which is much more porous than the inner region, which was not affected by the CO_2 action. The higher porosity of the region nearer to the external edge presents a morphology similar to that of the P_{C24h} paste, which explains the slightly higher water absorption than that of P_{REF} paste [6]. The morphology of the inner regions with a much lower porosity resembles that of paste $P_{REF,}$ and considering the respective NMR spectrum results, its slightly higher condensed C-S-H phases that those of P_{REF} explain the slightly higher elastic modulus than that obtained for the reference paste. At the same time, it's more porous outer surface explains the slightly higher plastic deformation that occurred in the mechanical assay results for the P_{C1h} paste, when compared to those of the reference, [6] which does not show this porosity gradient at the regions near its external surface.

4.Conclusions

- 1h of carbonation promotes a porous morphology at the more external regions, but the relatively nonporous structure typical of C-S-H is displayed by the more inner region. The 1h-carbonated paste shows greater loss of C_2S/C_3S than the reference sample, which may be the cause of the slightly greater elastic modulus for this sample compared to the reference.

- In the case of 24h of carbonation, the absence of $Ca(OH)_2$ after 28 days of setting, the highly altered morphology, and the much more highly condensed silicate structure shown in the NMR, all indicate that the hydration has followed a greatly different chemical path compared to the reference sample. That altered path leads to a paste with much higher porosity and substantially lowered compressive strength. The modifications on the C-S-H structure depend on the different carbonation times, as well as the type of carbonated phases formed. Those structures are similar for P_{REF} and inner parts of P_{C1h} pastes, with a little denser C-S-H solid matrix for the latter,

while in the 24h carbonation case, a much smaller amount of C-S-H crystalline phase is present, very probably due to the formation of a new and more condensed carbonated calcium silicate structure, which being too porous, affects negatively the resulting mechanical resistance.

- The radial transitory morphology of the P_{C1h} paste, caused by the carbonation treatment for 1h, damaged the region near to the external exposed surface, turning it more porous. This explains the slight increase of the water absorption for the paste P_{C1h} as well as its slightly higher plastic behavior than P_{REF}.

Acknowledgments The authors acknowledge the experimental assistance of the Rio de Janeiro Federal University Chemical School Thermal Analysis and Civil Engineering Structure Laboratories and the financial support of the National Research Council (CNPq).

References

1. Rostami V, Shao Y, Boyd AJ. Microstructure of cement paste subject to early carbonation curing. Cem Concr Res. 2012;42(1): 186–93.
2. Knopf FC, Roy A, Samrow HA, Dooley KM. High-pressure molding and carbonation of cementitious materials. Ind Eng Chem Res. 1999;v 38;2641-2649.
3. Castellote M, Fernandez L, Andrade C. Chemical changes and phase analysis of OPC paste carbonated at different CO_2 concentration. Mat Struc. 2009:4;515-525.
4. Chaipanich A, Nochaiya T. Thermal analysis and microstructure of Portland cement fly ash silica fume paste. J Therm Anal Calorim 2010:2;487-493.
5. Neves Junior A, Dweck J, Toledo Filho RD, FairBairn EMR. A study of the carbonation profile of cement paste by thermogravimetry and its effect on the compressive strength. J Therm Anal Calorim.2013;114 (3)
6. Neves Junior A, Dweck J, Toledo Filho RD, FairBairn EMR. The effects of the early carbonation curing on the mechanical and porosity properties of high initial strength Portland cement pastes To be submitted 2014.

7. Brazilian Association of Technical Standards. High initial strength Portland cement. NBR 5733. Rio de Janeiro. 1991.
8. Brazilian Association of Technical Standards. Moderate sulphate resistance Portland cement and moderate hydration heat (MRS) and high sulphate resistance NBR 5737. Rio de Janeiro. 1986.
9. Neves Junior A, Dweck J, Toledo Filho RD, FairBairn EMR. Early stages hydration of high initial strength Portland cement—Part I—thermogravimetric analysis on calcined mass basis. J Therm Anal Calorim. 2012;108:725–31.
10. Neves Junior A, Dweck J, Toledo Filho RD, FairBairn EMR. CO_2 sequestration by high initial strength Portland cement pastes. J Therm Anal Calorim. 2013; 113: 1577-1584.
11. Pinto C.A, Sansalone J.J, Cartledge F.K, Dweck J, Dias F..V, Bucher P.M. Cement stabilization of runoff residuals: A study of stabilization/solidification of urban rainfall-runoff residuals in type 1 Portland cement by XRD and ^{29}Si NMR analysis. Wat A Sol Poll. 2008; 188:261-270.
12. Pinto C.A, Dweck J, Sansalone J.J, Cartledge F.K, Hamassaki L.T, Diaz F.R.V, Albanez N, Buchler P.M. Evaluation of S/S process of tannery waste in cement by structural and mechanical analysis. Mat Sci For;2010, 1130-1136.
13. Neves Junior A, Toledo Filho R.D, Dweck J, Fairbairn E.M.R. A study of CO_2 capture by high initial strength Portland cement pastes at early curing stages by non conventional thermogravimetry and differential thermal analysis. To be submitted 2014.

ARTIGO H - Neves Junior A, Ferreira S.R, Toledo Filho R.D, Dweck J, Fairbairn E.M.R. Early carbonation curing of high initial strength Portland cement and lime composites with sisal fibers. To be submitted 2014.

Early carbonation curing of high initial strength Portland cement and lime composites with sisal fibers.

Alex Neves Junior[a], Saulo Rocha Ferreira[a], Romildo Dias Toledo Filho[a], Jo Dweck[b] and Eduardo de Moraes Rego Fairbairn[a]

[a] Civil Engineering Program – COPPE – Rio de Janeiro Federal University, Brazil

[b] School of Chemistry - Rio de Janeiro Federal University, Brazil.

To be submitted to an international journal

2014

Abstract

This paper presents a study of two different composites treated with CO_2 at early curing stages and reinforced with long sisal fibres. Using the best conditions of CO_2 capture previously determined by the authors, the aim of this work was to develop two composites, where the CO_2, besides being captured by Portland cement matrix, also allows the reinforcement of this matrix with a natural fibre, by the pH decrease promoted by carbonation reactions, increasing the durability of the resulting material. Another lime/pozzolanic material composite, was also treated with CO_2 at early stages of formation, with the carbonation and pozzolanic reactions acting simultaneously to deplete the $Ca(OH)_2$, thus improving its durability.

Key Words: Early carbonation curing, sisal fibre, mortar, composite materials, lime composites, accelerated ageing, SEM, thermogravimetry, derivative thermo- gravimetry

1.Introduction

The strategies to improve the durability of composites reinforced with vegetables fibres has been studied by many authors [1-4]. One of the worse problems of this kind of composites is the mineralisation of those fibres due to the migration of hydration products, specially calcium hydroxide to the fibre lumen, wall and voids [2,3]. Among the strategies to avoid this damage caused by the high alkalinity, one is to decrease the high pH of this matrix by manufacturing Portand cements blended with pozzolanic materials [4]. Another way to reduce the $Ca(OH)_2$ content in the matrix, ensuring the survival of the natural fibres, is through CO_2 carbonation reactions where $Ca(OH)_2$ can be consumed, reducing the pH of the matrix [2].

In this work, the authors propose to study two types of composites reinforced with long sisal fibres, a Portland cement composite and a lime composite, both being treated with CO_2 at early stages at the best conditions of capturing previously studied by the authors [5], to solve the problem of the mineralization of the fibre, as well as to create an ecologic composite by absorbing CO_2 as $CaCO_3$ increasing the resistance and improving the durability. To compare the influence of the CO_2 in the performance of the carbonated composites, Portland cement and lime composites blended with fly ash and metakaolin were prepared without carbonation treatment. The composites were analysed by 4 point bending tests at 28 days and after 10 and 20 controlled cycles of wetting and

drying. The mechanical and durability performance of the composites were discussed using the results of flexural tests performed on 80 x 400 x 12 mm specimens. Backscattered electron imaging in the scanning electron microscopy (SEM) was used in order to detect any change in the fibres microstructure. Thermogravimetry and derivative thermogravimetry (TG/DTG) analysis of the matrix were used to analyse the hydrated and carbonated products formed, explaining the influence in the fibres's structure and mechanical results.

2.Materials and methods

In this study, a high initial strength and sulfate-resistant Portland cement (HS SR PC) [6] was used to prepare the mortars specimens, which allow to reach high strengths at early hydration stages. This kind of cement may have a maximum of 5% of carbonates addition and aggregation of blast furnace slag or pozzolanic materials [7].

The chemical composition of the cement (HS SR PC), metakaolin (MK), fly ash (FA) and lime, were determined by XRF and is presented in the Table 1.

Table 1 – Chemical composition of HS SR PC, MK, FA and lime

Compound	Content (%)			
	HS SR PC	MK	FA	Lime
CaO	66.92	0.27	1.76	50.7
SiO_2	16.45	42.82	51.63	0.78
Al_2O_3	5.00	42.01	32.61	-
SO_3	4.44	1.14	1.56	0.43
Fe_2O_3	3.30	4.65	5.12	0.18
TiO_2	0.40	1.45	1.16	-
K_2O	0.35	1.37	3.12	0.05
MnO	0.28	-	-	0.02
SrO	0.25	-	-	0.08
ZnO	0.03	-	-	-
ZrO_2	0.02	-	0.14	-
MgO	-	-	-	14.29
P_2O_5	-	0.81	0.8	1.87
BaO	-	-	0.46	-
LOI	2.55	5.49	1.63	31.6

For this work was used a quartz sand river, with specific mass of 2.63 g/cm³. The particle size is smaller than 0,84mm (ABNT sieve nº20). The granulometric distribution curve of the fine aggregates and HS SR PC used to produce the mortars are presented in Figure 1.

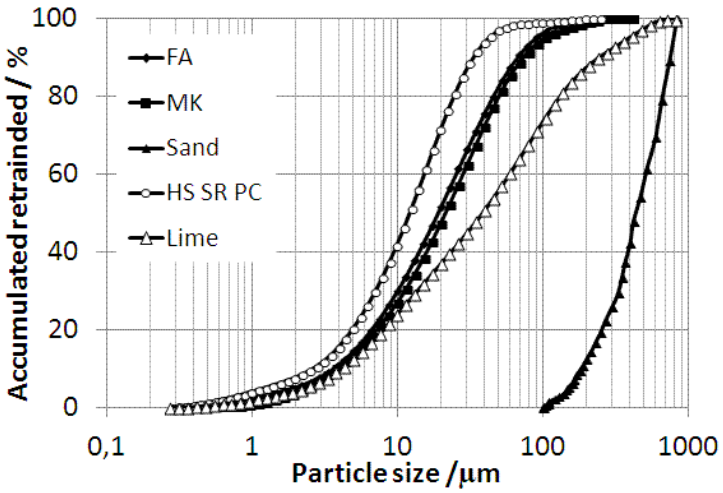

Figure 1 – Granulometric distribution of the HS SR PC, MK, FA, lime and sand.

The superplasticizer used was the type PA (polyacrylate, Glenium 51) with solids content of 31.20%, density of 1073 kg / m³ and pH 6,2.

The natural sisal fibres used in this investigation were obtained from the county of Valente-BA. Before being used to prepare the composites, the fibres were previously washed in hot water (80 – 100°C). After been washed, the fibres were disposed in a room with medium temperature of 40°C to dry and brushed for alignment being cut with length of 50mm.

The composites were prepared in a mortar mixer of 20l of capacity by the following steps:

- Mixing the water with the superplasticizer during 30 sec in the mortar mixer.
- Premixing the fines (in bags) during 1 min and then placing in the mortar mixer during 2 min.
- Stopping during 30 sec to remove the material retained in the mortar mixer.
- Mixing during more 2 min.
- Pouring the fibrous reinforcement inside the mortar mixer during 2-6 min. In all composites, 4% of fibres in relation to the volume were used.

After the above steps, the mixtures were put into aluminum molds with dimensions of 250mm (width) x 400m (length) x 15 mm (thickness), with bottom and upper lids of acrylic. For each composite plate, after the curing process, 3 specimens of 80 mm (width) x 400 mm (length) x 15 mm (thickness) were extracted with the aid of a circular saw, for the mechanical tests, at the proposed ages.

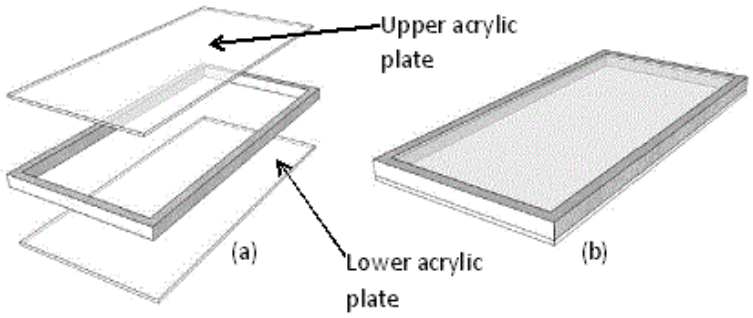

Figure 2 – Upper and lower acrylic plates (a) and acrylic mold (b)

Two types of Portland cement named CSAND and CMKFA and a lime composite named LMKFA, both reinforced with sisal fibres were studied in this work. The table 2 presents the traces used to produce the composites.

Table 2 – Trace of mixtures

Composite name	Matrix (kg/m³)						
	HS SR PC	Lime	Sand	MK	FA	Water	SP
CSAND	1098	-	549	-	-	437	3
CMKFA	362		543	290	435	425	14
LMKFA	-	362	723	217	145	572	4

The following nomenclature to reference the specimens will be used :

- [*Composite name*_*i*CO_2_C*j*], "*i*" is the time of exposition to CO_2 and "*j*" the number of cycles of wetting and drying.

27 test specimens were cast for the CSAND composites, 9 test specimens for the CMKFA composites and 18 test specimens for LMKFA composites. Some specimens of CSAND composites were treated with CO_2 during 1 and 24h, after 6h of hydration, when they were demolded to allow a multidirectional flow, based in a previous work of the authors [5], and others without carbonation to compare as reference. The specimens of CMKFA composite which were not submitted to CO_2 treatment, were compared with

the respective CSAND composite, knowing that this composites are free of $Ca(OH)_2$ [2,3]. Some specimens of LMKFA composites were treated with CO_2 during 1h immediately after the casting, with a unidirectional flow normal to the exposed surface, and others without carbonation, as references. The carbonation treatment were performed in a controlled climatic chamber with a CO_2 controlling device according to Fig 3 and 4. During the CO_2 treatment, the temperature and RH inside the chamber were 25°C and RH=60% respectively, following best previous indicated conditions [5].

Figure 3 – Controlled climatic chamber

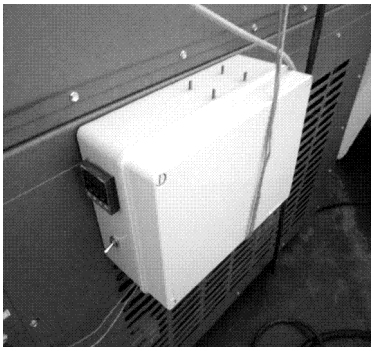

Figure 4 – CO_2 controlling device

Some specimens of the CSAND, CMKFA and LMKFA were submitted to an accelerated ageing test after 28 days, which was performed in a forced ventilation chamber. All the specimens were conditioned in a room with RH=100% until performing the mechanical test.

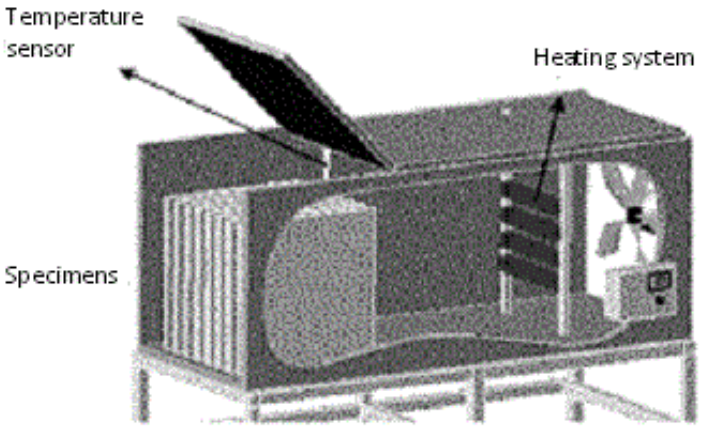

Figure 5 – Schematic of the forced ventilation chamber

In this experiment, the specimens were completely saturated in water at 30±1°C, followed by a drying step in the forced ventilated chamber. Considering that after 24h of immersion in water, the specimen absorbed 90% of the water necessary to its total saturation and after 48h of drying, it has lost 70% of the mass gained during its saturation, a cycle of 3 days was adopted (1 day submerged in water followed by 2 days drying inside the forced ventilated chamber).

Table 3 shows the used experiment conditions.

Table 3 – Experiments conditions

Specimens	W/MC (%)	N° of cycles of wetting/drying	Demolding time for exposition to CO2 (h)	Exposition to CO2 time (h)	Age of the specimens
CSAND_0CO2_C0	0,4	-	-	-	28d
CSAND_1CO2_C0	0,4	-	6	1	28d
CSAND_24CO2_C0	0,4	-	6	24	28d
CMKFA_0CO2_C0	0,4	-	-	-	28d
CSAND_0CO2_C10	0,4	10	-	-	58d
CSAND_1CO2_C10	0,4	10	6	1	58d
CSAND_24CO2_C10	0,4	10	6	24	58d
CMKFA_0CO2_C10	0,4	10	-	-	58d
CSAND_0CO2_C20	0,4	20	-	-	78d
CSAND_1CO2_C20	0,4	20	6	1	78d
CSAND_24CO2_C20	0,4	20	6	24	78d
CMKFA_0CO2_C20	0,4	20	-	-	78d
LMKFA_0CO2_C0	0,79	-	-	-	28d
LMKFA_1CO2_C0	0,79	-	6	1	28d
LMKFA_0CO2_C10	0,79	10	-	-	58d
LMKFA_1CO2_C10	0,79	10	-	1	58d
LMKFA_0CO2_C20	0,79	20	-	-	78d
LMKFA_1CO2_C20	0,79	20	-	1	78d

In this work, the forced ventilated chamber, was set for a temperature of 36±1°C and wind speed of 0.5 m/s. Some specimens were submitted to a 10 and 20 cycles of wetting and drying.

At the established ages, the specimens were stored in a room with controlled temperature of 21±1°C for a period of 30h, when they were tested. Before the test, the specimens were white painted, with a PVA based paint to better verify the appearance of cracks. A four points bending test was performed in a Universal Shimadzu AGX-100kN model with a test speed of 0.5mm/min. The load points were far 100 mm between each other and the span between supports was 300 mm.

From the 4 points bending test, the load and the displacement at the middle of the span were obtained, but the results were expressed in equivalent stress, using the equation:

$\sigma = \frac{30F}{bd^2 10}$ where,

σ =Equivalent stress (MPa)

F =Force (kN)

b =width of the specimen (cm)

d =height of the specimen (cm)

The toughness index of the specimens was calculated using the Belgium standard method, according to the equation:

$P^* = P_n / P_{1^oC}$

Where,

P_n = Are the loads corresponding to the displacements n=1, 2, 3 and 6 mm

$P_{1°C}$ = First crack load.

After the mechanical test, aliquots of the matrix for thermal analysis were taken from the region located at the mid-span of the specimens and put immediately into a little glass bottle containing 3 mL of acetone, to stop the hydration process. After, they were conditioned in little sealed plastic bags until the test.

The extraction of the fibres from the inside of the composites was made from a small piece of composite (2 cm x 2 cm) which was crushed with a locking plier and after crushing, the fibres were separated from the matrix with a sieve. Their surface was manually cleaned.

Thermogravimetric and derivative Thermogravimetric analysis (TG/DTG) was performed in a TA Instruments, SDT Q600 model, simultaneous TGA/DTA/DSC apparatus, at a heating rate of 10 °C min^{-1}, from 35 to 1000 °C, by using 100 $mL.min^{-1}$ of nitrogen flow. Before this heating step, they were dried inside the equipment initially

heating at 1 °C min-1 from 25 to 35°C and then by an isothermal step at 35°C for 1 h, to eliminate any residual non combined free water. The analyses were performed in platinum pans. The TG/DTG curves data of the CSAND and CMKFA matrices were presented on the initial cement mass basis, according to the procedure described in previous works of the authors [8,9]. The TG/DTG curves of the LMKFA matrices will be presented on the initial lime mass basis, following the same procedure as explained for the cement mass basis [8]. Fig 6 presents the TG/DTG curves of the HS SR PC and lime on respective sample initial mass basis.

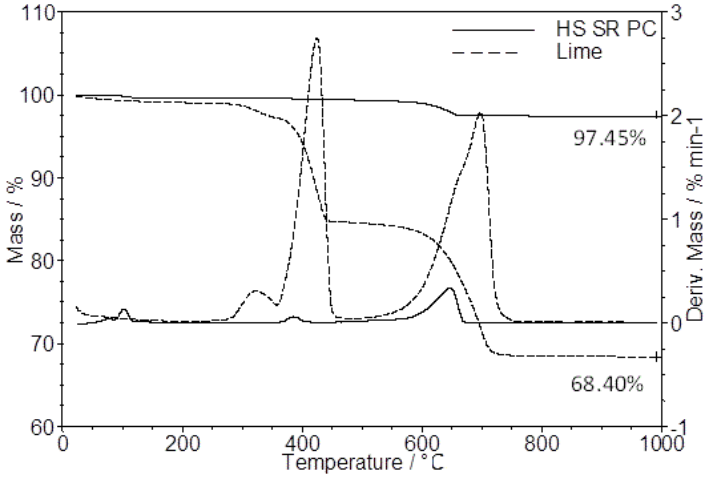

Figure 6 – TG/DTG curves of the HS SR PC and Lime on the calcined mass basis

For the microstructural analysis of the cross section of the fibres, they were cut with the aid of sharp blade. To improve the conditions of the cut, the fibres were immersed in water for 48h and then submitted to cutting.

The sisal fibre's microstructure was investigated using a HITACHI 3000 scanning electron microscope, under high vacuum environment and 15 kV accelerating voltage. The diameter of the circular holder was 10mm and a pre-coating with gold, approximately 20 nm deep was required. The images were post-processed using Image J software.

3.Results

Figures 7(a), (b) and (c) present the flexural mechanical data results for the CSAND and CMKFA containing composites.

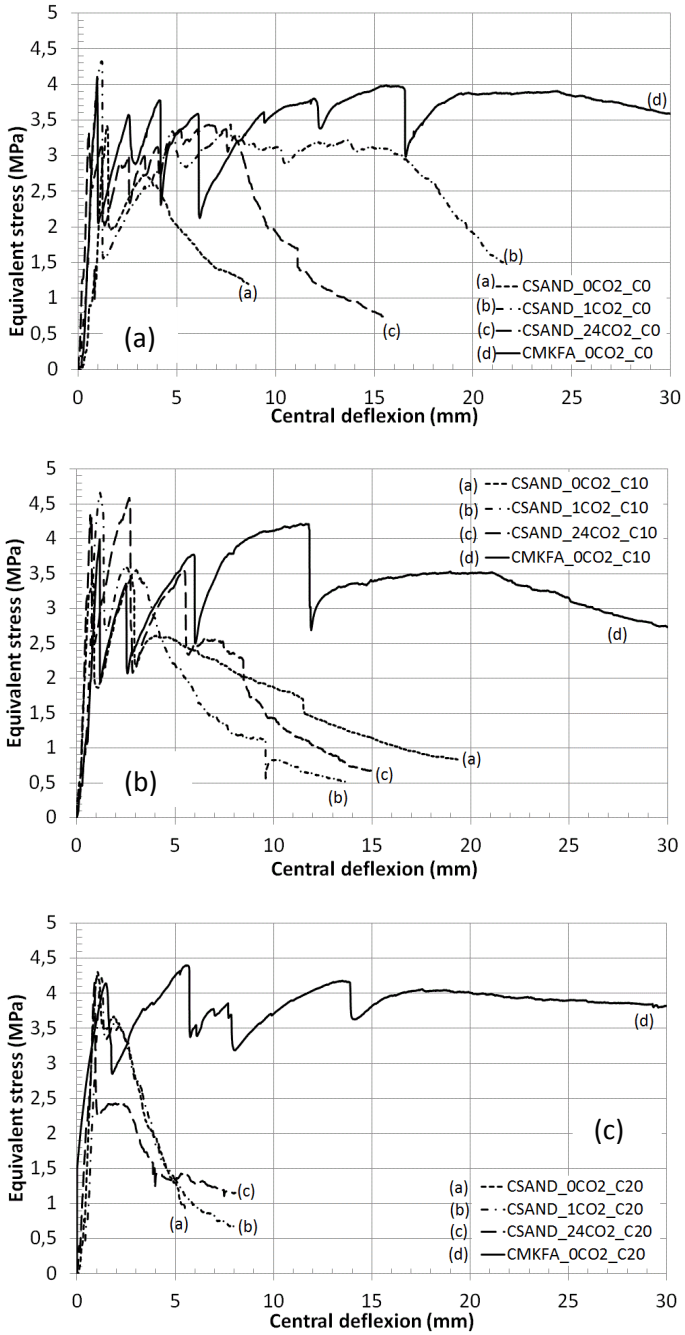

Figure 7-Equivalent stress x Central deflection curves of the composites. (a) CSAND and CMKFA without accelerated ageing; (b) CSAND and CMKFA with 10 cycles of accelerated ageing; (c) CSAND and CMKFA with 20 cycles of accelerated ageing

Figures 8(a), (b) and (c) present the mechanical results under flexural for the LMKFA composites.

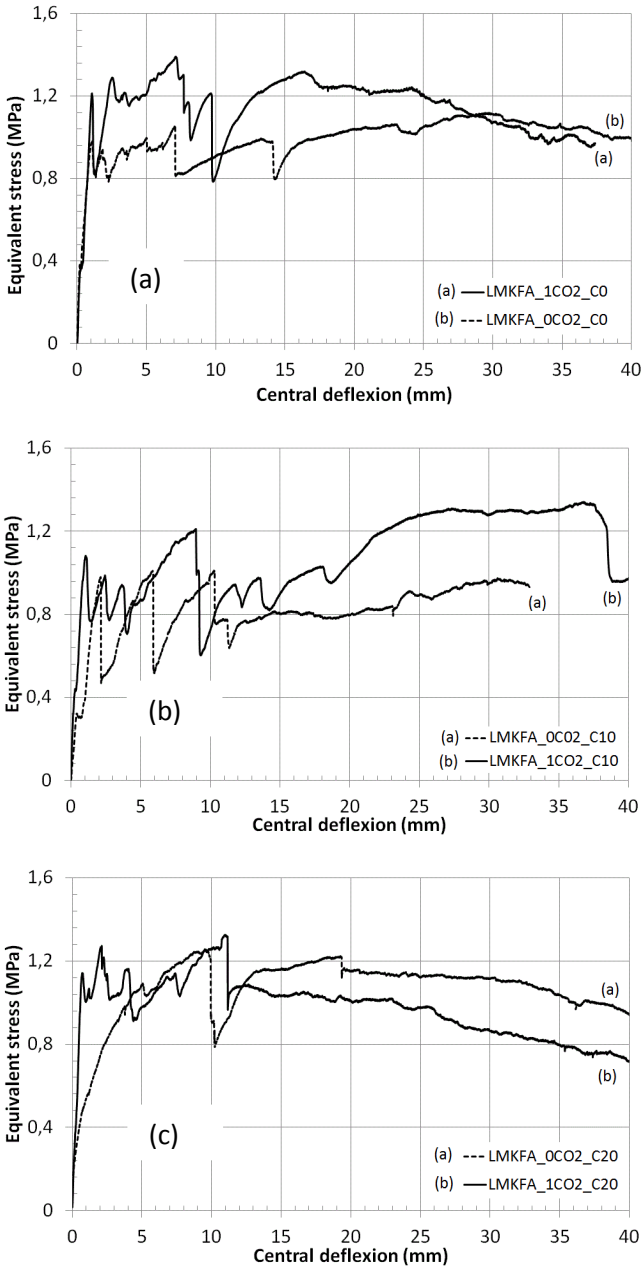

Figure 8 – Equivalent stress x Central deflection curves of the LMKFA composites: without accelerated ageing (a), with 10 cycles of accelerated ageing (b) and with 20 cycles of accelerated ageing (c)

According to Figures 7(a), (b) and (c) the composites CMKFA-0CO2-C0, CMKFA-0CO2-C10 and CMKFA-0CO2-C20, showed the better mechanical performance than the other composites, through the strain hardening behaviour.

For Fig 7(a), considering the composites without the wetting and drying cycles, the composite CSAND-1CO2-C0, presents the higher maximum stress crack than the other composites, showing a small behaviour of strain hardening. Only the composite CSAND-0CO2-C0 showed the worst performance with a visible strain softening

behaviour. For the composite treated with CO_2 during 24h (CSAND-24CO2-C0), the matrix presented a decrease of the resistance, probably due to the conditions of the proposed treatment, as the lower relative humidity and the excess of CO_2 time exposure, which were not favourable to improve the mechanical properties, as occurred with the pastes [10].

For Fig 7(b), with 10 cycles of wetting and drying, the composite CSAND-1CO2-C10, continued to present the higher maximum stress crack, but all the composites presented a decrease of the multiple cracks behavior, losing their deformability, in relation to the experiments without accelerated ageing. (Fig.7 (a)).

Increasing the number of cycles to 20, in Fig.7(c), we can notice that the mechanical behavior of the composites CSAND-0CO2-C20, CSAND-1CO2-C20 and CSAND-24CO2-C20 worsened considerably, all presenting a strain softening behaviour. The maximum stress crack for these composites is practically equal.

The mechanical efficiency demonstrated by the CMKFA in relation to the CSAND composites, due to the evident strain hardening behaviour, shows that this type of matrices continue to be more attractive to improve the global resistance of the composites.

From Fig 8(a), (b) and (c), all the LMKFA composites presented a strain hardening behaviour. The composites LMKFA-1CO2-C0 and LMKFA-1CO2-C10 presented a better mechanical performance than the respective composites without carbonation, showing also a higher maximum stress crack. For the LMKFA composites with 20 cycles of wetting and drying (Fig 8(c)), the composite without carbonation (LMKFA-0CO2-C20), presented a loss of the mechanical performance, probably due to the effect caused by the accelerated ageing, which produced initial cracks in the matrix, before the test. We can notice that, 1h of carbonation was enough for the composite LMKFA-1CO2-C20, to improve the resistance of its matrix for the accelerating ageing test in relation to the LMKFA-0CO2-C20.

Figure 9(a), (b) and (c) presents the toughness index results obtained by using the Belgian standard method for the CSAND and CMKFA composites.

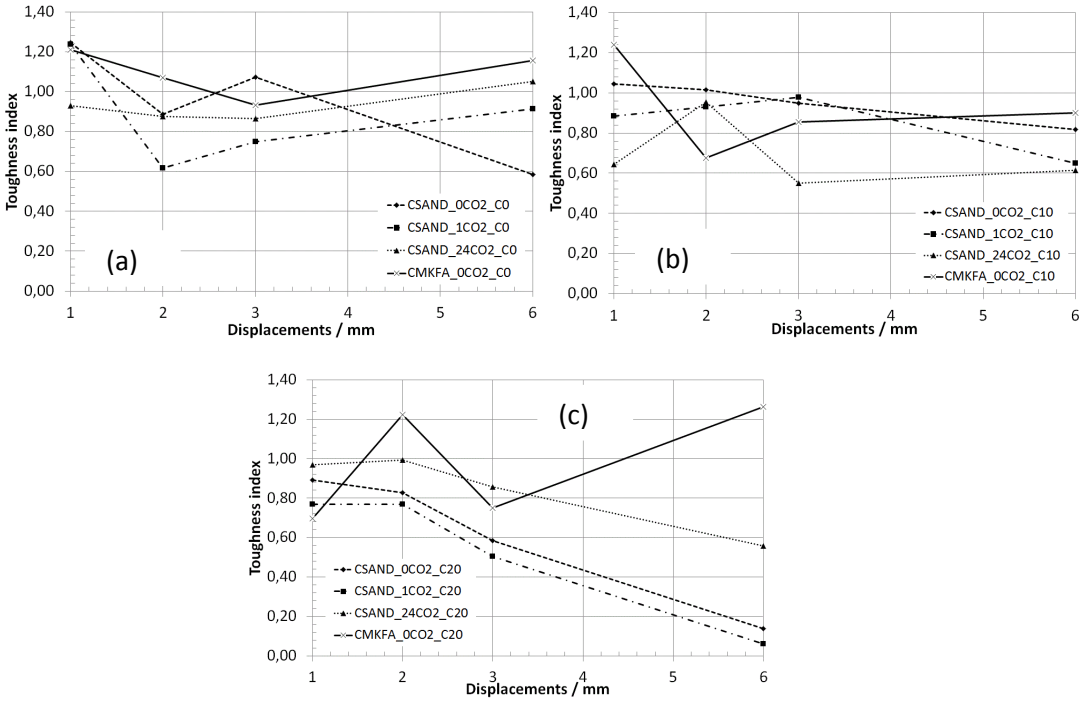

Figure 9 – Toughness by Belgian standard method of the CSAND and CMKFA composites without accelerated ageing (a), CSAND and CMKFA with 10 cycles of accelerated ageing (b), CSAND and CMKFA with 20 cycles of accelerated ageing (c)

Figures 10(a) (b) and (c) present the toughness index results obtained by using the Belgian standard method for the LMKFA composites.

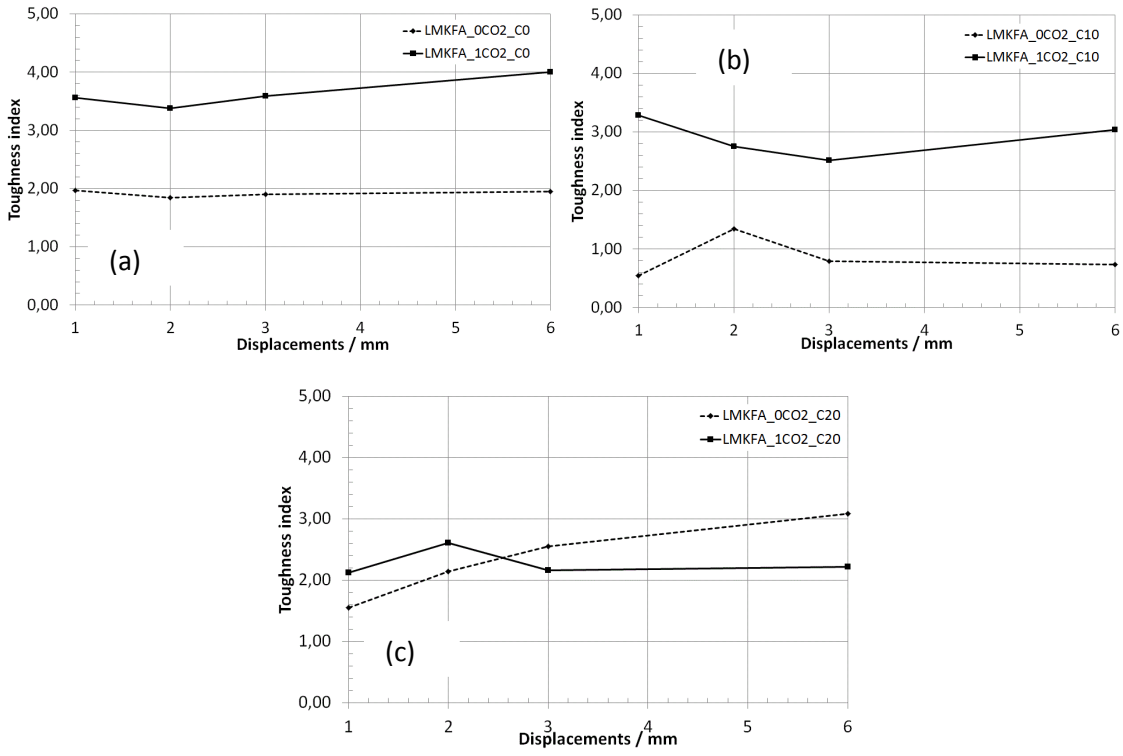

Figure 10 – Toughness by Belgian standard method of the composites LMKFA without accelerated ageing (a), LMKFA with 10 cycles of accelerated ageing (b), LMKFA with 20 cycles of accelerated ageing (c)

In Fig 9(a), the composites CSAND-0CO2-C0, CSAND-1CO2-C0 and CMKFA-0C02-C0, presented a softening behaviour until 2mm of displacement and an elasto-plastic hardening behaviour between 2 and 6mm.

From Fig 9(b), the composites CSAND-0CO2-C10 and CSAND-1CO2-C10, presented a softening behaviour from 3mm displacement. The CMKFA-0CO2-C10 composite presented a recovery of the hardening behaviour from 2mm, but the Pn/P1°C is less than 1 in relation to the CMKFA-0CO2-C0, showing the influence of the ageing process.

Fig 9(c) corroborates the results shown in Fig 7(c), showing the softening process of the composites CSAND-0CO2-C20, CSAND-1CO2-C20 and CSAND-24CO2-C20 from 2mm of displacement. The CMKFA-0CO2-C20 confirmed the hardening tendency with Pn/P1°C higher than 1, showing the increase of the capacity of the matrix to absorb energy.

According to the Figures 10(a) and (b), the Pn/P1°C is higher for the LMKFA-1CO2-C0 and LMKFA-1CO2-C10 specimens than the respective non-carbonated LMKFA-0CO2-C0 and LMKFA-0CO2-C10 ones, showing the beneficial effects of the carbonation to improve the resistance of the composites by the strain hardening behaviour.

In Fig 10(c), a hardening process occurs until 2mm for LMKFA-0CO2-C20 and LMKFA-1CO2-C20 composites. From 2mm LMKFA-1CO2-C20 lost mechanical performance when compared to LMKFA-0CO2-C20 composite, despite this matrix presents initial cracking due to the ageing according to Fig 8(c).

Fig.11 presents the TG/DTG curves of the matrix of the composites studied on initial cement mass basis for the CSAND and CMKFA composites.

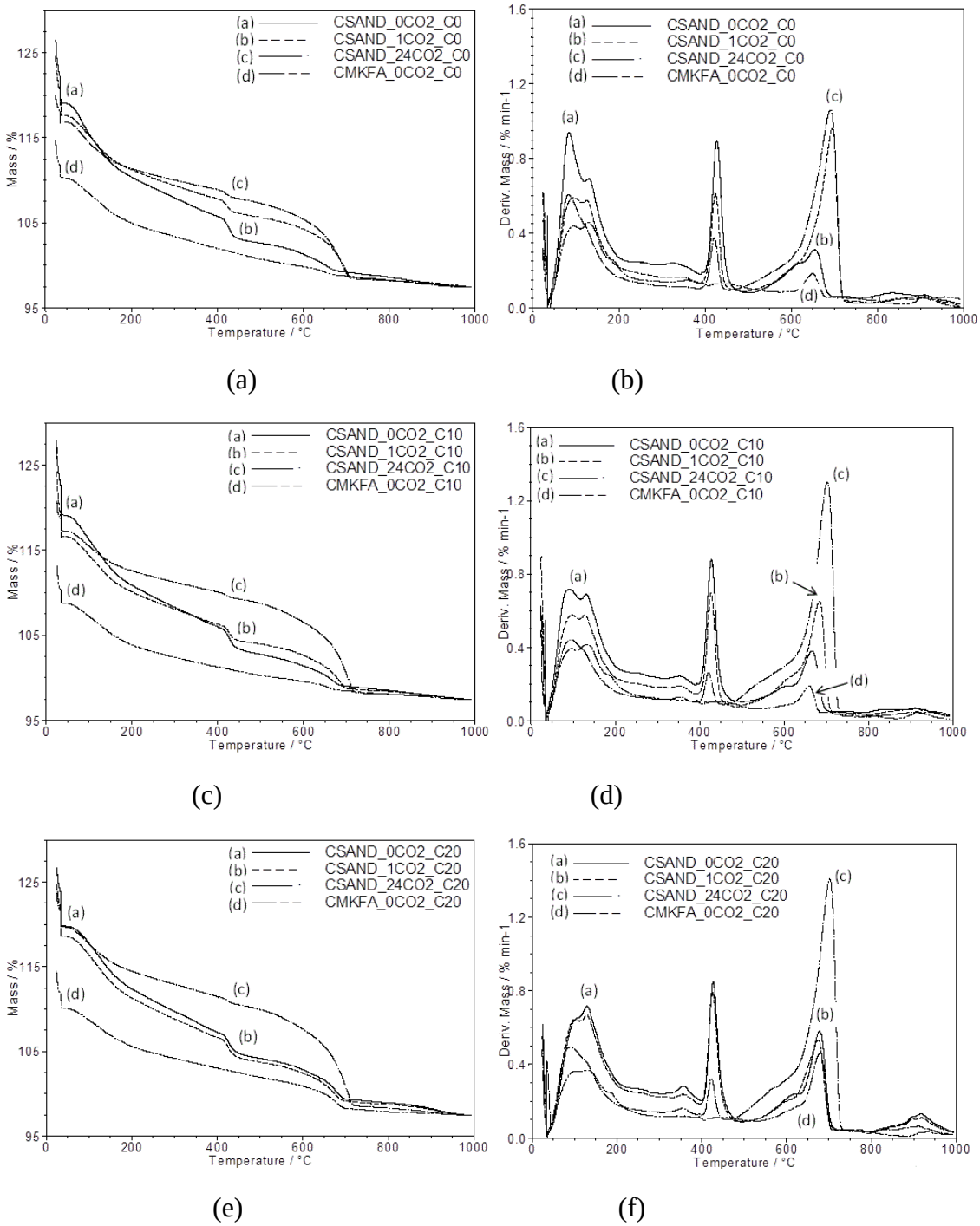

Figure 11 – TG/DTG curves on initial cement mass basis for the CSAND and CMKFA composites, without accelerated ageing (a,b), with 10 cycles of accelerated ageing (c,d) and with 20 cycles of accelerated ageing (e,f)

Figure 12 presents the TG/DTG curves of the LMKFA composite matrices on initial lime mass basis.

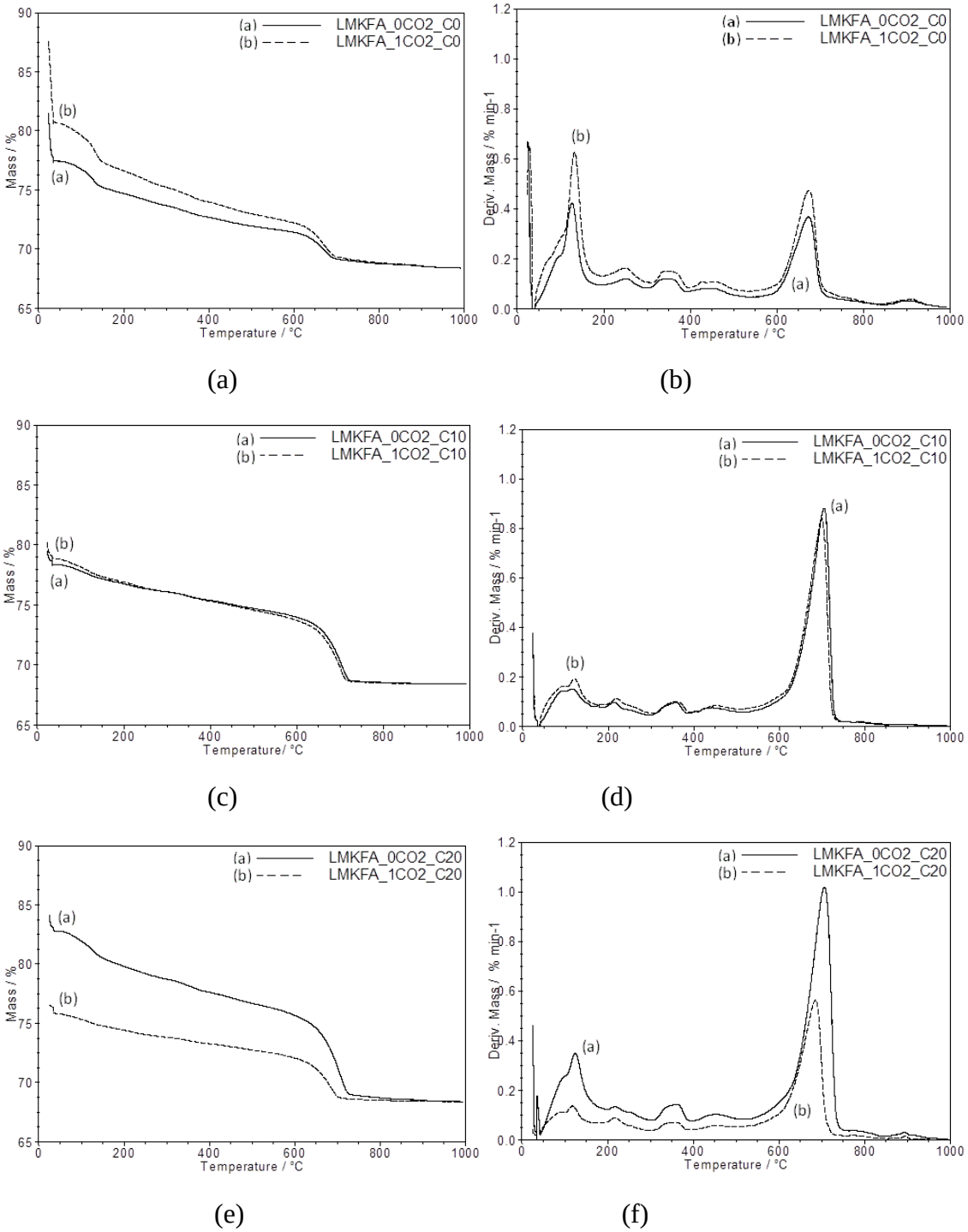

Figure 12 – TG/DTG curves of the LMKFA composite matrices on initial lime mass basis, without accelerated ageing (a,b), with 10 cycles of accelerated ageing (c,d) and with 20 cycles of accelerated ageing (e,f)

According to Fig 11, it is noticed the complete $Ca(OH)_2$ consumption for all CMKFA composites (CMKFA-0CO2-C0, CMKFA-0CO2-C10 and CMKFA-0CO2-C20). For the CSAND composites without carbonation (CSAND-0CO2-C0, CSAND-0CO2-C10 and CSAND-0CO2-C20), the expected peak of $Ca(OH)_2$ is present . For the carbonated composites (CSAND-1CO2 and CSAND-24CO2), the peak of the $Ca(OH)_2$ decreases as

well as the respective peak of $CaCO_3$ increases. The treatment with 24h of carbonation (CSAND-24CO2) was not enough to consume all the $Ca(OH)_2$, differently of what occurred with the carbonated pastes [5].

The TG/DTG results of the CMKFA composites shows that a cementitious matrix blended with pozzolans (MK and FA) is more efficient to produce matrices free of $Ca(OH)_2$ in comparison to the CSAND composites treated with CO_2.

According to the Fig 12(a)(b)(c)(d)(e) and (f), we can notice the complete consumption of the $Ca(OH)_2$ for all the LMKFA composites. For the composites without accelerated ageing, the treatment with 1h of carbonation for the LMKFA-1CO2-C0 increased the $CaCO_3$ peak in relation to the LMKFA-0CO2-C0 as expected. The composites with accelerated ageing of 10 cycles (Fig 12(c) and (d)) presented the same $CaCO_3$ content, probably due to the inherent carbonation of the LMKFA-0CO2-C10 sample.

Increasing the accelerated ageing to 20 cycles, the $CaCO_3$ peak of the LMKFA-1CO2-C20 decreased in relation to the LMKFA-0CO2-C20, probably due to the water leaching effect, which affected the matrix and its mechanical performance as seen in the Fig 8(c) and 10 (c).

Scanning electron micrographs of the cross section of the sisal fibres from the CSAND and CMKFA composites without accelerated ageing are presented in Fig 13, as examples.

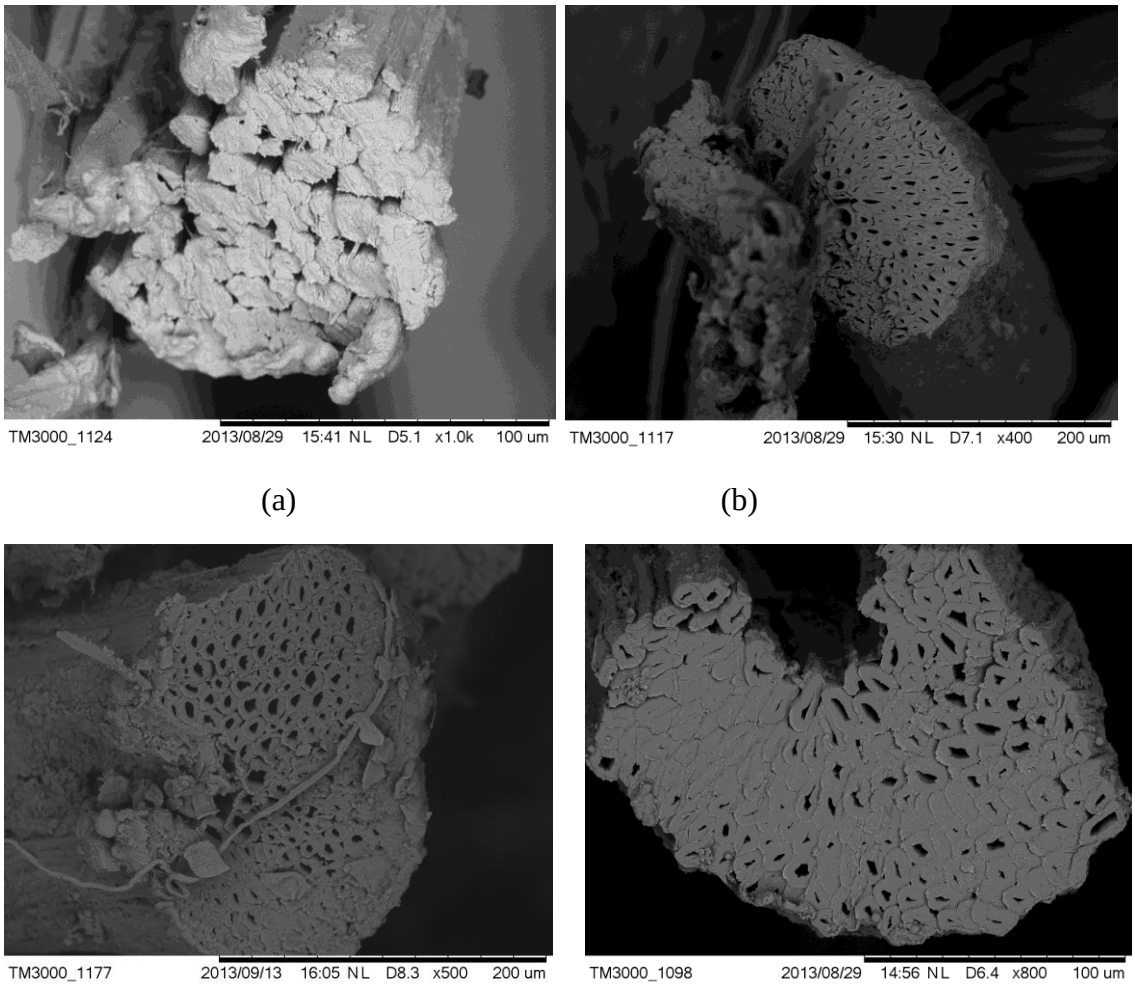

Figure 13 – Backscattered images of the cross-section of the sisal from the composites CSAND-0CO2-C0 (a) CSAND-24CO2-C0 (b), CSAND-1CO2-C0 (c) and CMKFA-0CO2-C0 (d)

The photomicrographs reveal that fibres from the CSAND-0CO2-C0 (Fig 13(a)) presents high deterioration, as expected, due to the high alkalinity as indicated by the TG/DTG results (Fig.11 (a) and (b)). Although, the carbonation treatment with 24h and 1h for the composites CSAND-24CO2-C0 and CSAND-1CO2-C0 respectively (Fig 13 (b) and (c)) has not been enough to consume all the $Ca(OH)_2$ (Fig 11 (a) and (b)), it allowed to reduce the alkalinity of the matrix and to preserve apparently the characteristic of the fibres, as shown in Fig 13 (b) and (c). The complete consumption of the $Ca(OH)_2$ as indicated by the TG/DTG curves for the CMKFA composites (Fig 11

(a) and (b)) confirms to be ideal to maintain the structure of the fibres (Fig 13(d)), as expected.

Scanning electron micrographs of the cross section of the sisal fibres of LMKFA composites with 1h of carbonation are presented in Fig.14, as examples.

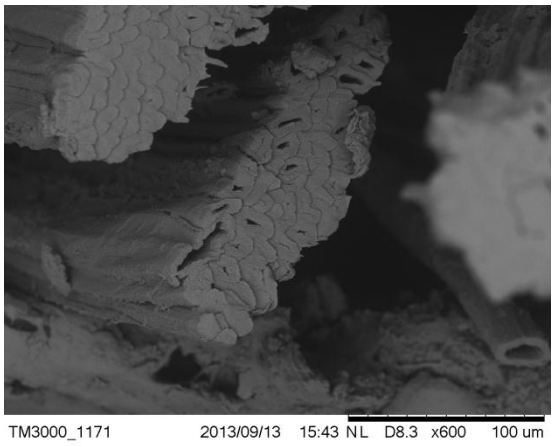

(a)

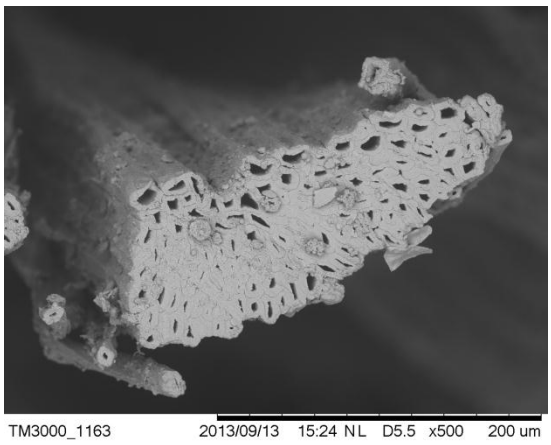

(b)

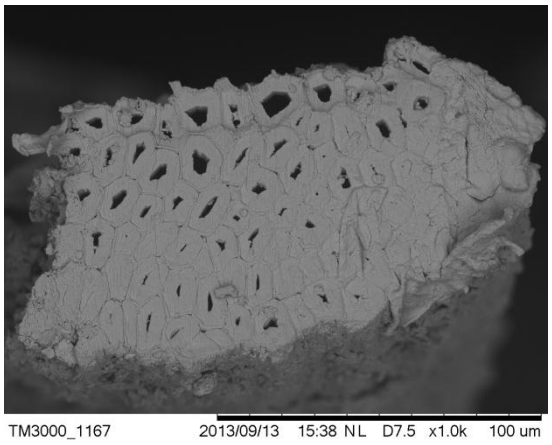

(c)

Figure 14 – Backscattered images of the cross-section of the sisal from the composites LMKFA-1CO2-C0 (a) LMKFA-1CO2-C10 (b), LMKFA-1CO2-C20 (c)

The photomicrographs of the fibres present in LMKFA-1CO2-C0 and LMKFA-1CO2-C10 composites (Fig 14(a) and (b)) show that the pozzolanic activity and the carbonation reaction were efficient to consume the $Ca(OH)_2$, preserving the fibre structure. With 20 cycles of accelerated ageing (Fig 14(c)), despite the consumption of

the $Ca(OH)_2$ showed in Fig 12 (e) and (f), a light degradation of the fibres has started, probably caused by the influence of the ageing process on the matrix .

4.Conclusions

- CMKFA composites present better mechanical results than CSAND composites, with a strain hardening behavior without and with accelerated ageing.
- CSAND composites with 1h of carbonation (CSAND-1CO2) present higher maximum stress crack than the other composites (CSAND-0CO2 and CSAND-24CO2) without and until 10 cycles of accelerated ageing.
- CSAND composites present a decrease of their mechanical resistance as ageing is applied and intensified to 20 cicles, changing the light strain hardening behavior presented without ageing to a strain softening behavior after 10 and 20 cycles of ageing.
- The cementitious matrices blended with pozzolans show to be more effective with respect to all $Ca(OH)_2$ consumption.
- The 24h of carbonation of CSAND composites was not enough to deplete all the $Ca(OH)_2$ and despite apparently the micrographs shows a small modification of the sisal fiber structure, the little presence of $Ca(OH)_2$ with the increasing of the ageing cycles contributes to decrease the mechanical performance of these composites.
- All LMKFA composites present their matrices free of $Ca(OH)_2$ with a strain hardening behavior, indicating to be efficient matrices to maintain the fiber induced mechanical properties of these composites .
- All the LMKFA_1CO2 composites present a higher maximum stress crack than the LMKFA-0CO2 composites, promoted by the formed carbonated products.
- Increasing the ageing cycles from 10 to 20, the LMKFA-1CO2 composite starts to be affected by the ageing action, showing a possible water leaching effect of their components as indicated by the TG/DTG curve data.

Acknowledgments The authors acknowledge the experimental assistance of the Rio de Janeiro Federal University Chemical School Thermal Analysis and Civil Engineering

Structure Laboratories and the financial support of the National Research Council (CNPq).

References

1. Silva FA, Chawla N, Toledo Filho, RD. 2010. Mechanical Behavior of Natural Sisal Fibers. J Bio Mat and Bio. 2010; (8):106-113.
2. Toledo Filho RD, Scrivener S, England GL, Ghavas. Durability of alkali-sensitive sisal and coconut fibres in cement mortar composites. Cem Con Comp.2000;22:127-143.
3. Toledo Filho RD, Ghavami K, England GL, Scrivener K. Development of vegetable fibre-mortar composites of improved durability. Cem Con Comp.2003;25:185-196.
4. Silva AF, Mobasher B, Soranakom C, Toledo Filho RD. Effect of fiber shape and morphology on interfacial bond and cracking behaviors of sisal fiber cement based composites. Cem Con Comp. 2011;33:814-823.
5. Neves Junior A, Dweck J, Toledo Filho RD, FairBairn EMR. CO_2 sequestration by high initial strength Portland cement pastes. J Therm Anal Calorim. 2013; 113: 1577-1584.
6. Brazilian Association of Technical Standards. High initial strength Portland cement. NBR 5733. Rio de Janeiro. 1991.
7. Brazilian Association of Technical Standards. Moderate sulphate resistance Portland cement and moderate hydration heat (MRS) and high sulphate resistance NBR 5737. Rio de Janeiro. 1986.
8. Neves Junior A, Dweck J, Toledo Filho RD, FairBairn EMR. Early stages hydration of high initial strength Portland cement—Part I—thermogravimetric analysis on calcined mass basis. J Therm Anal Calorim. 2012;108:725–31.
9. Neves Junior A, Dweck J, Toledo Filho RD, FairBairn EMR. Early stages hydration of high initial strength Portland cement—Part II—NCDTA and Vicat analysis. J Therm Anal Calorim. 2013;113:659–65.

10. Neves Junior A, Dweck J, Toledo Filho RD, FairBairn EMR. A study of the carbonation profile of cement paste by thermogravimetry and its effect on the compressive strength. J Therm Anal Calorim.2013;114 (3)